Nonlinear Vibration and Frequency Response Analysis of Piezoelectric-based Nanotube Resonators

by

ZIA SAADATNIA

A Thesis Submitted in Partial Fulfillment
of the Requirements for the Degree of

Master of Applied Science
Mechanical Engineering

The Faculty of Engineering and Applied Science
Department of Mechanical Engineering

University of Ontario Institute of Technology

April 2015

Abstract

To study the vibration behaviour of nanotube-based structures, different models of nanotubes under the effects of piezoelectric layer, intermediate mass, fluid flow and structure curvature are developed. The frequency responses of proposed models for both free and forced vibrations under single frequency, multi-frequency and parametric excitations are investigated. The Hamiltonian principle and Lagrangian method are associated with non-local non-classical theory to develop the nonlinear vibration models and two strong methods known as Galerkin technique and multiple scales method are employed to find the solutions of the developed systems equations. Accordingly, the governing equations for transverse vibration of a nanotube carrying an intermediate mass are obtained and the internal-external resonances are considered for the obtained structure. Then, the vibration model of piezoelectric-layered nanotube structure is developed and the system behaviour under single frequency and multi-frequency excitations is analyzed. In the next model, the nonlinear vibration of piezoelectric-layered nanotube conveying fluid flow is developed considering the fluid-structure interaction and the influence of constant and harmonic applied voltages are examined on the vibration behaviour of proposed system. In the last model, transverse vibration of the piezoelectric-layered nanotube with a geometrical curvature is presented and the structure vibration under external and parametric excitation for different curves are studied. Effects of various physical, mechanical and geometrical properties on the vibrations of developed models are investigated. It is shown that consideration of non-local theory can remarkably influence the frequency-amplitude responses of the nano structures. The importance of intermediate in changing the frequency responses of the system is studied. Effects of piezoelectric layer

and applied voltage on the natural frequency and frequency-amplitude behaviour of the structure are also examined. It is observed that fluid flow plays an important role in the vibration behaviour and the system stability. The curved structure is also analyzed and the nonlinear hardening-softening behaviour owing to the nanotube curvature is studied.

Dedication

This thesis is dedicated to my mother for her endless support and inspiration. It is also dedicated to my family for encouraging me in all steps of my education.

Acknowledgement

I am pleased to express my deepest appreciation to Professor Ebrahim Esmailzadeh for his steadfast support and insightful supervision during my research and education at UOIT. Truly, without his sympathetic supports and encouragement, I would never be in this stage of my academic career.

I wish to express my gratitude to the advisory committee members for their generous and careful contribution.

I would like to appreciate Dr. Davood Younesian not only for his great helpfulness in this thesis, but also for his invaluable advice and thoughtful criticisms during my undergraduate and graduate studies.

I would like to have special thanks to my respectful friend, Hassan Askari, for his countless motivation and assistance in the past 7 years. I am also very thankful to my friends Dr. Fereydoon Diba, Saeed Jami and Amir Ghandehariun for their constant helps in past two years.

The financial support provided by the Natural Science and Engineering Research Council (NSERC) of Canada to complete this research is gratefully acknowledged.

Table of Contents

Table of Figures

List of Tables

Nomenclature

A	Cross section area (m^2)
a	Internal characteristic length (m)
D	Dielectric displacement (C/m^2)
D_x	Electrical displacement in axial direction (C/m^2)
d	Piezoelectric charge constant (C/N)
E	Young's modulus (N/m^2)
E_1	Linear elastic constant of piezoelectric (N/m^2)
E^x	Electric field in axial direction (V/m)
$\tilde{E}$	Compliance of the medium (m^2/N)
e_0	Nanotube material constant
e_1	Piezoelectric constant (C/m^2)
F	External excitation (N)
I	Cross section moment of inertia (m^4)
k_1	Dielectric constant (F/m)
L	Structure length (m)
l	External characteristic length (m)
M	Dimensionless intermediate mass
$\overline{M}$	Bending moment ($N.m$)
m	Mass of intermediate particle (kg)

$\overline{N}$	Shear force (N)
P	Axial load (N)
R	Nanotube radius (m)
r	Quadratic curve waviness (maximum point)
s	Stress tensor (N/m^2)
T	Kinetic energy (J)
U	Potential energy (J)
$\hat{U}$	Dimensionless fluid velocity
u	Longitudinal displacement (m)
u_i	Displacement vector (m)
$\vec{V}$	Velocity vector (m/s)
V_0	Amplitude of constant voltage (V)
V_1	Amplitude of harmonic voltage (V)
$\overline{V}$	Volume (m^3)
v	Constant fluid flow velocity (m/s)
W	Work of external force (J)
w	Transverse displacement (m)
$\bar{x}$	Cubic curve waviness (position of maximum point)
Z	Structure curvature function
α	Dimensionless vibration amplitude
Δ	Dirac function

$\in$	Electrical field (V/m)
ε	Strain tensor
μ	Dimensionless damping coefficient
μ_0	Dimensionless non-local parameter
ξ	Dielectric permittivity (F/m)
ρ	Structure density (kg/m^3)
ρ_f	Fluid density (kg/m^3)
σ	Detuning parameter
τ	Time parameter ($1/s$)
φ	Electric potential (V)
Ω	Frequency of excitation (rad/s)
ω	Natural frequency (rad/s)

Chapter 1: **Introduction**

1.1. NANOTUBE, PROPERTIES AND APPLICATION

The role of carbon nanotubes can be extensively found in science and engineering due to their exceptional properties since their discovery in past decades. Carbon nanotubes are one of the main carbon allotropes with a cylindrical formation firstly discovered by Iijima in 1991 during his research on the surface of graphite electrodes in an electric arc discharge[1, 2]. Actually, due to the unique properties of carbon, various allotropes have been found for this element such as diamond, graphite, fullerenes (e.g., buckyballs, nanotubes) graphene sheets, etc., [3]. The two first ones are the most well-known allotropes such that in diamond each carbon atom is bonded to four other carbon atoms while in graphite the carbon atoms are only bonded in two dimensions [3]. Nanotubes are known as members of fullerenes family which are constructed by rolling the graphene sheets [3]. The atomic formation of these sheets are in hexagonal lattices of carbon atoms and the way of rolling the sheets determines the nanotubes exceptional properties [3]. The diameter of these structures can vary from 1 to 100 nm and they can have the length of up

to millimeters [2, 4]. Nanotubes also have Young's modulus more than $1\,Tpa$, density around $1.3\,g/cm^3$ and the length to diameter ratio of up to 132,000,000:1 [2, 5, 6].

Indeed, the nanotubes display outstanding mechanical, thermal and electrical behaviours superior than the other materials [2, 7]. Therefore, applications of these structures are observed in a variety of mechanical, electrical biomedical devices as well as fundamental science. In addition, number of research works about the understanding and development of nanotube-based systems has been interestingly increased in current decades. Basically, there are two types of nanotubes namely single walled nanotube and multi-walled nanotube. The first one has three microstructure formations including zigzag, arm-chair and chiral which could be shaped as rolled graphene sheets [2, 7]. The schematic illustration of three main carbon nanotube structures is depicted in Figure 1-1 [7]. Single walled nanotubes can be fabricated by different techniques such as arc-discharge generators, laser ablation and chemical vapor deposition [2]. The second one is an array of concentric cylinders which is fabricated either by arc-discharge generators or more commonly by chemical vapor deposition [2].

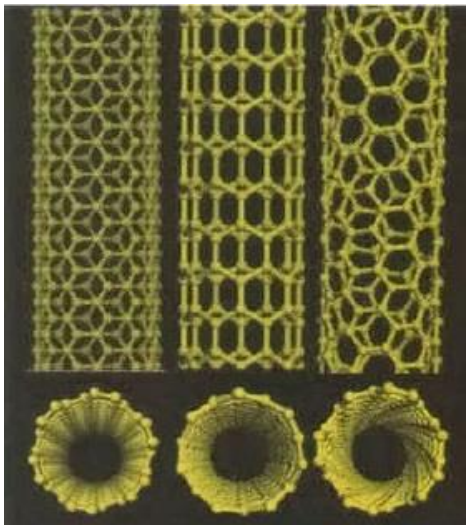

(a) (b) (c)

Figure 1-1 Nanotube schematic structures a) arm-chair b) zigzag c) chiral [7].

Regarding the nanotubes properties, the exceptional mechanical, electrical and thermal properties of these structures have made them as one of the key elements in electrochemical devices, hydrogen storage systems, field emission devices, nanometer-sized electronic devices, sensors, actuators and probes [7]. In terms of mechanical properties, nanotubes have shown great stiffness, elasticity and tensile strength by having very high Young's modulus which can be implemented in a variety of bending, twisting and torsional mechanisms [7-9]. In terms of electrical properties, some nanotubes show a high conductivity even in the room temperature due to their microstructures and consequently they are able for carrying high currents and electronic transport, which is very important in electronic devices and circuits [7-10]. In terms of thermal properties, nanotubes greatly have thermal stability and conductivity which has been proved both by experiments and other simulation methods and accordingly they can efficiently be employed in heat transfer applications in comparison with the other materials [7, 8, 11, 12].

In this section several examples of nanotubes applications are briefly presented to show the importance and capability of these structures for various systems. One of the main applications of nanotubes is to be implemented as ideal fillers for composite structures [2, 13-15]. Due to the unique properties, they can be an appropriate candidate for reinforcement of composites to enhance their strength as well as thermal and electrical conductivities [2, 14]. Figure 1-2 shows transmission electron microscopy (TEM) for a sample of polyamide-6 reinforced by nanotubes for improving its mechanical and electrical characteristics [13].

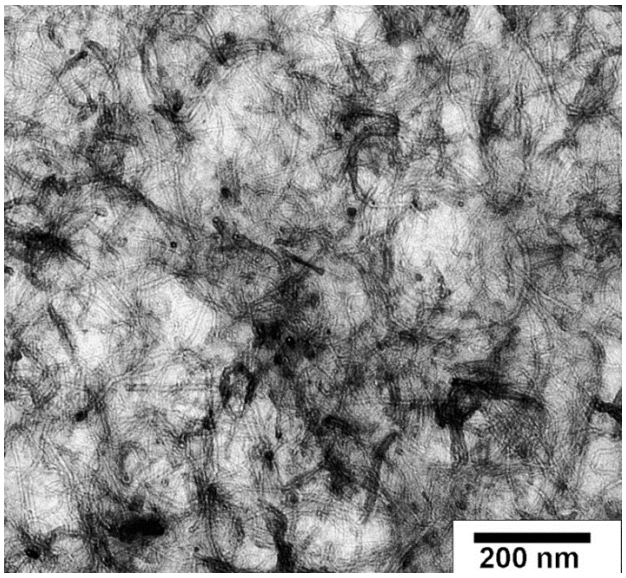

Figure 1-2 TEM-micrographs of polyamide-6 filled with carbon nanotubes [13].

Nanotubes are also efficient structures for resonance-based sensors which are applicable for mass detection, biomedical applications and chemical reaction monitoring [16-18]. This feature is originated from the high sensitivity of nanotubes to very small added masses which leads to a frequency shift on the system and consequently the change on the frequency is the key point for diagnoses of small bio particles as well as humidity [16, 19]. A nanotube resonator with the application of mass detection has been shown in Figure 1-3 using electron microscopy image [17].

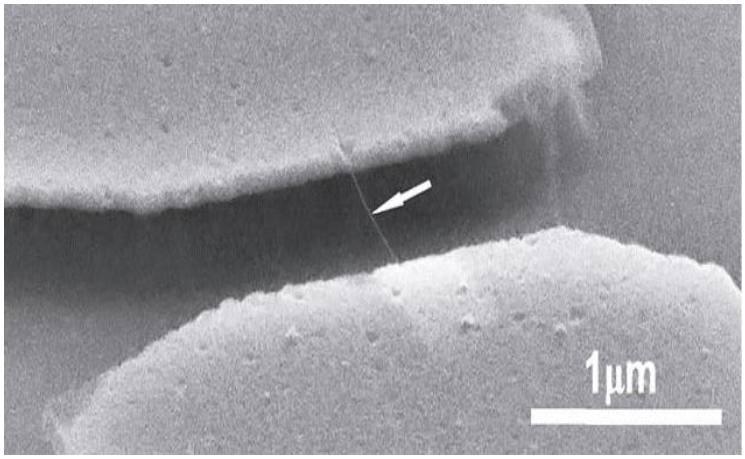

Figure 1-3 Scanning electron microscopy image of the nanotube resonator [17].

Another important use of nanotubes is that they can be employed as ideal fluid conveyors in nanopiping system [20-22]. This application could be seen in probing cells or transporting drugs and proteins inside cells with least intrusion and damage [20]. Also, due to the almost frictionless interface at some nanotubes walls and fluids, a very high fluid velocity can be achieved which is applicable for biological channels [21]. As one sample of nanotubes for nanopiping targets, the scanning electron microscope micrograph of a carbon nanopipe with deposited polypyrrole has been depicted in Figure 1-4 using bipolar electrochemistry methods [20].

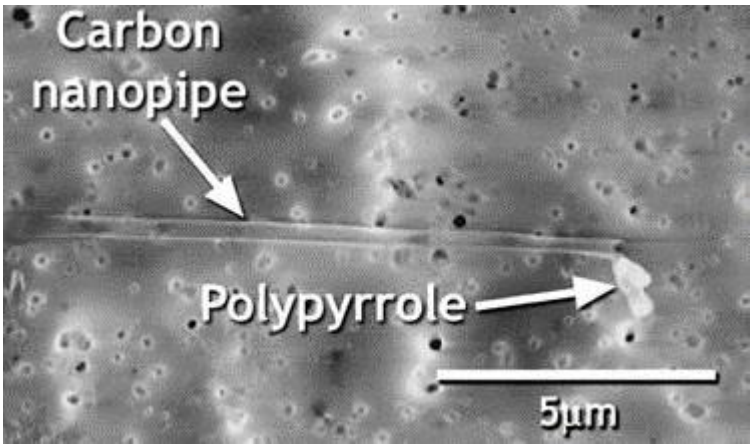

Figure 1-4 Electron microscope micrograph of nanopipe with polypyrrole [20]

In addition, surveying the literature reveals that a variety of other electromechanical applications can be found for nanotubes such as nanotube based bearing for rotational motions [23] carbon nanotubes for nanorobotics [24], nano sized mechanical switches [25] and many other instances [26-28].

1.2. NONLOCAL THEORY

Dynamic modeling and analysis of nano structure has been studied by a number of researchers due to the differences that the very small dimension brings into the models. Therefore, various techniques have been proposed recently to investigate the mechanical behaviour of such systems including experimental methods, molecular dynamics and continuum mechanics [29]. However, the experimental methods are quite difficult and limited due to the restrictions in the experiments [29]. On the other hands, molecular dynamics method is rather challenging owing to the difficult accurate formulation for the system as well as costly and intensive solution processes [29]. Thus, application of continuum mechanics has been interestingly considered in order to analyze the aforementioned structures [29]. Although the classical continuum mechanic theories would reach to the relevant findings to some extent, the accuracy of the results have always been questionable owing to the differences that small length scale adds to the system, which is not considered in classical methods [29]. The reason is that in small length scales, the material microstructure such as lattice formation of atomic configuration and internal atomic forces play an important role, and consequently the discrete microstructure cannot be standardized as continuum model [29].

Hence, the non-classical theories were developed to consider these effects and one of the main theories was nonlocal elasticity theory proposed by Eringen [30-33]. According to this theory, the stress at a reference point is taken to be related to strain field at every point in the body [32]. So, the stress tensor at a specific point is the function of strain tensors at all points while in classical models the stress and strain tensors are uniquely dependent to each other at the same point [32]. The nonlocal assumption would consider a range of

internal microstructure forces into the constitutive equations which is potentially applicable for nano scale structure modeling [34]. Detailed discussions regarding the nonlocal Eringen's theory can found in the literature [30, 32-34], however a brief formulation is presented here. Accordingly, for a homogeneous isotropic material with no body force the basic equations are constructed as [33, 35]:

$$s_{ij,j}(x) = \int \alpha(|x - x'|, \tau) C_{ijkl} \varepsilon_{kl}(x') d\overline{V}(x'), \quad \forall x \in \overline{V}, \tag{1.1}$$

$$\varepsilon_{ij} = \frac{1}{2}(u_{i,j} + u_{j,i}), \tag{1.2}$$

In above equations s_{ij} and ε_{ij} are the stress and strain tensors, respectively and C_{ijkl} shows the classical elastic modulus tensor [35]. u_i is the displacement vector and $\alpha(|x - x'|, \tau)$ indicates nonlocal effects at the reference point originated from the local strain at the point namely attenuation function where $|x - x'|$ is the Euclidian distance [35]. The parameter $\tau = e_0 a / l$ is obtained for each material such that e_0, a and l denote material constant, internal and external characteristic lengths, respectively and they can be found based on the material microstructure properties including wavelength, lattice formation, atomic dynamics, etc. [35]. The analysis of above integral-partial differential equation is quite difficult however it was shown that for a specific class of physically allowable kernel, it could be reduced to singular partial differential equations [35]. It has been proved that by using Hooke's law the uniaxial stress equation could be derived as [35]

$$s(x) - (e_0 a)^2 \frac{d^2 s(x)}{dx^2} = E\varepsilon(x), \tag{1.3}$$

where E indicates the material Young's modulus and the constant coefficient is associated with the small length scale of the nano structure. Hence, this equation and other resultant equations can be implemented to provide more accurate models for the mechanical behaviors of nano size systems. As examples, Peddieson, et al. employed nonlocal elasticity theory for nanobeams in conjunction with Euler-Bernoulli beam theory [34]. Sudak presented the column buckling analysis for multi-walled carbon nanotubes by means of this theory to show the effects of small length effects [29]. Wang applied nonlocal theory to study the wave propagation in Euler-Bernoulli and Timoshenko beams and the effect of small size on the wavelengths were analyzed [35]. Reddy and Pang formulated the general equations of motions for static bending, vibration and buckling of Euler-Bernoulli and Timoshenko beams and then various boundary conditions were examined [36]. Nonlocal nonlinear formulations for deformations beams and plates which can be applicable for nano structure were extended by Reddy [37]. Considering elastic substrates, post buckling and bending of carbon nanotubes were investigated by means of nonlocal continuum theory [38]. In another work, vibration of initially pre-stressed coupled nano beams were analysed using nonlocal elasticity method [39]. Using nonlocal theory, forced responses of single walled carbon nanotubes for various boundary conditions were carried out by Claeyssen, et al. [40]. Also in a recent study, resonance frequency of zeptogram-scale nanosensors targeted for mass detection application were obtained employing nonlocal theory [41]. In all aforementioned articles as well as many other researches, the influence of considering small scale parameter on the systems responses were observed comparing to the classical theories.

1.3. PIEZOELECTRIC MATERIALS

Piezoelectric material is basically referred to a type of solid state materials which shows a coupling between is electrical, mechanical, and thermal states by applying mechanical stress to dielectric crystals [42]. It was revealed that when an electric field is applied to these materials, mechanical stress or strain are observed in their behaviours and on the other hand, mechanical deformation leads to electric charge [42]. Different categorizations have been defined for piezoelectric materials. For example, some piezo materials are known as natural piezoelectric materials such as Quartz, Rochelle salt, ammonium phosphate, and paraffin and the others are known as synthetic piezoelectric materials such as zirconate titanate (PbZrTiO3–PbTiO3, known as PZT), barium titanate, barium strontium titanate (BaSTO), lead lanthinum zirconate titanate (PLZT), lithium sulfate, and polyvinylidene fluoride (PVDF) and PVDF copolymers, etc. [42]. On the other hand, these materials are put in ceramic and polymeric categories and for example PZT compounds are in ceramic form [42].

Due to the superior properties of piezoelectric materials, they can widely been implemented into a variety of electromechanical systems. For example, PZT materials are appropriate for electromechanical transducers such as generators (e.g., spark ignition, solid-state batteries), sensors (e.g., accelerometers and pressure transducers), and actuators (e.g., pneumatic and hydraulic valves) [42]. Also, PVDF copolymers can extensively be utilized for industrial applications such as ultrasonic transducers, hydrophones, microphones, and vibration damping [42].

The aim of this section is to present a brief description for the mechanical behavior of piezoelectric materials and the detailed modeling and analysis of the targeted materials can

be found in the references [42-44]. Accordingly, the expression of dielectric displacement, D, in an unstressed linear medium under the influence of the electrical field $\in$ is ideally written as [42]:

$$D = \xi \in \tag{1.4}$$

In which ξ shows the absolute dielectric permittivity of the medium [F/m] [42]. Also, the mechanical strain-stress relationship in the same linear medium without the presence of electric field is given as:

$$\varepsilon = \tilde{E}s, \tag{1.5}$$

where s and ε show the applied stress and strain, respectively. Also, $\tilde{E}$ indicates the compliance of the medium (i.e. inverse of the material stiffness). For the piezoelectric materials, the coupling between the interacting mechanical and electrical fields can be linearly approximated by the following sets of equations [42]:

$$\varepsilon = \tilde{E}s + d \in \tag{1.6-a}$$

$$D = ds + \xi \in \tag{1.6-b}$$

In above equations d refers to the piezoelectric charge constant which is found for each piezoelectric material. It should be noted that the stress, strain, electric field and constant parameters of above coupled equations are generally expressed in matrix and tensor forms as seen in the references [42]. However, according to the material type and some geometrical simplifications, these relations are reduced to simpler forms which can be used in the system mathematical models [42].

The applications of piezoelectric material in very small size structures has been interestingly studied in recent research works owing to their exclusive characteristics. As some instances, the Piezoelectric-based vibration control systems for micro and nano sizes as well as macro structures were investigated [42]. In that study a variety of piezoelectric-based devices which could be employed in vibration controllers, positioning systems, cantilever sensors and nano-size sensors and actuators were developed [42]. Gao and Wang investigated the piezoelectric potential distribution of nanowires as nanogenerators and it was shown that the produced voltage due to the structure displacement is much higher than the voltage caused by thermal effects [45]. In another work, a novel composite nanostructure produced by coating carbon nanotubes with piezoelectric zinc oxide ZnO, were developed [46]. The model was then analysed using Timoshenko beam theory and the application of it for nanoresonators were taken into the account [46]. The piezoelectric ZnO carbon nanotube were studied under axial strain and electric voltage and the buckling phenomena were investigated for the targeted structure [47]. Momeni and Attariani investigated the electromechanical characteristics of one dimensional zinc oxide nano piezoelectric systems by considering the influence of small size and surface parameters [48]. Also, Khan, et al. studied various types of composite nanowires for harvesting piezoelectric potential implanted in specific textiles [49].

Chapter 2: **Vibration of nanotube-based structures**

2.1. DYNAMIC MODELING AND VIBRATION OF NANOTUBES

Investigation to dynamic and vibration of nanotube-based structures have been found in a number of research articles in two past decades owing to the unique properties of these systems. As one of the earlier works, Poncharal, et al. studied the static and dynamic mechanical deflections of multi-walled nanotubes under the transmission of electron microscope when the structure is cantilevered [50]. The resonance excitations at the fundamental frequency as well as higher modes were targeted to study and compared with model of elastic beams as depicted in Figure 2-1 [50]. It was shown how the proposed model can be employed for detection of small particles in biomedical applications [50]. In another work, the atomic force microscopy were implemented to measure the lateral deflections of nanocantilever systems in resonance conditions [51]. The experimental method were evaluated by a nonlinear electromechanical model and the results were checked for static and dynamic excitations [51]. Davis and Boisen developed and fabricated aluminum nanostructures as high sensitivity mass sensors by determining their dynamic characteristics [52]. They compared the proposed sensor model system with silicon one and found out that aluminum could be a better option in terms of high sensitivity applying experimental tests [52].

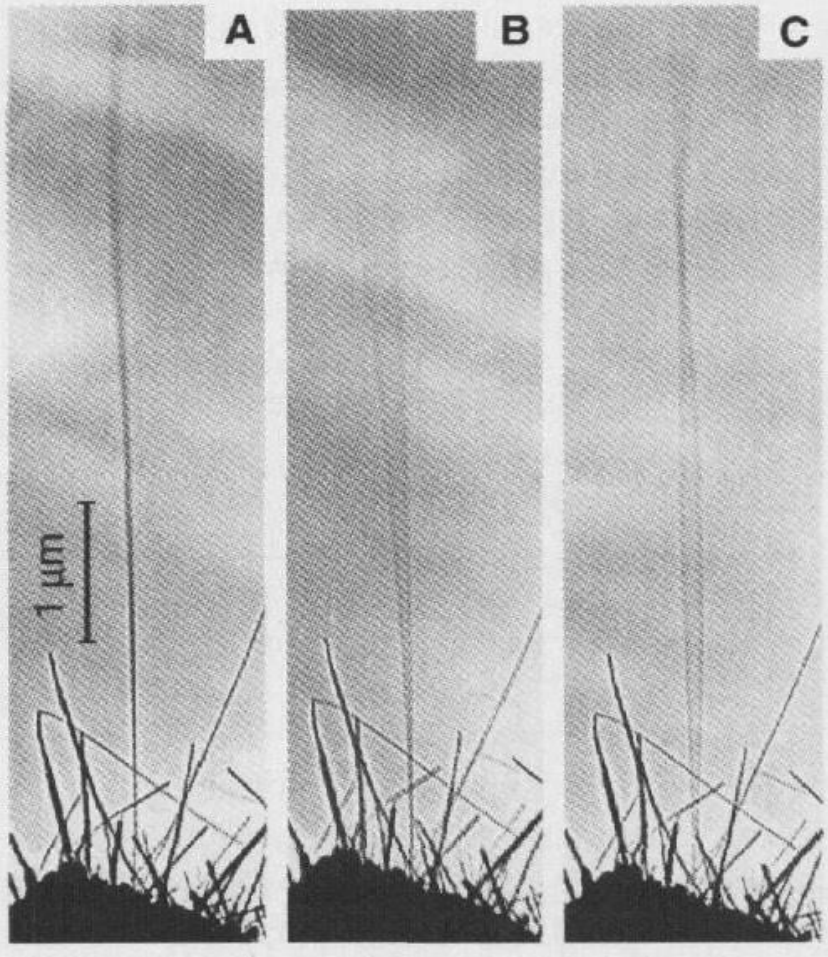

Figure 2-1 Nanotube under A) non, B) first mode, C) second mode, resonances [50]

Kim et al., employed the molecular dynamics simulation to obtain the elastic properties of silicon nanostructures such as Young's moduli [53]. Effects of dimensional scaling on the moduli were taken into the account and compared to experimental findings and continuum mechanic modeling showing how this parameter dependent to the dimensions [53]. Adali developed variational principles to investigate the transverse vibration of multi-walled carbon nanotubes considering nonlocal theories [54]. Free vibration of the proposed model were considered and the Rayleigh quotients were obtained for finding the system natural frequencies and then numerically examined for an example [54]. Effects of surface energies on the nonlinear static and dynamic mechanical behaviour

of nanobeams were analyzed by Fu et al. including geometrical nonlinearity [55]. For that purpose, the transverse normal stress was considered for the surface stresses balances unlike the classical models [55]. Presented results proved that this factor which is related to the small length scales would lead to considerable differences in comparison with the classical ones [55]. Forced vibration analysis of nano-electromechanical systems under electrostatically excitation of an electrode was studied by Kacem, et al. [56]. The proposed system was developed using Galerkin decomposition method and averaging method for clamped-clamped boundary conditions and analytically solved considering different nonlinearity sources and fringing field influences [56]. Also, a parameter study were carried out focusing on the effect of applied electric filed on the system vibration responses [56]. Generalized differential quadrature method were employed to investigate the free vibration of multi-walled carbon nanotubes considering Timoshenko beam theory [57]. Different boundary conditions and van der Waals forces were taken into the account and the impact of boundaries, geometrical parameters and Pasternak foundation properties were examined on the nonlinear frequency- amplitude responses of the structure [57]. Longitudinal vibration of single-walled carbon nanotubes with an attached buckyball mass using nonlocal assumptions was analyzed by Murmu and Adhikari [58]. The aim of that article was to find out the significant effect of attached mass on the resonant frequency of the system [58]. The analytical expressions for the structure frequency were then obtained and the results were compared with molecular dynamic method as well as classical solutions [58]. Effect of the mass and nonlocal parameter on the frequency shifts were then studied and it was observed that increase on the concentrated mass would result in higher shifts on the model frequencies [58]. Application of grapheme-based nano-electro-

mechanical systems for mass detection purpose was developed by investigating the nonlinear vibration of these structures [59]. The model was constructed based on the continuum elastic theory for plates and it was shown that in plane tension is significantly effective in vibrational behaviour and resonances of the model [59]. Frequency analysis of carbon nanotubes as biosensors were carried out by Murmu and Adhikari considering nonlocal theory [60]. To evaluate the findings, a molecular dynamics analysis was employed and it was shown that both techniques find similar results but different from the classical ones [60]. In addition, the influence of adding mass to the structure on the frequencies of the proposed system were studied and compared for both methods [60]. Free vibration and primary resonance of carbon nanotubes under harmonic excitation were investigated by Rafiee, et al. [61]. The model was established based on classical theories and von Karman strain displacement relations and then solved by means of multiple scales method [61]. Effect of various parameters such as foundation properties and system geometry on the free vibration responses and nonlinear hardening behavior of the system forced vibration were numerically and graphically represented [61]. Adomian decomposition and Pade approximation were utilized to analyze the nonlinear vibration and stability of nanocantilever switches by Noghreabadi, et al. [62]. The results of the developed solution procedure were then verified by numerical solutions [62]. As the system was under the nano actuator, effect of actuation parameters such as the gap between structure and actuator and applied voltage were taken into the account [62]. Natural frequencies and mode shapes of double-walled carbon nanotubes carrying a bacterium tip mass by means of continuum theory [63]. The proposed model was then solved by means of finite difference method and then examined for a variety of bacteria and accordingly the

frequency shift could be implemented for detection of very small masses [63]. Nordenfelt investigated the flexural vibrations of nano-ribbons and nanotubes under the electromagnetic field and the possibility of self-excitation for higher mode vibration were targeted in the study [64]. A constant magnetic field were considered in the model and the advantage of using graphene and carbon nanotube in terms of reaching to desired amplitudes of vibration were observed [64]. Also in a recent study, application of strain gradient theory in frequency analysis of nano resonators were analyzed by Mani-Miandoab, et al. [65]. Also, effects of electrostatic actuation and non-classical assumption on the frequency responses and stability of the system were examined and graphically represented for various numerical values [65].

2.2. VIBRATION OF FLUID-CONVEYING NANO STRUCTURES

Due to the important application of nanotubes as nanopiping systems for transfer of nanoparticles, these structures can be significantly implemented in biomedical devices for drug delivery mechanisms. Understanding the mechanical behaviour, particularly the vibrational responses and frequency analysis have involved a number of researchers in current years. For example, dynamic modeling of viscous fluid flow inside nanotubes were carried out using classical methods [66]. In that paper, multi-walled carbon nanotube conveying fluid was modeled by Euler-Bernoulli beam theory and the linear Navier-Stoke equation for different boundary conditions [66]. The frequency expressions and critical velocities were analytically found and examined for two viscous fluids namely Acetone and Methanol [66]. Also, the stability of the structure were analyzed considering different geometries for the nanotube structure [66]. In another classical study, the vibration of

axially loaded fluid conveying nanotubes considering the Euler-Bernoulli beam theory was investigated [67]. The nonlinear frequency-amplitude responses were carried out and effects of linear foundation and fluid velocity on the frequency responses were studied [67]. The structure aspect ratio and axial load were two other important parameters which were taken into the account and the sensitivity of system stability to aforementioned parameters were described [67]. Considering small length effect, nonlinear vibration and stability of double walled carbon nanotubes were investigated applying continuum mechanical theories [68]. It was shown that the assumption of small length effect is effective on the natural frequencies but that effect is not considerably observable in critical fluid velocity of their model [69]. Ghavanloo, et al. employed finite element method to accomplish the frequency analysis of Euler-Bernoulli beam type nanotubes including fluid flow [70]. The foundation was taken to be viscoelastic and the non-viscous fluid effect were modeled using steady flow velocity and flow mass density [70]. The properties of structure foundation and fluid motion were taken to perform a parameter study for the resonance frequencies of the system [70]. Transverse vibration of a single walled carbon nanotube under the motion of viscous fluid and divergence stability of the structure were investigated in another work [71]. For this model, the nanotube was embedded in a Kelvin-Voigt foundation and the sensitivity of system stability and frequency responses to the foundation parameters were characterized [71]. Prediction of surface effects on the vibration of fluid conveying nano conveyors were investigated by Wang employing non-local elasticity theory [72]. Effect of these parameters on the frequency of the system and critical fluid velocity were examined as well as geometrical properties of the structure [72]. It should be noted that in that paper both circular and rectangular cross sections were modeled for the

nanosystem which might be helpful for different designs [72]. Hashemnia and Emdad considered carbon-water bond potential energy and nonlocal effect to model the free vibration of single walled carbon nanotubes conveying water [73]. They showed that their assumptions would lead to higher natural frequencies in comparison with the continuum mechanic models. Again effects of foundation parameters and structure geometries on the fundamental natural frequencies were examined [73]. Wang employed modified nonlocal beam theory based on new nonlocal stress model to investigate the vibration and stability of fluid conveying nanotubes [74]. According to the developed model of that study, higher natural frequencies were obtained comparing to partial nonlocal beam theory which is also effective on the critical velocities [74]. In another paper, Wang employed gradient elasticity theory for modeling the aforementioned structure [75]. Two material length scale parameters were combined in that work to show the dependency of the system behavior to the small size effect [75]. It was shown that the results are noticeably different for the studies which considered only one material length scale parameter namely stress gradient model [75]. Soltani and Farshidianfar employed the energy balance method to find the nonlinear natural frequencies of a nonlocal nanotube conveying fluid [76]. Using this method, the periodic solution and frequency expressions were analytically obtained and then compared with numerical solutions. Effects of initial conditions, axial tension, nonlocal parameter, fluid velocity and Winkler-Pasternak foundation on the nonlinear natural frequency variation were evaluated in their work [76]. Kiani utilized nonlocal Rayleigh beam model to investigated the vibration of inclined single walled carbon nanotube with simply supported boundaries [77]. Effects of various parameters such as nonlocal parameter and inclination angle on the maximum dynamic amplitude factors and

nonlocal axial and flexural forces were examined and graphically represented [77]. Also, flow of pulsating and viscous fluid were considered to investigate the vibration and stability of a single walled carbon nanotube by Liang and Su [78]. The assumption of pulsating fluid was originated from this fact that in some nano electro mechanical devises, the power systems driving the fluid inside the structure are pulsative producing intermittent behaviour on the fluid flow [78]. The problem were solved by means of averaging method and the stability boundary curves were extracted for numerical values and then compared with the classical model results [78].

2.3. DYNAMICS OF CURVED NANOTUBES

In some nanotube-based systems, the structure might have a curvature on its shape which can be as a result of the natural geometrical properties of the structure or it is intentionally shaped on the model to reach specific mechanical properties for the model. This curvature can play a critical role in the system mechanical behavior. Thus, investigation to the effect of structure curvature on the nanotube mechanical behavior has been a very attractive topic in past recent years. Figure 2-2 [79] shows a real configuration of a nanotube having a curvature along the structure. As one of the pioneer works, Berhan et al. investigated the effects of these non-straight shapes on the mechanical properties of nano structures [80]. Their modeling showed that the Young's moduli in nanotube ropes is directly dependent to the waviness of these structures [80]. They have also found how the formation of nanotubes could improve the overall properties of nano sheets made by aforementioned curved nanotube ropes [80].

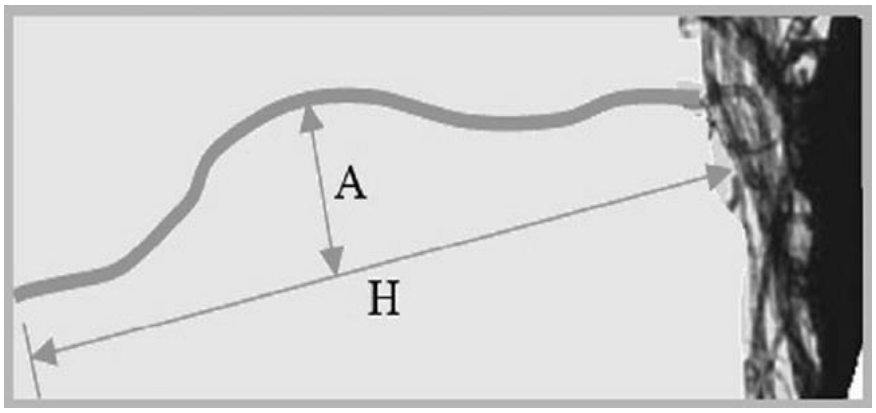

Figure 2-2 Model of a nanotube associated with a curvature [79].

Effect of surface deviations in double walled nanotubes was investigated by Patel et al., which are applicable in nano-mechanical sensors [79]. They employed finite element method to model the double walled carbon nanotubes with bridged and cantilever ends and according to their findings, the frequency shift can occur by changing the structure curvature which is attributed to the change of system stiffness [79]. Mayoof and Hawwa investigated the chaotic behavior of curved nanotube when the harmonic excitation is applied to the system [81]. The periodic doubling which turned to chaotic behavior where found in the system due to the nonlinear terms that were caused by the curved configuration of the nanotube [81]. In another paper, the vibration characteristics of a fluid-conveying nanotube with a curved longitudinal shape was investigated [82]. This work studied the effects of circular shape associated with the fluid flow on the system natural frequency and the stability of the structure were analyzed and it was shown that the stability is very dependent to the presence of curvature [82]. Lee and Chang considered the non-uniformity on the cross section of a nanotube using the nanocantilever beam model [83]. The sensitivity of system parameter to the non-uniform shape and small scale parameter were investigated by finding the frequency-amplitude relations of the structure free vibration [83]. In a very interesting research, the effect of wavy nanotube on the stress transfer of

single-walled carbon nanotube reinforced polymer composites was taken into the account [84]. This model provided a prediction for axial and interfacial shear stresses along a curved nanotube embedded in a matrix [84]. This work showed that value of maximum interfacial shear stress is increasingly related to the nanotube wavelength unlike the axial one [84]. Effect of initially curved nanotube on the natural frequencies and mode shapes of nanotube based actuators were analyzed by Ouakad and Younis [85]. They found the natural frequency numerically for various system parameters to show the critical impact of structure shape on the stability and natural frequencies of the system [85]. In a recent research a unified approach is developed to model the vibration of curved nanotubes by mean of Non-Uniform Rational B-Spline method (NURBS) [8]. In in that study a variety of curvatures that might be seen in the nanotube structures were considered and effects of shape waviness on the frequency responses were carried out [8]. Saadatnia, et al. employed the idea of previous work to investigate the vibration of fluid-conveying nanotube with quadratic curvature [86]. They found that the system nonlinear behavior including softening and hardening is remarkably related to the curvature waviness [86].

2.4. VIBRATION OF PIEZOELECTRIC-BASED MICRO/NANO STRUCTURES

The superior properties of piezoelectric materials and their significant application in small scale electromechanical structures have attracted the scientists to investigate the dynamics and vibrational behaviors of piezoelectric-based nanostructures. As examples, Yan and Jiang investigated the vibrational and buckling behaviors of piezoelectric nanobeams [87]. In that study, the surfaces effects including residual surface stress, surface

elasticity and surface piezoelectricity where taken into the account they found that the resonant frequencies and stability of the structure is very dependent on these effects [87]. They could tune the resonant frequency by adjusting the applied voltage for zirconate titanate material PZT-5H [87]. The vibrational behaviour of zinc oxide- carbon nanotubes were studied as pressure stress sensors by Wang and Chew [88]. This structures have been fabricated by coating the piezoelectric material on the nanotube and linear assumptions were developed for modeling the corresponding vibration [88]. The dependency of system frequency to the applied pressure were analyzed and a linear elation were observed between the two parameters [88]. Ke, et al. applied nonlocal theory to model the nonlinear vibration of piezoelectric nanobeams considering Timoshenko beam theory [89]. Effects of applied voltages and uniform temperature were added to the system. The free vibration of proposed model were taken into the account and differential quadrature method were implemented to solve it and to find the natural frequencies and mode shapes [89]. It was shown that the system behavior and the frequency ratio is dependent to the small scale parameter and increase on the applied temperature would lead to higher frequencies [89]. It was shown that for piezoelectric material PZT-4, the change of voltage amplitude from positive to negative values would decrease the frequency ratio and the system responses are very sensitive to the type of boundary conditions [89]. Thermoelectric mechanical vibration of piezoelectric nanobeams were investigated by Ke and Wang using Eringen's Nonlocal theory [69]. The differential quadrature method were used as previous work to find the frequencies and mode shapes and the thermoelectric- mechanical loading sensitivity were evaluated for the system responses [69]. It was shown that the electric loading is further effective that the thermal one on the system natural frequencies [69]. In another work, the

Boron-Nitrate nanotubes and PVDF material for piezoelectric fiber reinforced composites were taken into the account and effect of fluid motion on the vibration of reinforced structure were analyzed [90]. Therefore, the nonlinear Donnell's shell theory was associated with nonlocal theory as well as energy methods to establish the governing equations of motion [90]. Effect of fluid flow on the system natural frequency were fully investigated and it was shown how the increase on the fluid velocity would lead to the system instability [90]. It was also observed that the orientation of Boron-Nitrate nanotubes as piezoelectric fibers inside the composite structure is remarkably effective on the vibration behaviour of the developed model [90]. Large vibration of a composite structure reinforced by nanotubes and having two piezoelectric layers on top and bottom were investigated [91]. Effects of the nanotubes distributions inside the structure namely uniform distribution and functionally graded distribution were investigated linear and nonlinear frequencies of the proposed model were calculated for different configurations [91]. The important results for their model was the smaller impact of applied voltage on the frequencies of the systems unlike other models [91]. It was also seen that the functionally graded reinforcement is very influencing on the nonlinearity of the structure [91]. Torsional buckling behaviour of a double-walled Boron-Nitrate nanotube a as piezoelectric structure were studied using nonlocal elasticity and piezoelectricity theories [92]. The structure was modeled as a cylindrical shell embedded in a Winkler-Pasternak foundation and the energy method were employed to obtain the governing equations of the system [92]. It was concluded that the buckling loads are sensitive to the small scale parameter, temperature change and foundation characteristics of the developed model [92]. Free vibration of piezoelectric-layered nanobeam considering surface effect were

published [93]. The Jaconi elliptic functions were implemented to find the exact relations of nonlinear natural frequency for the system and the obtained expressions were numerically examined [93]. It was revealed that the sign and amplitude of applied voltage to the piezoelectric layer has significant impact on the system frequencies [93]. Also, the influence of surface effects and the nanobeam material such as aluminum and silicon on the frequencies were tested and it was found that the aluminum nanobeam is more sensitive to the surface effects [93]. In a very recent research, the application of vibrating piezoelectric ultrathin films for detecting very small masses were studied [94]. the structure were considered to be under thermo-electro-mechanical loads and the nonlocal elasticity theory were taken for the systems development [94]. Two types of formations including single layer and double layer nanofilms were modeled for the proposed mass detection system and the Winkler foundation were added to the system [94]. A parameter study were carried out for the small mass, applied voltage, small scale nonlocal parameter and the frequency shift were noticeably observed by changing those parameters [94].

2.5. THESIS MOTIVATION

The importance of studying nanotubes vibrations, especially piezoelectric-layered nanotubes is obvious as observed in some examples presented in previous sections. However, different considerations have not been taken in some recent researches yet. In some papers, the effect of small scale structure is neglected which may reduce the accuracy of obtained solutions comparing to the real model responses. In some other studies, the effect of nonlinearity has not been taken into the account due to the complexity that this effect may bring into the system model. The forced vibration of aforementioned structures

is another essential issues which has been found in few research articles. Also, in a number of problems including piezoelectric layer, a constant applied voltage has been taken and its effect on the natural frequency has been studied. More specifically, the various resonance cases which may occur to the system due to the external loads as well as variable voltage have not been considered in several current researches.

Therefore, in the present work four models of nanotube vibrations associated with intermediate mass, piezoelectric layer, fluid flow and planer curvature are developed. In all models, effect of small scale size is embedded by employing Eringen's nonlocal theory. Also, various nonlinearities are added to the systems models due to presence of suggested assumptions such as large vibration and structure curvature. In addition, different excitations are considered for the models such as single frequency, multi-frequency and parametric excitations. Both constant and variable voltages effects are evaluated for the piezoelectric-layered structures and a variety of resonance cases are taken into the account and solved for the developed structures vibrations.

2.6. THESIS OUTLINE

This work presents four models of nanotube-bases structures from Chapters three to six. In Chapter three, nonlinear vibration of a nanotube carrying an intermediate mass is modeled. Galerkin method is applied for two-mode vibration. Then, the multiple scales method is employed to solve the obtained equations. Effects of different parameters such as intermediate mass, nonlocal parameter, applied load on the system vibration responses are represented and discussed in details.

In Chapter four, transverse vibration of a nanotube having a slender piezoelectric layer on the nanotube is modeled. The Galerkin and the multiple scales methods are implemented to find the system solutions. Two cases of forced vibration including single frequency and multi-frequency excitations are taken and various resonance cases such as simultaneous combination resonances are analyzed. The influence of non-local effect, applied voltage, piezoelectric thickness are studied in the frequency responses.

Chapter five is dedicated to investigating the vibration of piezoelectric-layered nanotube containing a fluid flow. The governing equations of motion considering the fluid-structure interaction are derived and solved by means of Galerkin method and multiple scales method. The applied voltage is taken to be both constant and harmonic and the fluid is assumed to have constant velocity. The primary, parametric and the simultaneous resonances are taken into account for the system. Obtained solutions are examined for different parameters such as applied voltage, fluid velocity, and piezoelectric thickness.

The last developed model in Chapter six represents the transverse vibration of a curved piezoelectric nanotube. Accordingly, the governing equations of the proposed system is obtained considering a general two dimensional curvature along the structure. The system frequency-amplitude relationships are carried out for various curvature shapes and the responses are plotted for primary and parametric resonances. The influence of non-local parameter, voltage amplitude, piezoelectric thickness on the response curves are studied.

It should be added that in the final Chapter i.e. Chapter seven, a summary of all presented works are provided for each developed model and some interesting ideas are suggested in order to carry on future researches.

Chapter 3: **Vibration of beam-model nanotubes carrying intermediate mass**

3.1. INTRODUCTION

In this Chapter vibrations of a carbon nanotube carrying an intermediate mass along it is investigated. For this purpose, the mathematical models for the transversal vibration of the system are obtained by applying the Euler-Bernoulli beam theory, Energy method, Hamiltonian principle and the non-local theories. Accordingly, the governing equations for the stress, strain, displacement, moment of inertia, shear force and so on are employed to construct the required terms for the kinetic and potential energies and external work and then the Lagrangian formula is implemented and combined with Eringen's non-classical theories. Obtained equation generally includes the effect of external excitation and important nonlinear terms. To solve the obtained equation and to find the system responses in various cases, the Galerkin method is utilized to discretize the corresponding partial differential equation and consequently the nonlinear differential equation of motion governing to the system time response is achieved using the orthogonality of normal modes. In next step, a strong perturbation technique known as Multiple Scales Method is implemented to solve the aforementioned equation. Various important cases for different boundary conditions including free and forced vibrations, internal and external resonances

are considered in this study. For the free vibration, the effect of external excitation are eliminated from the problem and the system response and also the nonlinear frequency of the system are obtained in analytical form. For the force vibration and by considering external harmonic excitation, the structure frequency responses considering important resonance cases are analytically found and the system motions are investigated.

Finally, the obtained solutions are evaluated for various numerical cases and the results are discussed by having a parameter study for the system.

3.2. MATHEMATICAL MODELING

The aim of this section is to obtain the governing equation of motion for the vibration of proposed model as shown in Figure 3-1. Based on the Euler-Bernoulli beam theory, the two dimensional displacement field is written as[76]

$$w(x,z,t) = w(x,t) \tag{3.1}$$

$$u(x,z,t) = u(x,t) - z\frac{\partial w}{\partial x} \tag{3.2}$$

where w and u represent the transverse and longitudinal displacements, respectively. Accordingly, the von Karman strain is developed as [37]

$$\varepsilon_{xx} = \varepsilon_0 + u_x(x,t) - zw_{xx}(x,t) + \frac{1}{2}(w_x(x,t))^2 \tag{3.3}$$

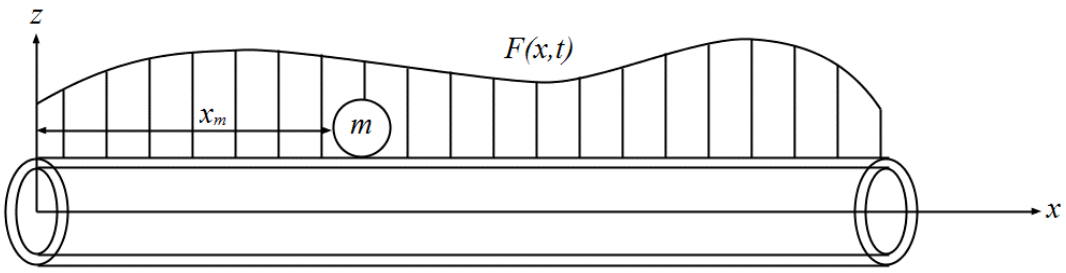

Figure 3-1 Schematic model of the nanotube carrying an intermediate mass.

where $\varepsilon_0 = P/EA$ denotes the initial strain due to the presence of the axial load P [95].

Also, the bending moment $\overline{M}$ and shear force $\overline{N}$ along the beam are as the following general formula

$$\overline{M} = \int_A z.s_{xx} dA,\ \overline{N} = \int_A s_{xx} dA, \tag{3.4}$$

in which A shows the cross section of the nanotube. To find the governing equation, the energy method and Hamiltonian principle are applied here. Accordingly, the Lagrangian function of the system is constructed as

$$L = T - U - W, \tag{3.5}$$

which T, U and W are represented the kinetic energy, potential energy and the external force work, respectively. Using the variational approach, the variation of the Lagrangian function in a period of time would be zero and consequently one can have

$$\delta \int_{t_1}^{t_2} L\, dt = \delta \int_{t_1}^{t_2} T - U - W\, dt = 0 \tag{3.6}$$

The strain energy for an Euler- Bernoulli beam model with the length L is written as

$$U = \int_{\bar{V}} s_{xx}\varepsilon_{xx} d\bar{V} = \int_0^L \int_A s_{xx}\varepsilon_{xx} dA dx \tag{3.7}$$

Applying Eqs. (3.4) and (3.5) into (3.7), leads

$$\begin{aligned} U &= \frac{1}{2}\int_0^L \int_A s_{xx}(\varepsilon_0 + u_x - z w_{xx} + \frac{1}{2} w_x^2)\, dA dx = \\ &\frac{1}{2}\int_0^L EA(\varepsilon_0^2 + 2\varepsilon_0 u_x + \varepsilon_0 w_x^2 + u_x^2 + u_x w_x^2 + \frac{1}{4} w_x^4) + EI w_{xx}^2 dx \end{aligned} \tag{3.8}$$

The variation of the strain energy is obtained as

$$\begin{aligned} &\int_{t_1}^{t_2} \delta U dt = \frac{1}{2}\int_{t_1}^{t_2} \{\int_0^L EA(2\varepsilon_0 \delta u_x + 2\varepsilon_0 w_x \delta w_x + 2u_x \delta u_x + w_x^2 \delta u_x + 2u_x w_x \delta w_x + w_x^3 \delta w_x) \\ &+ 2EI w_{xx} \delta w_{xx} dx\} dt = \frac{1}{2}\int_{t_1}^{t_2} [EA\{2\varepsilon_0 \delta u\Big|_0^L + 2\varepsilon_0 w_x \delta w\Big|_0^L - 2\int_0^L \varepsilon_0 w_{xx} \delta w dx + 2u_x \delta u\Big|_0^L \\ &- 2\int_0^L u_{xx} \delta u dx + w_x^2 \delta u\Big|_0^L - \int_0^L \frac{\partial}{\partial x}(w_x^2)\delta u dx + 2u_x w_x \delta w\Big|_0^L - 2\int_0^L \frac{\partial}{\partial x}(u_x w_x)\delta w dx \\ &+ w_x^3 \delta w\Big|_0^L - \int_0^L \frac{\partial}{\partial x}(w_x^3)\delta w dx\} + 2EI\{w_{xx}\delta w_x\Big|_0^L - w_{xxx}\delta w\Big|_0^L + \int_0^L w_{xxxx}\delta w dx\}]dt \end{aligned} \tag{3.9}$$

Using the boundary conditions properties, either of $\delta u, \delta w, w_x, \delta w_x, w_{xx}, and\ w_{xxx}$ are zero. Thus

$$\begin{aligned} \int_{t_1}^{t_2} \delta U dt = \int_{t_1}^{t_2} [\int_0^L &- EA\{(u_{xx} + w_x w_{xx})\delta u + (\varepsilon_0 w_{xx} + u_{xx} w_x + u_x w_{xx} + \frac{3}{2} w_{xx} w_x^2)\delta w\} dx \\ &+ \int_0^L EI w_{xxxx} \delta w dx] dt \end{aligned} \tag{3.10}$$

The kinetic energy considering the effect of intermediate mass equals to

$$T = \frac{1}{2}\int_0^L \rho A(w_t^2 + u_t^2)\, dx + \frac{1}{2} m(w_t^2 + u_t^2)\Big|_{x_m} \tag{3.11}$$

Where ρ denotes the density of nanotube and m shows the mass of intermediate particle. Note that the effect of rotary inertia is neglected due to the small sizes. The kinetic energy variation equals

$$\int_{t_1}^{t_2} \delta T dt = \int_{t_1}^{t_2} \{ \int_0^L \rho A (w_x \delta w_x + u_x \delta u_x) dx + m(w_x \delta w_x + u_x \delta u_x)\Big|_{x_m} \} dt \tag{3.12}$$

After changing the integration order and applying the integration by parts, one could reach

$$\begin{aligned} \int_{t_1}^{t_2} \delta T dt = \rho A \int_0^L \{ w_x \delta w \Big|_{t_1}^{t_2} - \int_{t_1}^{t_2} w_{tt} \delta w \, dt + u_x \delta u \Big|_{t_1}^{t_2} - \int_{t_1}^{t_2} u_{tt} \delta u \, dt \} dx + m \{ w_x \delta w \Big|_{t_1}^{t_2} \\ - \int_{t_1}^{t_2} w_{tt} \delta w \, dt + u_x \delta u \Big|_{t_1}^{t_2} - \int_{t_1}^{t_2} u_{tt} \delta u \, dt \} \Big|_{x_m} \end{aligned} \tag{3.13}$$

At t_1, t_2 the variations $\delta w, \delta u$ are zero. Hence

$$\int_{t_1}^{t_2} \delta T dt = \int_{t_1}^{t_2} \{ -\rho A \int_0^L (w_{tt} \delta w + u_{tt} \delta u) \, dx - m(w_{tt} \delta w + u_{tt} \delta u)\Big|_{x_m} \} dt \tag{3.14}$$

The external force $F(x,t)$ is considered to be applied in the transverse direction. So the variation of corresponding external work is

$$\int_{t_1}^{t_2} \delta W dt = \int_{t_1}^{t_2} \{ \int_0^L - F(x,t) \delta w \, dx \} dt \tag{3.15}$$

Applying Eqs. (3.10), (3.14) and (3.15) into Eq. (3.6) and factorizing the corresponding terms to δw and δu, and then setting them to zero, yields

$$\begin{aligned} &\delta w [\int_0^L \{ -\rho A w_{tt} + EA(\varepsilon_0 w_{xx} + u_{xx} w_x + u_x w_{xx} + \frac{3}{2} w_{xx} w_x^2) + F(x,t) - EI w_{xxxx} \\ &- m w_{tt} \Delta(x - x_m) \} dx] + \delta u [\int_0^L \{ -\rho A u_{tt} + EA(u_{xx} + w_x w_{xx}) - m u_{tt} \Delta(x - x_m) \} dx] = 0 \end{aligned} \tag{3.16}$$

$$\overline{M}_{xx} = (\rho A + m\Delta(x - x_m)) w_{tt} - EA(\varepsilon_0 w_{xx} + u_{xx} w_x + u_x w_{xx} + \frac{3}{2} w_{xx} w_x^2) - F(x,t) \tag{3.17}$$

Where Δ shows the Dirac function. To insert the effect of small size effect, the nonlocal theory is applied to the bending moment of the system. Accordingly, the following relationship is considered for the bending moment of the system based on the Eringen's theory[32]

$$\overline{M} - (e_0 a)^2 \overline{M}_{xx} = EIw_{xx} \tag{3.18}$$

Where E and I are the respective modulus of elasticity and cross-sectional moment of inertia for the nanotube and $e_0 a$ indicates the nonlocal parameter caused by the small scale of nanotube. Combining equations (3.17) and (3.18) and after some mathematical simplifications, one can find

$$\begin{aligned} &\rho A w_{tt} - EA(u_{xx} w_x + u_x w_{xx} + \frac{3}{2} w_{xx} w_x^2) + P w_{xx} - F(x,t) + m w_{tt} \Delta(x - x_m) + EI w_{xxxx} \\ &= (e_0 a)^2 \frac{\partial^2}{\partial x^2} \{\rho A w_{tt} - EA(u_{xx} w_x + u_x w_{xx} + \frac{3}{2} w_{xx} w_x^2) + P w_{xx} - F(x,t) + m w_{tt} \Delta(x - x_m)\} \end{aligned} \tag{3.19}$$

Above equation which represents the governing equation of motion for the dynamic of proposed system considering nano scale effect can also be written as the following format for further studies in the next section

$$\begin{aligned} &R(x,t) = \rho A w_{tt} - EA(u_{xx} w_x + u_x w_{xx} + \frac{3}{2} w_{xx} w_x^2) + P w_{xx} - F(x,t) + m w_{tt} \Delta(x - x_m) + EI w_{xxxx} \\ &- (e_0 a)^2 \frac{\partial^2}{\partial x^2} \{\rho A w_{tt} - EA(u_{xx} w_x + u_x w_{xx} + \frac{3}{2} w_{xx} w_x^2) + P w_{xx} - F(x,t) + m w_{tt} \Delta(x - x_m)\} = 0 \end{aligned} \tag{3.20}$$

To simplify above equation, one could find a relationship between the longitudinal and transversal displacements. Therefore, the inextensibility of the nanotube is associated with equation and the longitudinal displacement is approximated by the transversal one. Accordingly [95],

$$u \approx -\frac{1}{2}\int_0^x w_x^2 dx + \frac{x}{2L}\int_0^L w_x^2 dx \tag{3.21}$$

For simplicity and facilitating the solution procedure, the following dimensionless parameters are defined and applied into the main partial differential equation and therefore the obtained results and values are expressed in dimensionless form

$$x = L\hat{x},\ t = \tau\hat{t},\ w = L\hat{w},\ \tau = \sqrt{\frac{\rho A L^4}{EI}},\ M = \frac{m}{\rho A L},\ \mu_0 = \frac{e_0 a}{L},\ \hat{P} = \frac{pL^2}{EI} \tag{3.22}$$

3.3. VIBRATION SOLUTION OF NANOTUBE WITH INTERMEDIATE MASS

The Galerkin method is employed to solve the nonlinear partial differential equation obtained in previous section. Based on the concept of this method, the following solution is considered for the transverse vibration of the system

$$\hat{w}(\hat{x},\hat{t}) = \sum_{i=1}^{n} X_i(\hat{x}) Y_i(\hat{t}) \tag{3.23}$$

Where Y_i indicate the time responses and X_i denote the mode shapes of vibration for the nanotube with an intermediate mass which could be obtained from the linear system. The mode shapes of the system for different immovable boundary conditions are given in Table 3-1.

In a number of studies and for simplicity, it is convenient to take the first mode of motion where $i = 1$ in Eq. (3.23). However to find more precise solutions in this study, first and second modes where $i = 1, 2$ in this equation is chosen.

Table 3-1 Mode shape functions for different boundary conditions of a beam[96]

Cases	Mode shape	Value of $B_{i,\ i=1,2}$
Hinged-Hinged	$X_i(\hat{x}) = \sin(B_i\hat{x})$	$B_1 = \pi$ $B_2 = 2\pi$
Clamped-Clamped	$X_i(\hat{x}) = \sinh(B_n\hat{x}) - \sin(B_n\hat{x}) + a_n(\cosh(B_n\hat{x}) - \cos(B_n\hat{x}))$ $a_n = \left(\frac{\sinh(B_n) - \sin(B_n)}{\cos(B_n) - \cosh(B_n)}\right)$	$B_1 = 4.730041$ $B_2 = 7.853205$
Clamped-Hinged	$X_i(\hat{x}) = \sin(B_n\hat{x}) - \sinh(B_n\hat{x}) + a_n(\cosh(B_n\hat{x}) - \cos(B_n\hat{x}))$ $a_n = \left(\frac{\sin(B_n) - \sinh(B_n)}{\cos(B_n) - \cosh(B_n)}\right)$	$B_1 = 3.926602$ $B_2 = 7.068583$

Hence, the solution of Eq. (3.20) is reduced to the following form for any boundary conditions of the beam

$$\hat{w}(\hat{x},\hat{t}) = X_1(\hat{x})Y_1(\hat{t}) + X_2(\hat{x})Y_2(\hat{t}) \tag{3. 24}$$

Substituting above equation into the main equation and using the orthogonally of normal modes as below the governing equations of motion for two modes of nano beam vibration can be derived

$$\int_0^1 R(\hat{x},\hat{t})X_1(\hat{x})d\hat{x} = 0\,,\ \int_0^1 R(\hat{x},\hat{t})X_2(\hat{x})d\hat{x} = 0 \tag{3.25}$$

3.3.1. Clamped-Clamped ends and Hinged-Hinged ends

After some mathematical simplifications and by using the two mode shape functions for the clamped-clamped beam hinged-hinged the governing equations of motion for two modes of nano beam vibration is found in the following nonlinear ordinary coupled forms

$$\begin{cases} \ddot{Y}_1 + \omega_1^2 Y_1 + a_1 Y_1^3 + a_2 Y_1 Y_2^2 = \hat{q}_1(\hat{t}) \\ \ddot{Y}_2 + \omega_2^2 Y_2 + a_3 Y_2^3 + a_4 Y_2 Y_1^2 = \hat{q}_2(\hat{t}) \end{cases} \tag{3. 26}$$

Where expressions for the natural frequencies of each mode $\omega_{i,\, i=1,\, 2}$, the coefficients $a_{j,\, j=1,..,4}$ and forces $\hat{q}_i(\hat{t})_{,\, i=1,\, 2}$ are presented in Appendix *A*. To solve the nonlinear ordinary differential equation of motion seen in Eq. (3.26) and other nonlinear equations in next Chapters, a well-know and strong perturbation technique known as multiple scales method is employed [97]. According to the basic idea of this method, the following time scales are introduced

$$T_n = \varepsilon^n \hat{t},\ n = 0,\, 1,\, 2 \quad or\ T_0 = \hat{t},\, T_1 = \varepsilon \hat{t},\, T_2 = \varepsilon^2 \hat{t}, ... \tag{3.27}$$

where ε is the dimensionless perturbation parameter which is very small. Therefore, the derivatives with respect to the time t becomes

$$\begin{cases} \dfrac{d}{d\hat{t}} = \dfrac{dT_0}{dt}\dfrac{\partial}{\partial T_0} + \dfrac{dT_1}{dt}\dfrac{\partial}{\partial T_1} + ... = D_0 + \varepsilon D_1 + \varepsilon^2 D_2 + ... \\ \dfrac{d^2}{d\hat{t}^2} = D_0^2 + 2\varepsilon D_0 D_1 + \varepsilon^2 (D_1^2 + 2 D_0 D_1) + ... \end{cases} \tag{3.28}$$

Based on the applied method, the solution of problem is approximated as the following series

$$\begin{cases} Y_1 = \varepsilon Y_{11}(T_0, T_2) + \varepsilon^3 Y_{13}(T_0, T_2) + ... \\ Y_2 = \varepsilon Y_{21}(T_0, T_2) + \varepsilon^3 Y_{23}(T_0, T_2) + ... \end{cases} \tag{3.29}$$

To consider the influence of external forces, it is required to order the corresponding terms and consequently one can define $\hat{q}_i = \varepsilon^3 q_i$, $i = 1, 2$ [97]. Substituting aforementioned definitions and equations (3.27) to (3.29) into Eq. (3.26), and then equating the same power coefficient of ε , one can reach

$$\varepsilon : \begin{cases} D_0^2 Y_{11} + \omega_1^2 Y_{11} = 0 \\ D_0^2 Y_{21} + \omega_2^2 Y_{21} = 0 \end{cases} \tag{3.30}$$

and

$$\varepsilon^3 : \begin{cases} D_0^2 Y_{13} + \omega_1^2 Y_{13} = -2D_0 D_1 Y_{11} - \beta_1 Y_{11}^3 - \beta_2 Y_{11} Y_{21}^2 + q_1(T_0) \\ D_0^2 Y_{23} + \omega_2^2 Y_{23} = -2D_0 D_1 Y_{21} - \beta_3 Y_{21}^3 - \beta_4 Y_{21} Y_{11}^2 + q_2(T_0) \end{cases} \tag{3.31}$$

The solution of Eq. (3.30) is expressed as

$$\begin{cases} Y_{11} = A_1(T_2) \exp(i\omega_1 T_0) + C.C \\ Y_{21} = A_2(T_2) \exp(i\omega_2 T_0) + C.C \end{cases} \tag{3.32}$$

Where *C.C* shows the complex conjugate terms. Substituting Eq. (3.32) into (3.31), leads

$$\begin{aligned} D_0^2 Y_{13} + \omega_1^2 Y_{13} = {} & [-2i\omega_1 (A_1' - 3\beta_1 A_1^2 \overline{A}_1 - 2\beta_2 A_2 \overline{A}_2 A_1] . \exp(i\omega_1 T_0) - \beta_1 A_1^3 \exp(3i\omega_1 T_0) \\ & - \beta_2 A_1 A_2^2 \exp[i(\omega_1 + 2\omega_2) T_0] - \beta_2 A_1 \overline{A}_2^2 \exp[i(\omega_1 - 2\omega_2) T_0] + q_1(T_0) + C.C \end{aligned} \tag{3.33}$$

$$\begin{aligned} D_0^2 Y_{23} + \omega_2^2 Y_{23} = {} & [-2i\omega_2 A_2' - 3\beta_3 A_2^2 \overline{A}_2 - 2\beta_4 A_1 \overline{A}_1 A_2] . \exp(i\omega_2 T_0) - \beta_3 A_2^3 \exp(3i\omega_2 T_0) \\ & - \beta_4 A_2 A_1^2 \exp[i(\omega_2 + 2\omega_1) T_0] - \beta_4 A_2 \overline{A}_1^2 \exp[i(\omega_2 - 2\omega_1) T_0] + q_2(T_0) + C.C \end{aligned} \tag{3.34}$$

As seen from above equations, no internal resonances occurs in the system and the steady state motion in the forced vibration would be uncoupled which will be further discussed in the future. Let investigate the system free vibration first, which is important for finding the system natural frequencies, and then study the forced vibration in the next step.

- *Free vibration*

The aim of this section is to investigate the behavior of the system when it is freely vibrated. Accordingly, it is assumed that no external excitation is applied to the nanotube and consequently $F(x,t)$ and the corresponding terms become zero. The secular terms of above equations should be eliminated from its particular solution[97]. So the coefficients of $\exp(i\omega_j T_0), j=1,2$ are set to be zero as

$$\begin{cases} -2i\omega_1 A_1' - 3a_1 A_1^2 \overline{A}_1 - 2a_2 A_2 \overline{A}_2 A_1 = 0 \\ -2i\omega_2 A_2' - 3a_3 A_2^2 \overline{A}_2 - 2a_4 A_1 \overline{A}_1 A_2 = 0 \end{cases} \tag{3.35}$$

Now the polar representation $A_j = \frac{1}{2}\alpha_j \exp(i\theta_j)$ is utilized where α_j and θ_j are real. Substituting this definition into Eq. (3.35) and separating real and imaginary parts

$$\begin{cases} \omega_1 \alpha_1' = 0, \; -\omega_1 \alpha_1 \theta_1' + \frac{3a_1}{8}\alpha_1^3 + \frac{a_2}{4}\alpha_2^2 \alpha_1 = 0 \\ \omega_2 \alpha_2' = 0, \; -\omega_2 \alpha_2 \theta_2' + \frac{3a_2}{8}\alpha_2^3 + \frac{a_4}{4}\alpha_1^2 \alpha_2 = 0 \end{cases} \tag{3.36}$$

So $\alpha_j = \alpha_{0j}$ are constant and

$$\begin{cases} \theta_1 = (\frac{3a_1\alpha_{01}^2 + 2a_2\alpha_{02}^2}{8\omega_1})T_2 + \theta_{01} \\ \theta_2 = (\frac{3a_3\alpha_{02}^2 + 2a_4\alpha_{01}^2}{8\omega_2})T_2 + \theta_{02} \end{cases} \tag{3.37}$$

Where α_{0j} and θ_{0j} are constant to be obtained from the initial conditions. Thus,

$$\begin{cases} A_1(T_2) = \frac{1}{2}\alpha_{01}\exp[i((\frac{3a_1\alpha_{01}^2 + 2a_2\alpha_{02}^2}{8\omega_1})T_2 + \theta_{01})] \\ A_{21}(T_2) = \frac{1}{2}\alpha_{02}\exp[i((\frac{3a_3\alpha_{02}^2 + 2a_4\alpha_{01}^2}{8\omega_2})T_2 + \theta_{02})] \end{cases} \tag{3.38}$$

Substituting above equation into Eq. (3.38), finally the approximate solution for the structure free vibration is obtained as

$$\begin{cases} Y_1(\hat{t}) = \alpha_{01}\cos(\omega_1\hat{t} + \theta_{01}) + O(\varepsilon^3) \\ Y_2(\hat{t}) = \alpha_{02}\cos(\omega_2\hat{t} + \theta_{02}) + O(\varepsilon^3) \end{cases} \tag{3.39}$$

Where $O(\varepsilon^3)$ shows the higher order terms and the approximate nonlinear natural frequencies $\hat{\omega}_j$ equal

$$\begin{cases} \hat{\omega}_1 = \omega_1[1 + (\frac{3a_1\alpha_{01}^2 + 2\,a_2\alpha_{02}^2}{8\omega_1^2})] + O(\varepsilon^3) \\ \hat{\omega}_2 = \omega_2[1 + (\frac{3a_3\alpha_{02}^2 + 2\,a_4\alpha_{01}^2}{8\omega_2^2})] + O(\varepsilon^3) \end{cases} \tag{3.40}$$

- *Forced Vibration*

To analyse the force vibration of the structure, an external excitation is considered to be applied to the system. The proposed expression used for this purpose is written as

$$F(\hat{x},\hat{t}) = F_0\cos(\Omega\hat{t})\Delta(\hat{x} - \hat{x}_0) \tag{3.41}$$

This equation represents that a harmonic point load with the dimensionless amplitude F_0 and frequency Ω is applied to the nanotube at an arbitrary distance $\hat{x}_0$ along the structure using the Dirac function Δ. This load is taken as a common type of excitation having different applications in the forced vibration of such systems. Thus, by means of the

integrations provided in the Appendix *A*, the components of the applied forces for each modes can be obtained. In the forced vibration analysis of such systems using multiple scales method, it is convenient to add a small damping parameter $\varepsilon^2\mu$ into the both equations of the modes vibration [97]. So, by considering the applied force and aforementioned definition, equations (3.33) and (3.34) becomes

$$\begin{aligned} &D_0^2 Y_{13} + \omega_1^2 Y_{13} = [-2i\omega_1(A_1' + \mu A_1) - 3\beta_1 A_1^2 \overline{A}_1 - 2\beta_2 A_2 \overline{A}_2 A_1].\exp(i\omega_1 T_0) - \beta_1 A_1^3 \exp(3i\omega_1 T_0) \\ &- \beta_2 A_1 A_2^2 \exp[i(\omega_1 + 2\omega_2)T_0] - \beta_2 A_1 \overline{A}_2^2 \exp[i(\omega_1 - 2\omega_2)T_0] + \frac{1}{2} q_1 \exp(i\Omega T_0) + C.C \end{aligned} \tag{3.42}$$

$$\begin{aligned} &D_0^2 Y_{23} + \omega_2^2 Y_{23} = [-2i\omega_2(A_2' + \mu A_2) - 3\beta_3 A_2^2 \overline{A}_2 - 2\beta_4 A_1 \overline{A}_1 A_2].\exp(i\omega_2 T_0) - \beta_3 A_2^3 \exp(3i\omega_2 T_0) \\ &- \beta_4 A_2 A_1^2 \exp[i(\omega_2 + 2\omega_1)T_0] - \beta_4 A_2 \overline{A}_1^2 \exp[i(\omega_2 - 2\omega_1)T_0] + \frac{1}{2} q_2 \exp(i\Omega T_0) + C.C \end{aligned} \tag{3.43}$$

Now, two cases of external resonances are investigated for the vibration of nano beam. In the first case it is assumed that the frequency of external excitation Ω is close the natural frequency of the first mode i.e. $\Omega \approx \omega_1$. However for the second case $\Omega \approx \omega_2$ is considered. For the first case one can write

$$\Omega = \omega_1 + \varepsilon\sigma \tag{3.44}$$

In which σ shows the detuning parameter. Applying Eq. (3.44) into equations (3.42) and (3.43), and then by eliminating the secular terms, yields

$$\begin{cases} -2i\omega_1(A_1' + \mu A_1) - 3a_1 A_1^2 \overline{A}_1 - 2a_2 A_2 \overline{A}_2 A_1 + \frac{1}{2} q_1 \exp(i\sigma T_0) = 0 \\ -2i\omega_2(A_2' + \mu A_2) - 3a_3 A_2^2 \overline{A}_2 - 2a_4 A_1 \overline{A}_1 A_2 = 0 \end{cases} \tag{3.45}$$

Using the polar form A_j as before, substituting into Eq. (3.45) and separating real and imaginary parts, leads

$$\begin{cases} \sigma\omega_1\alpha_1 - \frac{3}{8}a_1\alpha_1^3 - \frac{1}{4}a_2\alpha_1\alpha_2^2 + \frac{1}{2}q_1\cos\gamma_1 = 0 \\ -\omega_1\alpha_1' - \mu\omega_1\alpha_1 + \frac{1}{2}q_{01}\sin\gamma_1 = 0 \\ \theta_2'\omega_2\alpha_2 - \frac{3}{8}a_3\alpha_2^3 - \frac{1}{4}a_4\alpha_2\alpha_1^2 = 0 \\ -\omega_2\alpha_2' - \mu\omega_2\alpha_2 = 0 \end{cases} \tag{3.46}$$

Where $\gamma_1 = \sigma T_0 - \theta_1$. Thus, the approximate solutions of the problem are obtained as

$$Y_{0j}(t) = \alpha_j \cos(\omega_j t + \theta_j) + O(\varepsilon^3) \tag{3.47}$$

in which α_j and θ_j are obtained by general solutions of the system of equations shown in Eq. (3.47). The steady state motion leads when [97] $a'_{i,i=1,2} = \gamma_1' = \theta_2' = 0$ and therefore, after some mathematical simplifications, one can find

$$\sigma = \left(\frac{3}{8}a_1\alpha_1^3 + \frac{1}{4}a_2\alpha_1\alpha_2^2 \pm (\frac{1}{4}q_1{}^2 - (\mu\omega_1\alpha_1)^2)^{1/2}\right) \Big/ (\omega_1\alpha_1),\ \alpha_2 = 0 \tag{3.48}$$

Above equation is known as the frequency-amplitude relationship, and finally, the approximate solution of steady state motion for the forced vibration of the first mode of proposed system considering resonance case is

$$Y_1(t) = \alpha_1 \cos(\Omega t - \gamma_1) + O(\varepsilon^3) \tag{3.49}$$

For the second resonance case the same manner as above could be applied.

Here, one can have

$$\Omega = \omega_2 + \varepsilon\sigma \tag{3.50}$$

Therefore, the secular terms are:

$$\begin{cases} -2i\omega_1(A_1' + \mu A_1) - 3a_1 A_1^2 \overline{A}_1 - 2a_2 A_2 \overline{A}_2 A_1 \\ -2i\omega_2(A_2' + \mu A_2) - 3a_3 A_2^2 \overline{A}_2 - 2a_4 A_1 \overline{A}_1 A_2 + \frac{1}{2} q_2 \exp(i\sigma T_0) = 0 \end{cases} \tag{3.51}$$

Therefore, in a similar way by using the polar notations and performing mathematical processes, the response of the steady state condition is achieved as

$$\sigma = \left(\frac{3}{8} a_3 \alpha_2^3 + \frac{1}{4} a_4 \alpha_2 \alpha_1^2 \pm (\frac{1}{4} {q_2}^2 - (\mu\omega_2\alpha_2)^2)^{1/2} \right) \Big/ (\omega_2 \alpha_2), \ \alpha_1 = 0 \tag{3.52}$$

3.3.1. Clamped -Hinged ends

Here by applying the two mode shape functions for the clamped-hinged the governing equations of motion for two modes of nano beam vibration is obtained as

$$\begin{cases} \ddot{Y}_1 + \omega_1^2 Y_1 + a_1 Y_1^3 + a_2 Y_1 Y_2^2 + b_1 Y_2 Y_1^2 + b_2 Y_2^3 = \hat{q}_1(\hat{t}) \\ \ddot{Y}_2 + \omega_2^2 Y_2 + a_3 Y_2^3 + a_4 Y_2 Y_1^2 + b_3 Y_1 Y_2^2 + b_4 Y_1^3 = \hat{q}_2(\hat{t}) \end{cases} \tag{3. 53}$$

Where the relations of the natural frequencies of each modes $\omega_{i,i=1,2}$, the coefficients $a_j, b_j, \ j = 1,...4$ and forces $\hat{q}_i(\hat{t})_{,i=1,2}$ are represented in Appendix *A* as before. Again the multiple scales method is utilized here. Using the same approximations for the solutions, ordering the forces and then equating the same power coefficient of ε, one can get

$$\varepsilon: \begin{cases} D_0^2 Y_{11} + \omega_1^2 Y_{11} = 0 \\ D_0^2 Y_{21} + \omega_2^2 Y_{21} = 0 \end{cases} \tag{3.54}$$

and

$$\varepsilon^3: \begin{cases} D_0^2 Y_{13} + \omega_1^2 Y_{13} = -2D_0(D_1 Y_{11} + \mu Y_{11}) - a_1 Y_{11}^3 - a_2 Y_{11} Y_{21}^2 - b_1 Y_{21} Y_{11}^2 - b_2 Y_{21}^3 + q_1(T_0) \\ D_0^2 Y_{23} + \omega_2^2 Y_{23} = -2D_0(D_1 Y_{21} + \mu Y_{21}) - a_3 Y_{21}^3 - a_4 Y_{21} Y_{11}^2 - b_3 Y_{11} Y_{21}^2 - b_4 Y_{11}^3 + q_2(T_0) \end{cases} \tag{3.55}$$

Substituting functions of Eq. (3.32) into (3.55), gives

$$
\begin{aligned}
&D_0^2 Y_{13} + \omega_1^2 Y_{13} = [-2i\omega_1(A_1' + \mu A_1) - 3a_1 A_1^2 \overline{A}_1 - 2a_2 A_2 \overline{A}_2 A_1].\exp(i\omega_1 T_0) - a_1 A_1^3 \exp(3i\omega_1 T_0) \\
&- a_2 A_1 A_2^2 \exp[i(\omega_1 + 2\omega_2)T_0] - a_2 A_1 \overline{A}_2^2 \exp[i(\omega_1 - 2\omega_2)T_0] \\
&- b_1 A_2 A_1^2 \exp[i(\omega_2 + 2\omega_1)T_0] - b_1 A_2 \overline{A}_1^2 \exp[i(\omega_2 - 2\omega_1)T_0] \\
&- b_2 A_2^3 \exp(3i\omega_2 T_0) - 3b_2 A_2^2 \overline{A}_2 \exp(i\omega_2 T_0) + q_1(T_0) + C.C
\end{aligned} \tag{3.56}
$$

$$
\begin{aligned}
&D_0^2 Y_{23} + \omega_2^2 Y_{23} = [-2i\omega_2(A_2' + \mu A_2) - 3a_3 A_2^2 \overline{A}_2 - 2a_4 A_1 \overline{A}_1 A_2].\exp(i\omega_2 T_0) - a_3 A_2^3 \exp(3i\omega_2 T_0) \\
&- a_4 A_2 A_1^2 \exp[i(\omega_2 + 2\omega_1)T_0] - a_4 A_2 \overline{A}_1^2 \exp[i(\omega_2 - 2\omega_1)T_0] \\
&- b_3 A_1 A_2^2 \exp[i(\omega_1 + 2\omega_2)T_0] - b_3 A_1 \overline{A}_2^2 \exp[i(\omega_1 - 2\omega_2)T_0] \\
&- b_4 A_1^3 \exp(3i\omega_1 T_0) - 3b_4 A_1^2 \overline{A}_1 \exp(i\omega_1 T_0) + q_2(T_0) + C.C
\end{aligned} \tag{3.57}
$$

Here, the internal resonance may occur in the system and due to the type of cubic nonlinearity this may be seen when $\omega_2 \approx 3\omega_1$. Without considering this case, the system solution would be same as previous resonance case. Also, the free vibration would be similar as well. Now, for more analysis in the proposed system let consider the internal-external resonance when a force is applied to the structure as taken in previous section. Accordingly, the detuning parameter of internal resonance is defined as

$$\omega_2 = 3\omega_1 + \varepsilon^2 \sigma_1 \tag{3.58}$$

Now two external resonances are investigated as explained below for the forced vibration of the system. For the first case, the resonance of the first mode is taken into the account and one could write

- Case *A* when $\Omega \approx \omega_1 \Rightarrow \Omega = \omega_1 + \varepsilon^2 \sigma_2$

Considering this external resonance case associated with the internal one, the secular terms of equations (3.56) and (3.57) become

$$-2i\omega_1(A_1' + \mu A_1) - 3a_1 A_1^2 \overline{A}_1 - 2a_2 A_2 \overline{A}_2 A_1 - b_1 A_2 \overline{A}_1^2 \exp(i\sigma_1 T_2) + \frac{1}{2} q_1 \exp(i\sigma_2 T_2) \tag{3.59}$$

$$-2i\omega_2(A_2' + \mu A_2) - 3a_3 A_2^2 \overline{A}_2 - 2a_4 A_1 \overline{A}_1 A_2 - b_4 A_1^3 \exp(-i\sigma T_2) \tag{3.60}$$

Applying the polar notation for A_j as before and separating the real and imaginary parts, yields,

$$\begin{cases} 8\theta_1'\omega_1\alpha_1 - 3a_1\alpha_1^3 - 2a_2\alpha_1\alpha_2^2 - b_1\alpha_2\alpha_1^2\cos\gamma_1 + 4q_1\cos\gamma_2 = 0 \\ 8\omega_1(\alpha_1' + \mu\alpha_1) + b_1\alpha_1^2\alpha_2\sin\gamma_1 - 4q_1\sin\gamma_2 = 0 \\ 8\theta_2'\omega_2\alpha_2 - 3a_3\alpha_2^3 - 2a_4\alpha_2\alpha_1^2 - b_4\alpha_1^3\cos\gamma_1 = 0 \\ 8\omega_2(\alpha_2' + \mu\alpha_2) - b_4\alpha_1^3\sin\gamma_1 = 0 \end{cases} \tag{3.61}$$

where $\gamma_1 = \sigma_1 T_2 + \theta_2 - 3\theta_1$, $\gamma_2 = \sigma_2 T_2 - \theta_1$. So the general solution of above system for would lead to the resonances of the considered case. Also by considering $\gamma_j = \alpha_j = 0$, the steady state motion can be obtained by the following sets of equations

$$\begin{cases} 8\sigma_2\omega_1\alpha_1 - 3a_1\alpha_1^3 - 2a_2\alpha_1\alpha_2^2 - b_1\alpha_2\alpha_1^2\cos\gamma_1 + 4q_1\cos\gamma_2 = 0 \\ 8\omega_1\mu\alpha_1 + b_1\alpha_1^2\alpha_2\sin\gamma_1 - 4q_1\sin\gamma_2 = 0 \\ 8(3\sigma_2 - \sigma_1)\omega_2\alpha_2 - 3a_3\alpha_2^3 - 2a_4\alpha_2\alpha_1^2 - b_4\alpha_1^3\cos\gamma_1 = 0 \\ 8\omega_2\mu\alpha_2 - b_4\alpha_1^3\sin\gamma_1 = 0 \end{cases} \tag{3.62}$$

- Case *B* when $\Omega \approx \omega_2 \Rightarrow \Omega = \omega_2 + \varepsilon^2\sigma_2$

For this case which shows the effect of external resonance on the second mode, the secular terms of equations (3.56) and (3.57), are found as

$$-2i\omega_1(A_1' + \mu A_1) - 3a_1A_1^2\bar{A}_1 - 2a_2A_2\bar{A}_2A_1 - b_1A_2\bar{A}_1^2\exp(i\sigma_1T_2) \tag{3.63}$$

$$-2i\omega_2(A_2' + \mu A_2) - 3a_3A_2^2\bar{A}_2 - 2a_4A_1\bar{A}_1A_2 - b_4A_1^3\exp(-i\sigma_1T_2) + \frac{1}{2}q_2\exp(i\sigma_2T_2) \tag{3.64}$$

Defining $\gamma_1 = \sigma_1T_2 - 3\theta_1 + \theta_2, \gamma_2 = \sigma_2T_2 - \theta_2$, by the similar procedure the responses of the system modes can be found by the following system of equations

$$\begin{cases} 8\theta_2'\omega_2\alpha_2 - 3a_3\alpha_2^3 - 2a_4\alpha_2\alpha_1^2 - b_4\alpha_1^3\cos\gamma_1 + 4q_2\cos\gamma_2 = 0 \\ 8\omega_2(\alpha_2' + \mu\alpha_2) - b_4\alpha_1^3\sin\gamma_1 - 4q_2\sin\gamma_2 = 0 \\ 8\theta_1'\omega_1\alpha_1 - 3a_1\alpha_1^3 - 2a_2\alpha_1\alpha_2^2 - b_1\alpha_2\alpha_1^2\cos\gamma_1 = 0 \\ 8\omega_1(\alpha_1' + \mu\alpha_1) + b_1\alpha_2\alpha_1^2\sin\gamma_1 = 0 \end{cases} \tag{3.65}$$

Finally, the steady-state motion is found for $\gamma_j = \alpha_j = 0$ as done in the previous case

$$\begin{cases} 8\sigma_2\omega_2\alpha_2 - 3a_3\alpha_2^3 - 2a_4\alpha_2\alpha_1^2 - b_4\alpha_1^3\cos\gamma_1 + 4q_2\cos\gamma_2 = 0 \\ 8\omega_2\mu\alpha_2 - b_4\alpha_1^3\sin\gamma_1 - 4q_2\sin\gamma_2 = 0 \\ \frac{8}{3}(\sigma_2 + \sigma_1)\omega_1\alpha_1 - 3a_1\alpha_1^3 - 2a_2\alpha_1\alpha_2^2 - b_1\alpha_2\alpha_1^2\cos\gamma_1 = 0 \\ 8\omega_1\mu\alpha_1 + b_1\alpha_2\alpha_1^2\sin\gamma_1 = 0 \end{cases} \tag{3.66}$$

Thus, a variety of cases in terms of the boundary conditions, free and forced vibrations, internal resonance, external resonance and the steady-state motions in detailed analytical forms were investigated.

3.4. RESULTS AND DISCUSSION

In this section the obtained solutions for the system responses is calculated for various numerical cases and effects of different physical and geometrical parameters on the vibrational behavior of the proposed structure is investigated. According to the mechanical properties of carbon nanotubes and based on the literature of the work, the following values and intervals are chosen for the system parameters [8]. For the free vibration, the frequency ratio, which is the ratio of nonlinear frequency to the linear frequency, is an important parameter is investigated for different cases. This parameter shows how the initial condition influences the frequency behavior of the system for the nonlinear systems unlike

linear once which are independent from it. Also, for the forced vibration, the frequency-amplitude response of the system is analyzed for different resonance cases.

Table 3-2 Physical and geometrical properties of the structure

Parameter	Value (unit)
E	$1-1.2(GPa)$
ρ	$1-2.3(g/cm^3)$
L	$10-100\,nm$
R (inner or outer radius)	$0.5-5\,nm$

The effects of external load, surface parameter, and the intermediate mass on the steady-state motion response of the Hinged-Hinged, Clamped-Clamped and Clamped-Hinged boundary conditions are investigated and presented in the Figures 3-2 to 3-5.

Figures 3-2 and 3-3 show the effect of initial amplitude on the frequency ratio of first mode and second mode of vibration, respectively. As seen, this parameter is very dependent on the initial condition for both cases. Also, effect of the initial condition of one mode on the frequency ratio of the other mode has been represented in which the increase of that parameter would lead to the increase of the ratio for both modes. However, the first mode is more sensitive rather than the second one. Figures 3-4 and 3-5 depict the impact of small scale parameter on the frequency ratio of both modes. The growth on the value of this parameter would enhance the frequency ratio. Comparing the results with the case that this parameter is zero corresponding to classical theories, reveals that small scale parameter is very important and should be taken into the account for vibration modeling and frequency analysis of such nano structures.

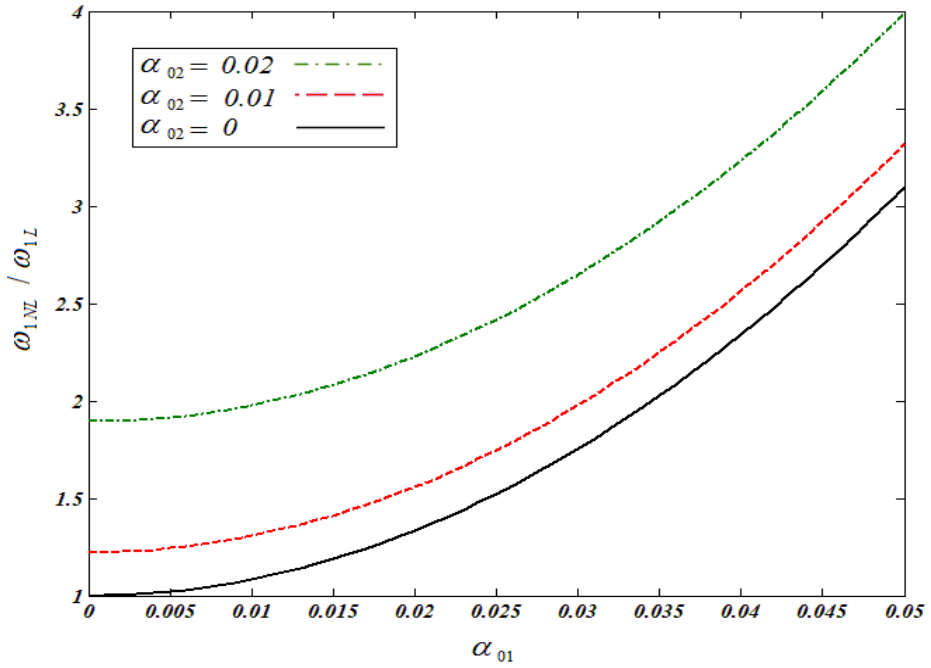

Figure 3-2 Variation of first mode frequency ratio for initial conditions, α_{01} and α_{02}

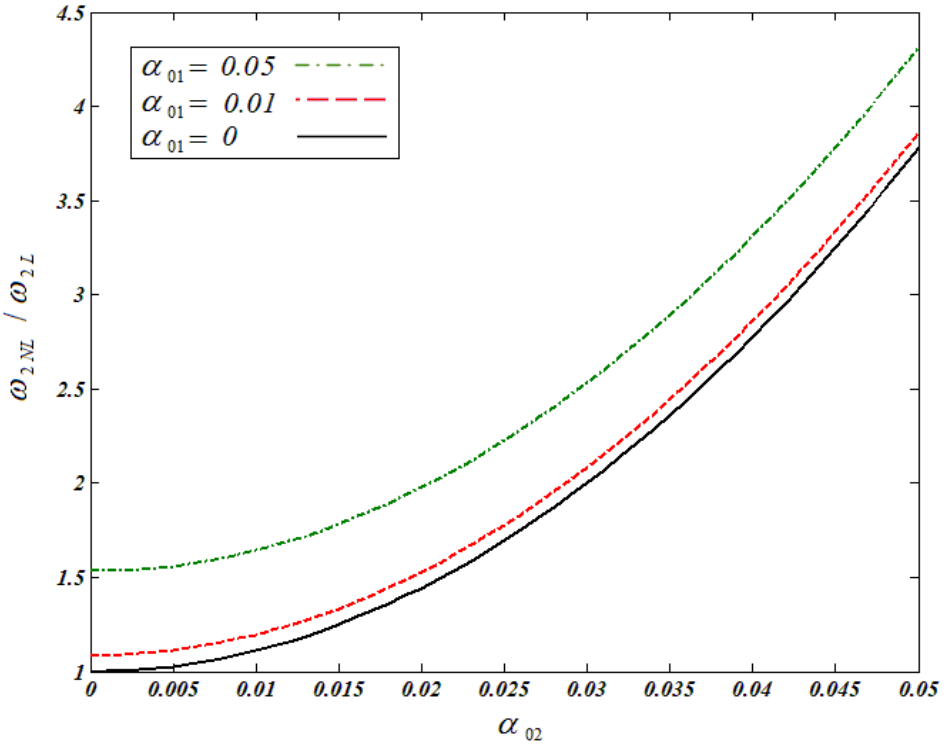

Figure 3-3 Variation of second mode frequency ratio for initial conditions, α_{01} and α_{02}

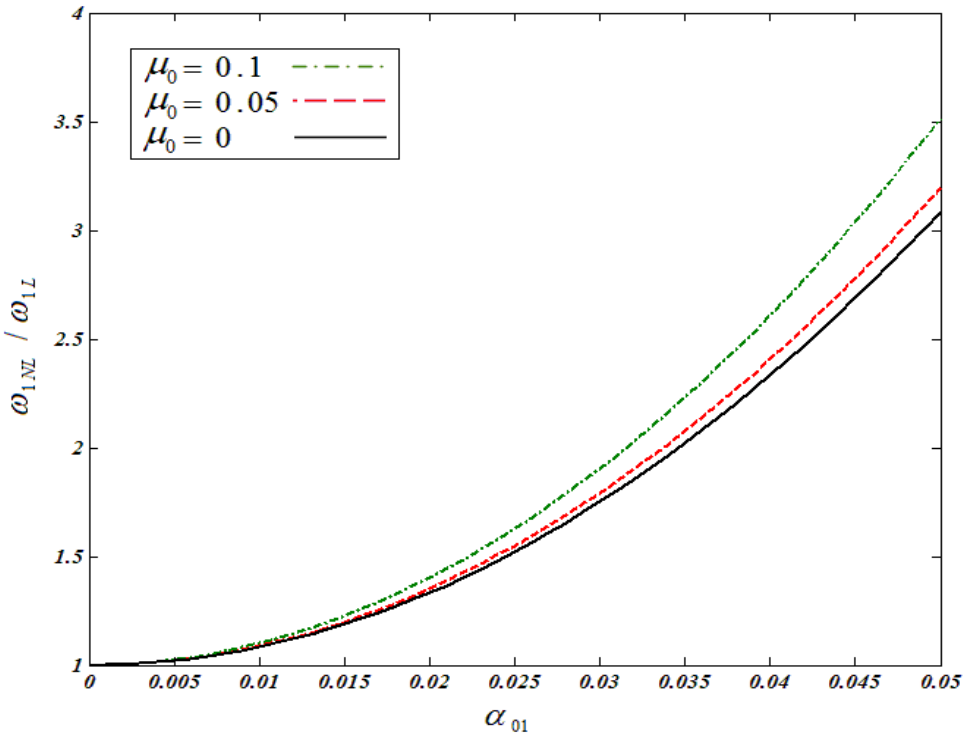

Figure 3-4 Effect of non-local parameter μ_0 on the frequency ratio of first mode.

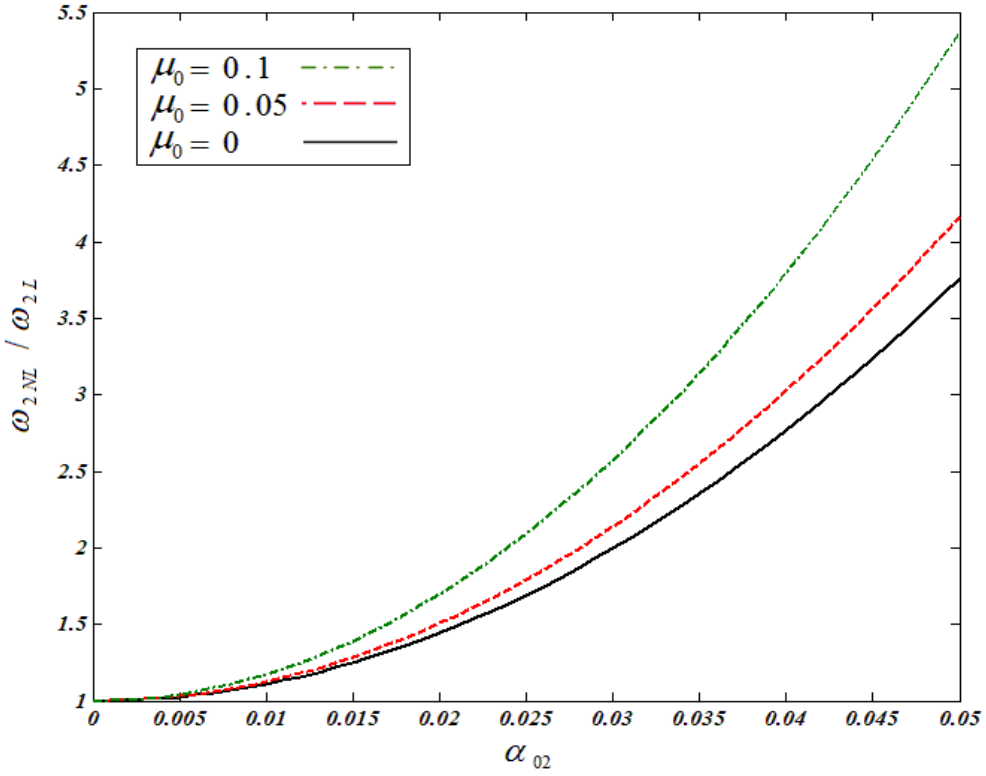

Figure 3-5 Effect of non-local parameter μ_0 on the frequency ratio of second mode.

Figures 3-6 to 3-8 represent the effects of nonlocal parameter, applied force and intermediate mass on the frequency response of the Hinged-Hinged (H-H) structure, respectively, when the first mode is under primary resonance. Similarly, figures 3-9 to 3-11 show the influence of aforementioned parameters for the Clamped-Clamped (C-C) boundary conditions. When the frequency response curve bends away to the right side of the vertical position (i.e., related to the linear system), the hardening behaviour is increased due to the system nonlinearity. As understood from these figures, the nonlocal parameter has a significant effect on the system response and increase on this parameter would make a considerable increase on the amplitude of vibration and hardening behaviour of the system in comparison with classical response in which this parameter is zero.

The C-C structure is more sensitive to this structure than the H-H one. In addition, the growth on the values of intermediate mass and applied force increase the amplitude of vibration as expected. Thus, these two parameters can be considered as the input parameters to reach the expected amplitudes especially in sensing applications. Also, the positions of intermediate mass and external point load are both in the middle of the nanotube to insert their maximum impact on the first mode vibration which is under resonance.

It should be noted that due to the properties of the boundary conditions, the maximum amplitude of vibration for H-H boundary is higher than the C-C owing to the more constraints that the second boundary condition applies to the system.

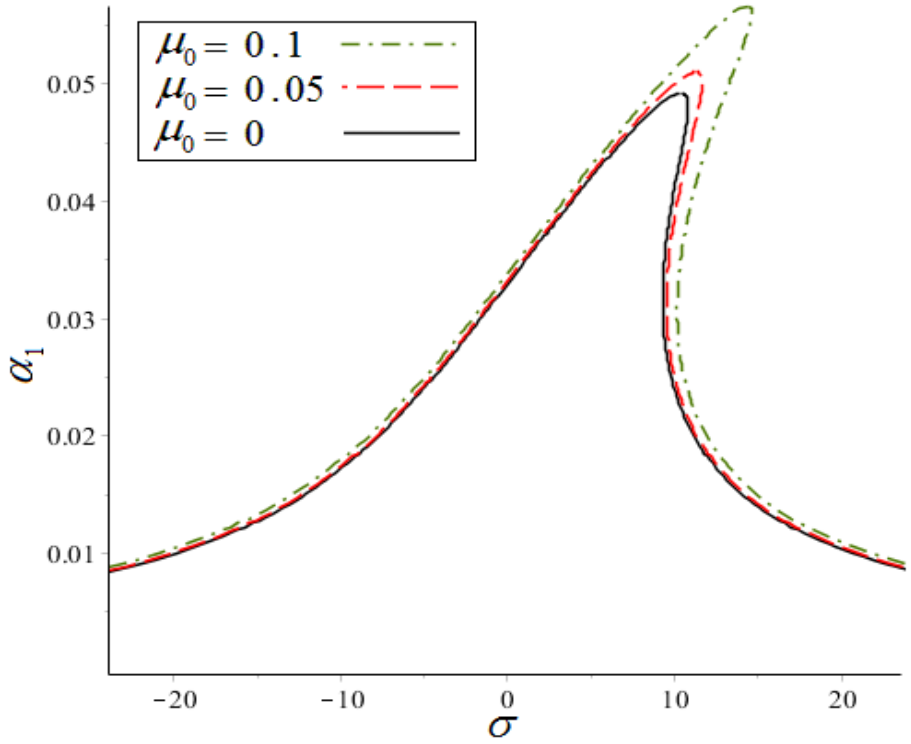

Figure 3-6 Non-local parameter μ_0 effect on frequency response (H-H boundaries).

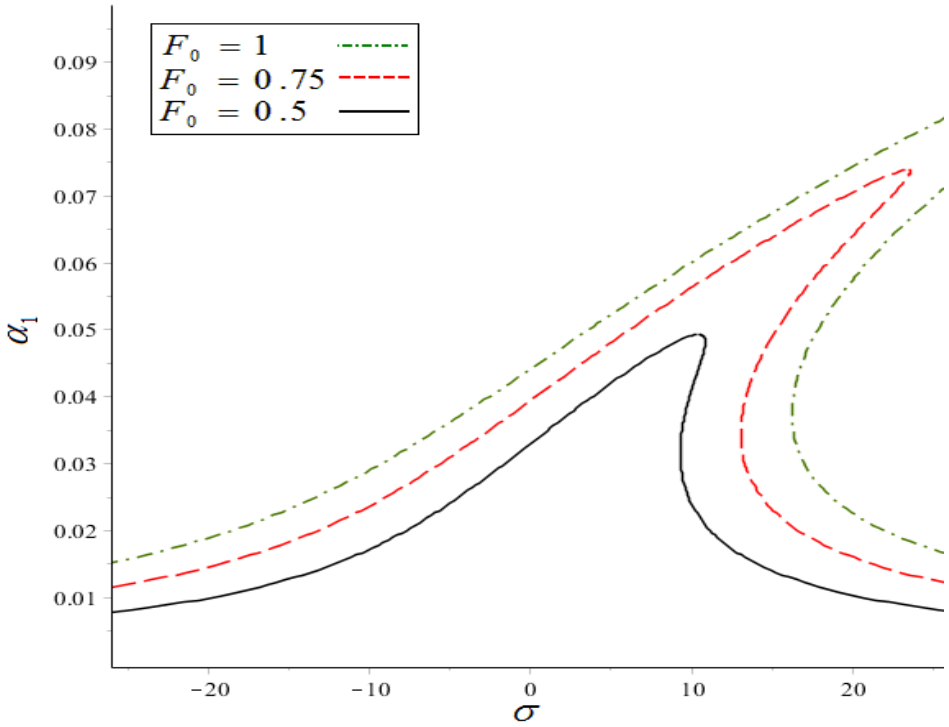

Figure 3-7 Force amplitude F_0 effect on frequency response (H-H boundaries).

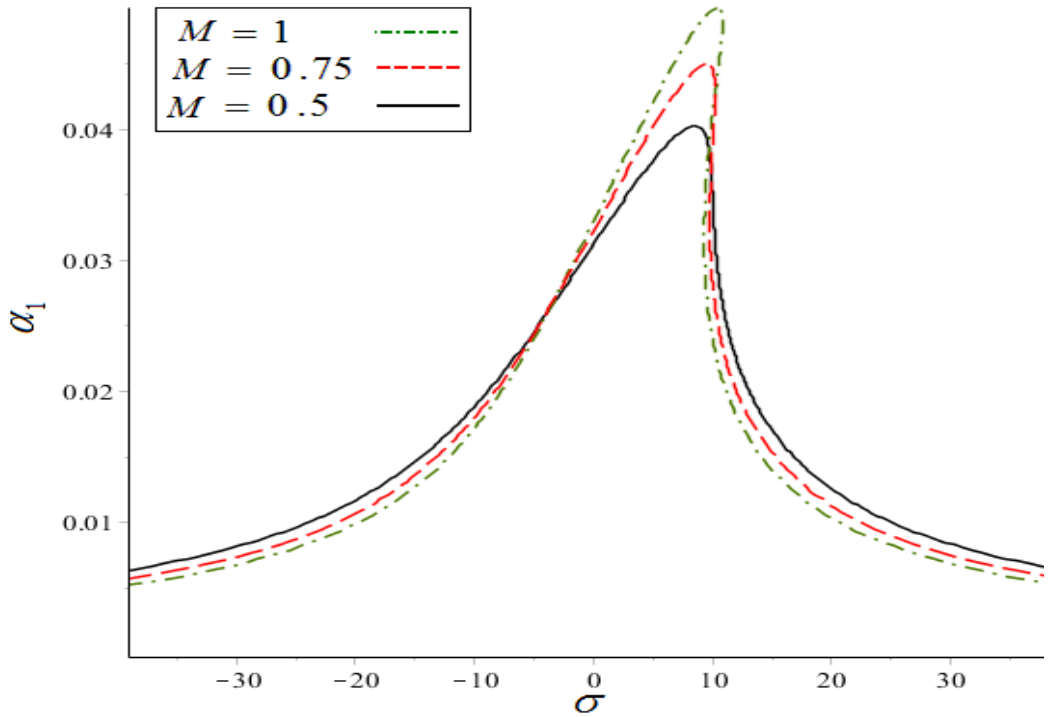

Figure 3-8 Intermediate mass M effect on frequency response (H-H boundaries).

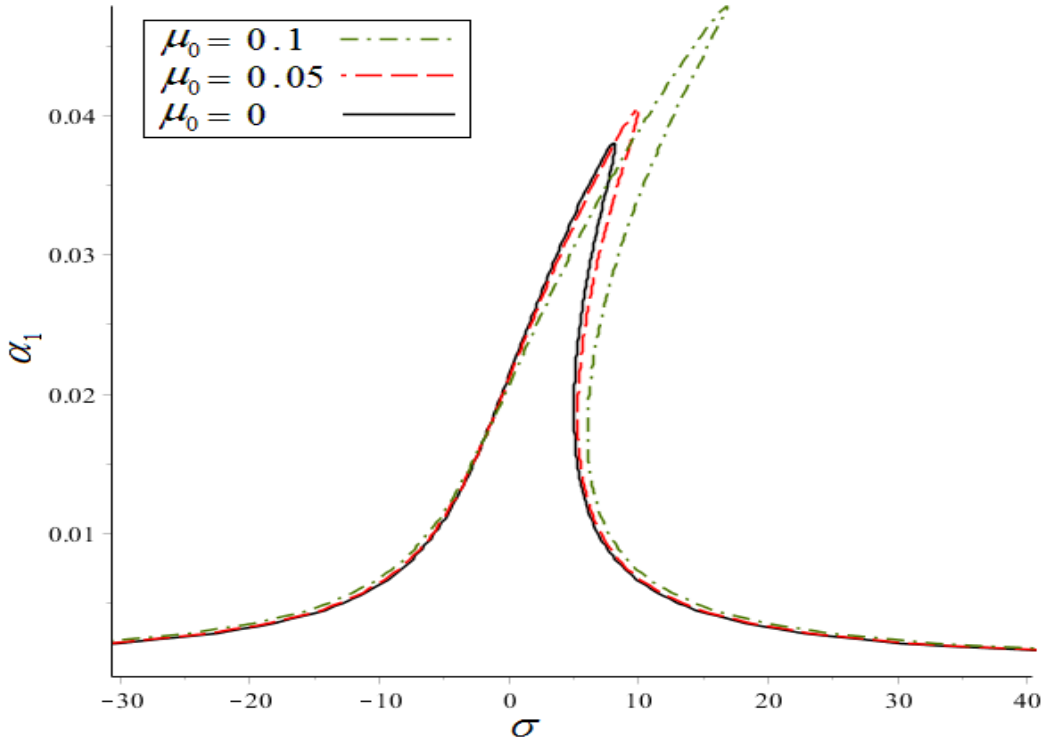

Figure 3-9 Non-local parameter μ_0 effect on frequency response (C-C boundaries).

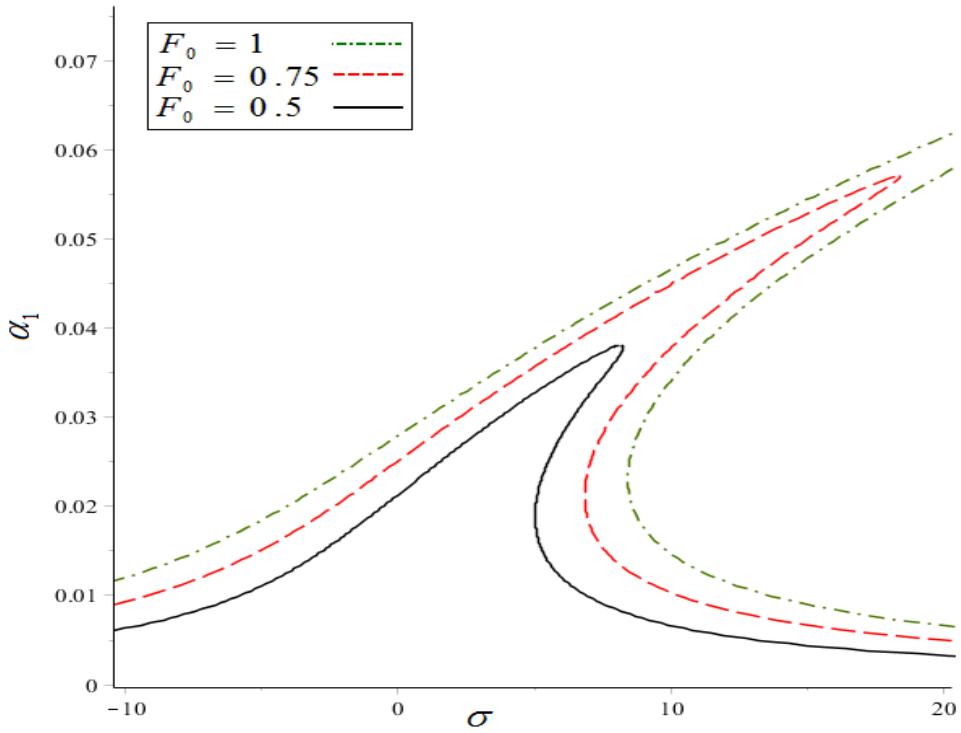

Figure 3-10 Force amplitude F_0 effect on frequency response (C-C boundaries).

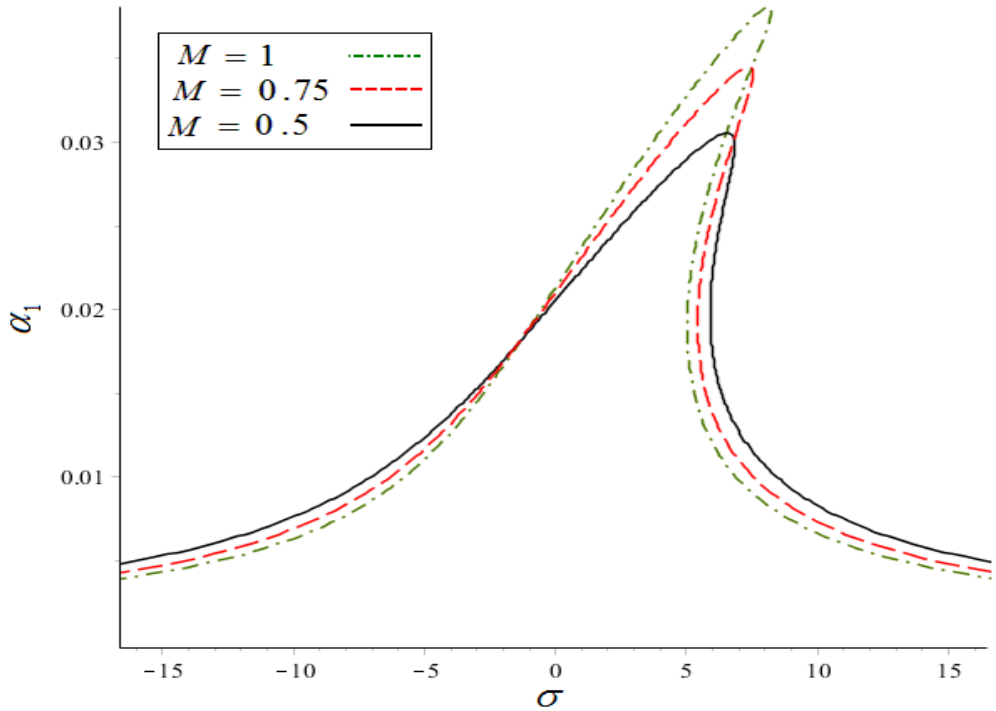

Figure 3-11 Intermediate mass M effect on frequency response (C-C boundaries).

For the Clamped-Hinged (C-H) system, as both internal and external resonances occur in the system modes, the effects of nonlocal parameter, applied force amplitude and intermediate mass have been represented for both modes frequency responses in figures 3-14 to 3-19. Figures 3-14, and 3-15 show the nonlocal parameter impact on the nonlinearity and amplitudes of vibration for mode one and mode two, respectively. The jump phenomena is illustrated in Figure 3-14 by solid and dotted arrows which is a very important phenomena in terms of physical view which the detailed understanding of the jump in the system could be found in the literature [97].

As brief explanation, by increasing the detuning parameter starting from the negative values, the amplitude of vibration increases and reaches to the maximum value following upper curve and then suddenly jumps down to the lower curve as shown by solid arrows. Also by decreasing the detuning parameters starting from positive values the amplitude of vibration increases by following the lower curve and then at a point suddenly jumps up to the upper curve as shown by dotted arrows.

In fact, the system response does not appear in the area between the two curves in reality. Indeed the jump phenomena makes a large shift in the amplitude of vibration. It should be reminded that changing the detuning parameter refers to the nearness of natural frequency to the frequency which causes resonance like the external frequency. Also, this fact exists for the primary resonances that were discussed previously for H-H and C-C boundaries when the hardening behaviour appears in the system. As it is obvious for the responses of the considered system, the jump phenomena is more obvious in the first mode vibration rather than the second mode. The effect of intermediate mass and applied force

on the increase of vibration amplitude have been seen as before. As expected the amplitude of vibration for the first mode is considerably greater than the second one which shows the importance of fundamental mode in vibration analysis of such systems. To compare the obtained results and the importance of using nanotubes for mass detection applications, the frequency responses of a nanotube resonator done by Cho, et al. are shown in Figure 3-12 for clamped-clamped ends [98]. As seen, an agreement is found between this figure and obtained results for the corresponding system behaviour. Also Figure 3-13 shows the results obtained by experimental measurements of a clamped nanotube with an intermediate mass [98]. Effects of mass on the frequency shift and jump phenomena is shown as expected which proves the application of proposed model for finding small masses. It should be noted that these results were presented actual dimensions of the system further information about the details can be found in the corresponding reference [98].

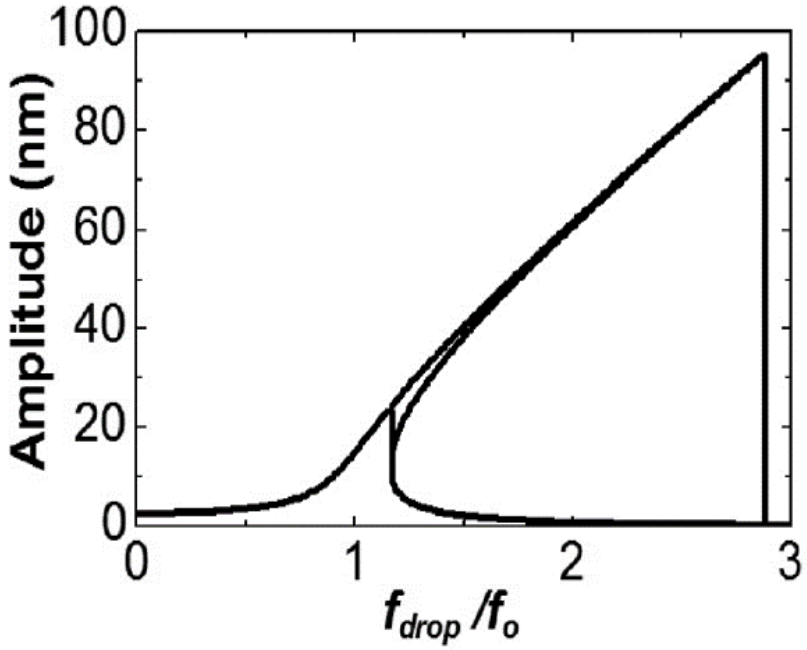

Figure 3-12 Frequency response of a nonlinear resonator for the parameters of carbon nanotube [98].

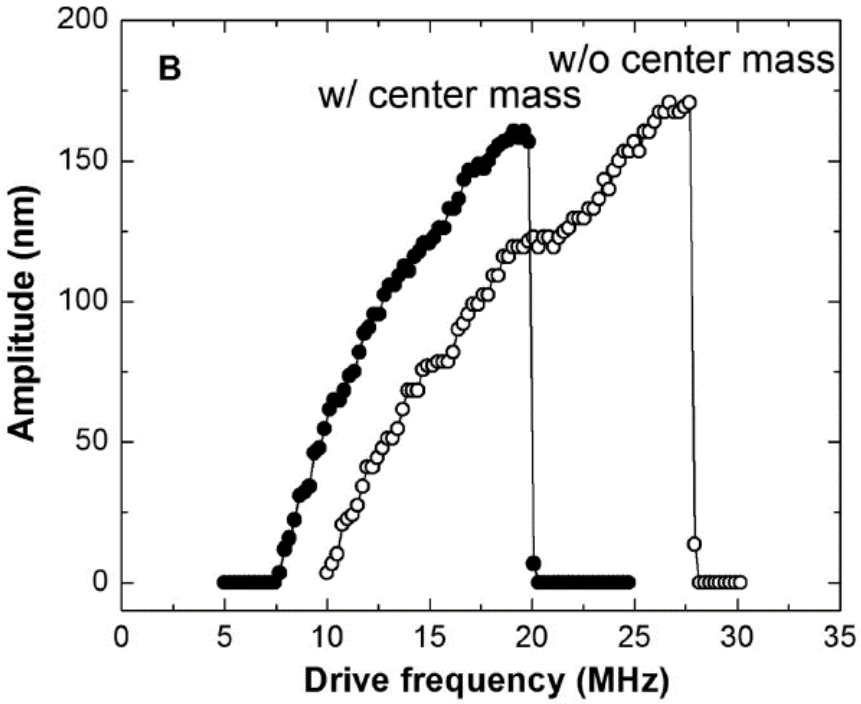

Figure 3-13 Effect of mass in the frequency response shift in mass sensing with a nanotube (experimental results) [98].

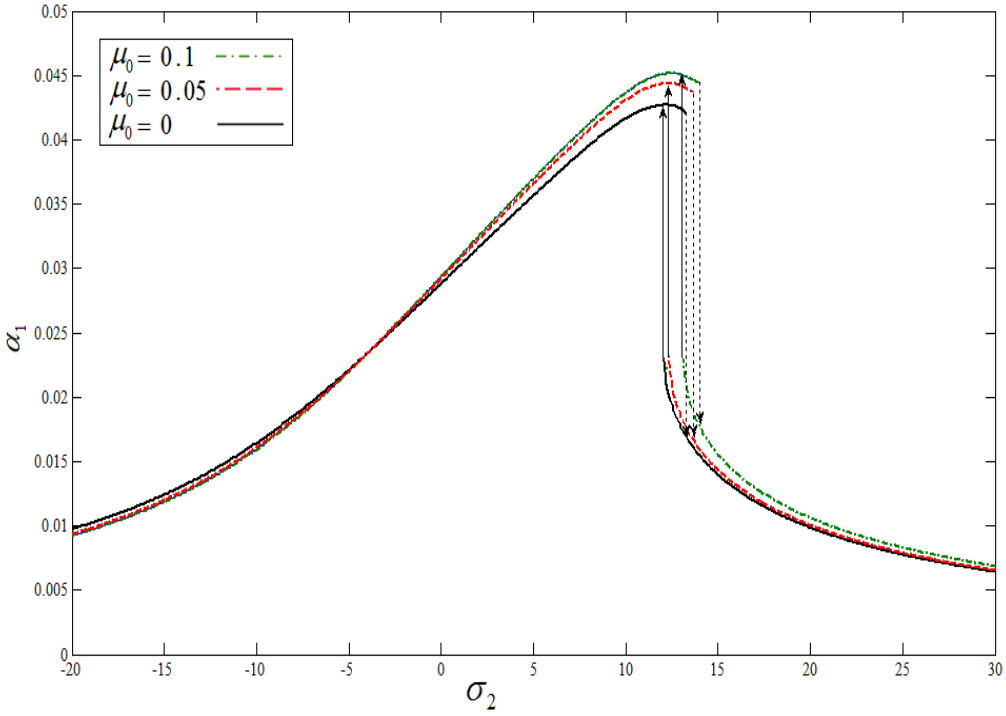

Figure 3-14 Non-local parameter μ_0 effect on frequency response of first mode (C-H boundaries).

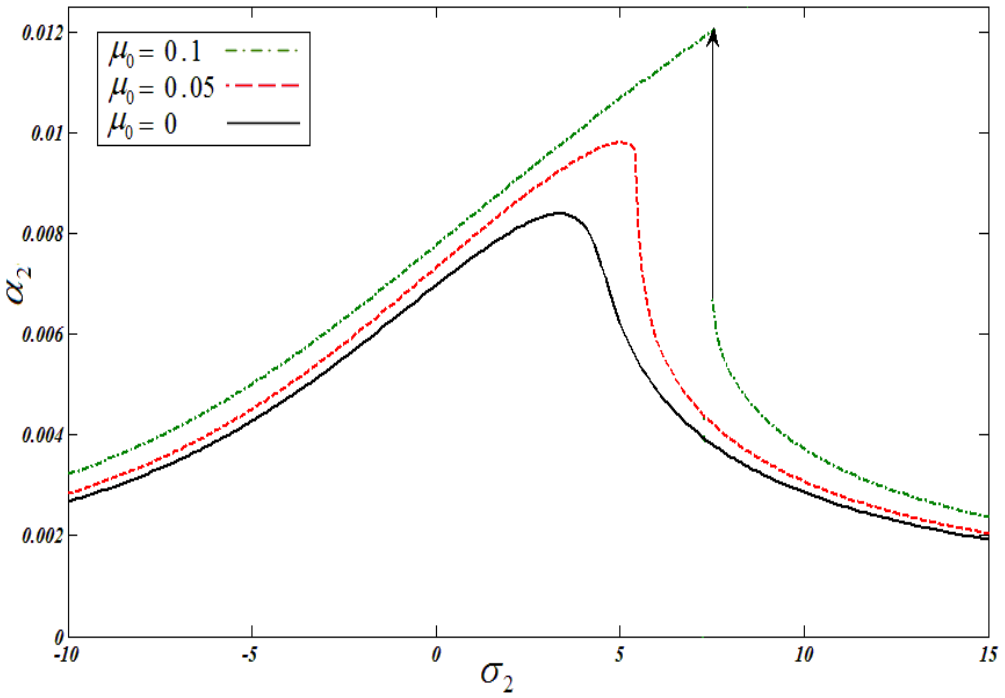

Figure 3-15 Non-local parameter μ_0 effect on frequency response of second mode (C-H boundaries).

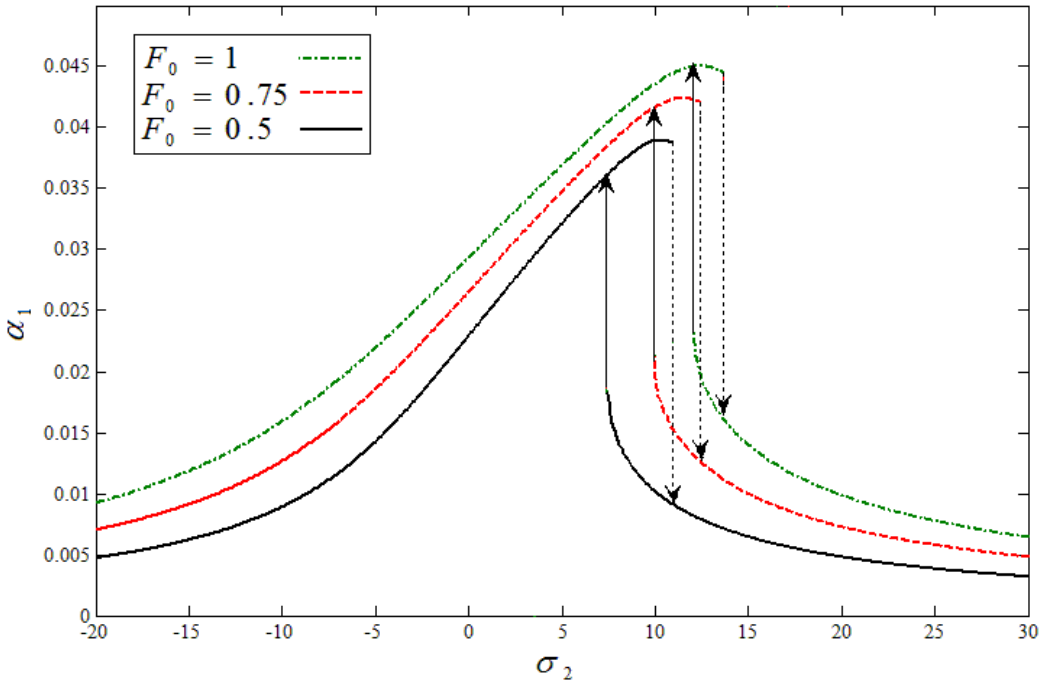

Figure 3-16 Force amplitude F_0 effect on frequency response of first mode (C-H boundaries).

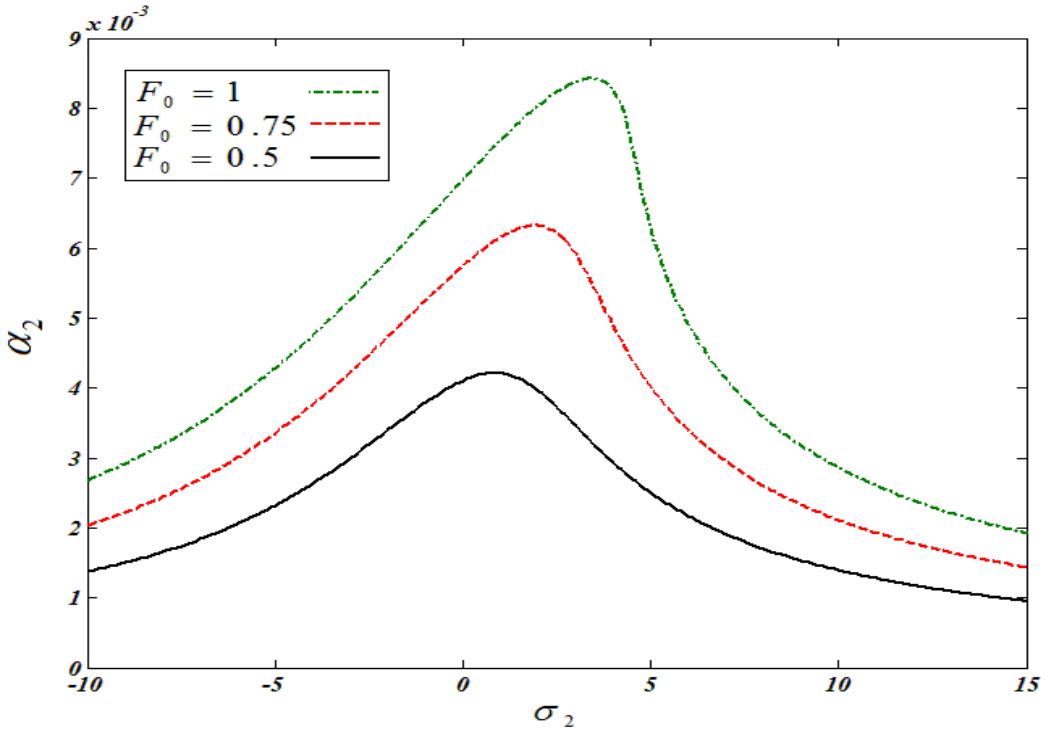

Figure 3-17 Force amplitude F_0 effect on frequency response of second mode (C-H boundaries).

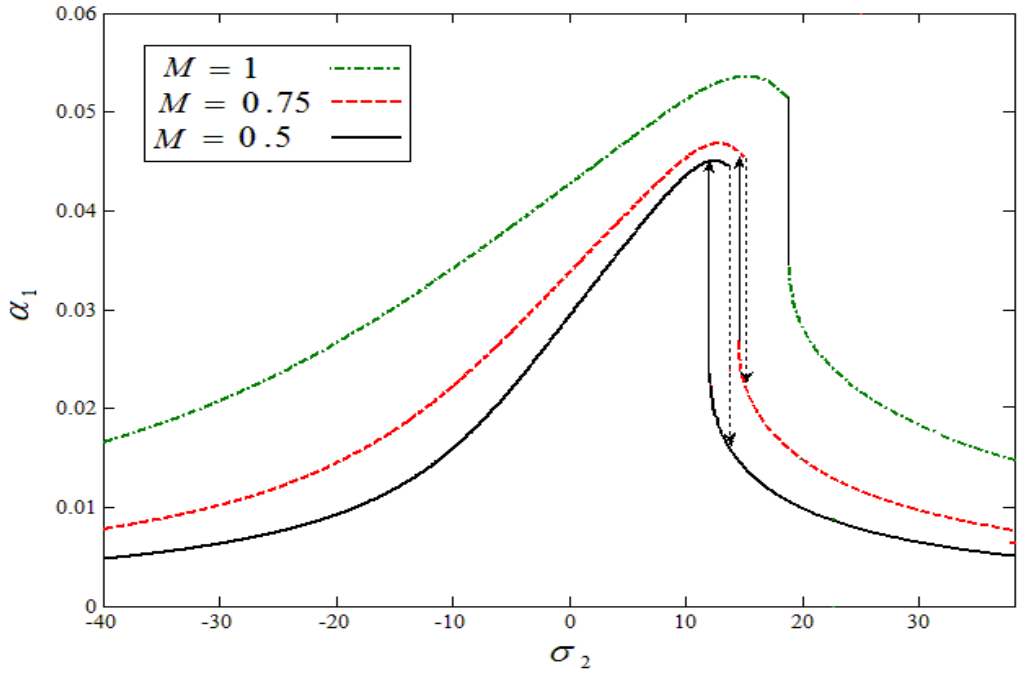

Figure 3-18 Intermediate mass M effect on frequency response of first mode (C-H boundaries).

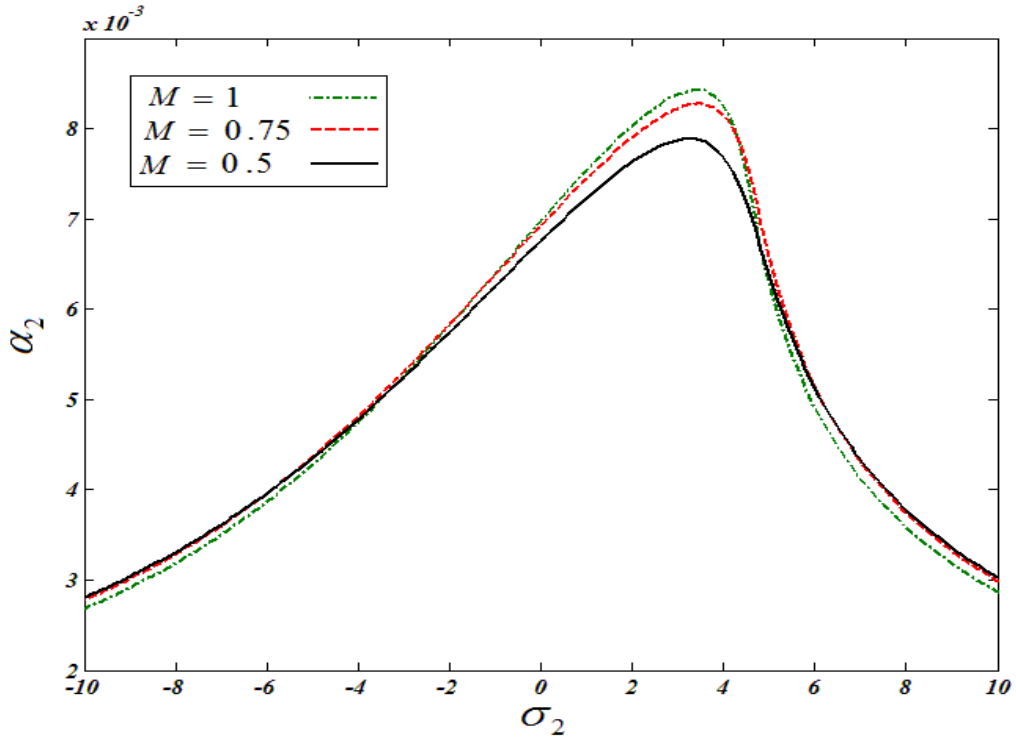

Figure 3-19 Intermediate mass M effect on frequency response of second mode (C-H boundaries).

Thus, the vibration responses of proposed system were investigated for various cases and effects of different parameters were analysed and discussed which would be helpful for understanding, predicting and also designing such small scale systems.

Chapter 4: **Vibration analysis of piezoelectric-layered non-local nanotubes**

4.1. INTRODUCTION

In this Chapter the vibration of a carbon nanotube having a piezoelectric layer around the nanotube is studied. The governing equations for the energy terms of both materials are developed by considering a slender piezoelectric material attached through the nanotube and the Hamiltonian and Lagrangian approaches are utilized to find the governing equation for the transversal vibration of the proposed system. Effects of intermediate mass and nonlocal theory are also added to the system model. Then the Galerkin method and multiple scales method are applied to solve the obtained equation as before. Here, the fundamental mode of vibration is taken into the account and the vibration of system under single frequency and multi-frequency excitations are investigated. For the single frequency excitation, the solution of primary resonance case is carried out and for the multi-frequency excitation, simultaneous combination resonances in which two resonance may occur at the same time where analyzed. Finally, the solutions of both cases are calculated for various numerical values and effects of different parameters, especially the parameters related to the presence of piezoelectric layer, on the frequency responses of the system are studied and discussed in details.

4.2. MATHEMATICAL MODELING

The dynamic modeling of a carbon nanotube having a layer of piezoelectric material on it is targeted here. The schematic model of proposed model has been depicted in Figure 4.1. Again, the Euler-Bernoulli beam theory is associated with nonlocal theory and the system is taken as a double walled nanotube in which the inner layer is the carbon nanotube and the outer one is the piezoelectric material and they have attached along each other. The general displacement field is considered as previous section for both layers.

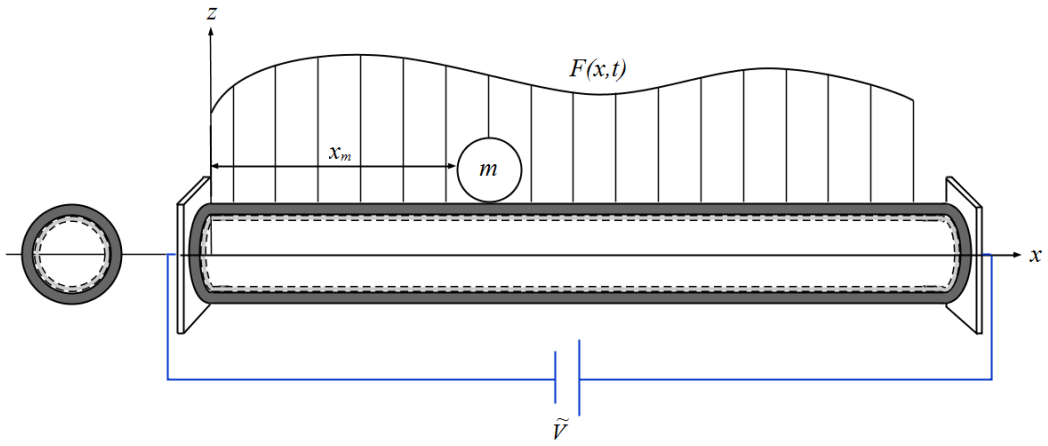

Figure 4-1 Schematic model of piezoelectric layered nanotube with intermediate mass.

The constitutive equations for the slender piezoelectric layer along the beam-type model is written as the following reduced form[47]

$$s_{xx} = E_1 \varepsilon_{xx} - e_1 E^x , \tag{4.1}$$

$$D^x = e_1 \varepsilon_{xx} + k_1 E^x , \tag{4.2}$$

where s_{xx} , ε_{xx} are the respective von Karman stress and the strain along the structure. E^x shows the electric field in axial direction such that $E^x = -\dfrac{\partial \varphi}{\partial x} = -\varphi_x$ and $\varphi(x,t)$ is the electric

potential. D_x denotes the electrical displacement in axial direction. Also, the constants E_1, e_1 and k_1 indicate the linear elastic constant of piezoelectric, piezoelectric constant, and the dielectric constant, respectively.

It should be noted that due to the symmetry and slenderness of the beam-type model of piezoelectric layer, the electrical effects on the other directions are not appear in the corresponding constitutive equations. Similar to previous Chapter, one can have the following relationships for the strains, Bending moments and shear forces of each layers

$$\begin{cases} \varepsilon_{xx,i} = \varepsilon_{0,i} + u_{x,i}(x,t) - z w_{xx,i}(x,t) + \dfrac{1}{2}(w_{x,i}(x,t))^2, \\ \overline{M}_i = \int\limits_{A_i} z.s_{xx,i}\, dA_i,\ \overline{N}_i = \int\limits_{A^i} s_{xx,i}\, dA_i, \end{cases} \quad and\ i = 1,2 \tag{4.3}$$

where $i = 1$ and $i = 2$ correspond to the outer layer and the inner nanotube, respectively. Also, $\varepsilon_{0,i} = P/(EA)_{,i}$ shows the initial strain of inside the structure as before. The energy method and Hamiltonian principle is used here as Chapter 3 to obtain the governing equation of motion of the system. Thus, the relationships of the strain energy, kinetic energy and the external force work should be developed here.

The strain energy of the proposed double walled system is presented as the following summation

$$U = \int_0^L \int\limits_{A_1} (s_{xx,1}\varepsilon_{xx,1} - D^x E^x)\, dA_1 dx + \int_0^L \int\limits_{A_2} s_{xx,2}\varepsilon_{xx,2}\, dA_2 dx \tag{4.4}$$

$$U = \frac{1}{2}\{\int_0^L \{E_1 A_1(\varepsilon_{01}^2 + 2\varepsilon_{01}u_{x,1} + \varepsilon_{01}w_{x,1}^2 + u_{x,1}^2 + u_{x,1}w_{x,1}^2 + \frac{1}{4}w_{x,1}^4)$$
$$+ e_1 A_1(\varphi_x u_{x,1} + \frac{1}{2}\varphi_x w_{x,1}^2) + E_1 I_1 w_{xx,1}^2\}dx$$
$$\int_0^L \{E_2 A_2(\varepsilon_{02}^2 + 2\varepsilon_{02}u_{x,2} + \varepsilon_{02}w_{x,2}^2 + u_{x,2}^2 + u_{x,2}w_{x,2}^2 + \frac{1}{4}w_{x,2}^4) + E_2 I_2 w_{xx,2}^2\}dx \quad (4.5)$$
$$+ \int_0^L D_1 \varphi_x dx\}$$

where

$$D_1 = A_1[e_1(\varepsilon_0 + u_{x,1} + \frac{1}{2}w_{x,1}^2) - k_1\varphi_{x,1}] \quad (4.6)$$

Due to the continuity equation and since it is considered that there is no friction between the layers caused by the attachment of each other, one can assume that the displacements of the layers would be equal [47]. Thus, by applying the relationships of Eq. (4.6) into Eq. (4.5), leads

$$U =$$
$$\frac{1}{2}\{\int_0^L (E_1 A_1 \varepsilon_{01}^2 + E_2 A_2 \varepsilon_{02}^2) - 4Pu_{x,1} - 2Pw_{x,1}^2 + \overline{EA}(u_x^2 + u_x w_x^2 + \frac{1}{4}w_x^4) \quad (4.7)$$
$$+ \overline{EI}w_{xx}^2 + A_1[2e_1\varepsilon_0\varphi_x + 2e_1(u_x + \frac{1}{2}w_x^2)\varphi_x - k_1\varphi_x^2]dx\}$$

And the variation of strain energy is expressed as

$$\int_{t_1}^{t_2}\delta U dt =$$

$$\frac{1}{2}\int_{t_1}^{t_2}\{\int_0^L -4P\delta u_x + 4w_x\delta w_x + \overline{EA}(2u_x\delta u_x + w_x^2\delta u_x + 2u_x w_x\delta w_x + w_x^3\delta w_x) + 2\overline{EI}w_{xx}\delta w_{xx}$$

$$+ A_1[e_1(\varepsilon_0\delta\varphi_x + \varphi_x\delta u_x + u_x\delta\varphi_x + \frac{1}{2}w_x^2\delta\varphi_x + \varphi_x w_x\delta w_x) - 2k_1\varphi_x\delta\varphi_x]dx\}dt =$$

$$\frac{1}{2}\int_{t_1}^{t_2}[\{-4P\delta u\Big|_0^L - 4Pw_x\delta w\Big|_0^L + 4\int_0^L Pw_{xx}\delta w dx\} + \overline{EA}\{2u_x\delta u\Big|_0^L$$

$$- 2\int_0^L u_{xx}\delta u dx + w_x^2\delta u\Big|_0^L - \int_0^L \frac{\partial}{\partial x}(w_x^2)\delta u dx + 2u_x w_x\delta w\Big|_0^L - 2\int_0^L \frac{\partial}{\partial x}(u_x w_x)\delta w dx \quad (4.8)$$

$$+ w_x^3\delta w\Big|_0^L - \int_0^L \frac{\partial}{\partial x}(w_x^3)\delta w dx\} + 2\overline{EI}\{w_{xx}\delta w_x\Big|_0^L - w_{xxx}\delta w\Big|_0^L + \int_0^L w_{xxxx}\delta w dx\}$$

$$+ A_1\{2e_1(\frac{\varepsilon_0}{2}\delta\varphi\Big|_0^L + u_x\delta\varphi\Big|_0^L - \int_0^L u_{xx}\delta\varphi dx + \varphi_x\delta u\Big|_0^L - \int_0^L \varphi_{xx}\delta u dx + \varphi_x w_x\delta w\Big|_0^L$$

$$- \int_0^L \frac{\partial}{\partial x}(\varphi_x w_x)\delta w dx\frac{1}{2}w_x^2\delta\varphi\Big|_0^L - \int_0^L \frac{\partial}{2\partial x}(w_x^2)\delta\varphi dx) - 2k_1(\varphi_x\delta\varphi\Big|_0^L - \int_0^L \varphi_{xx}\delta\varphi dx)\}]dt$$

Applying the boundary conditions properties similar to previous Chapter

$$\int_{t_1}^{t_2}\delta U dt = \frac{1}{2}\int_{t_1}^{t_2}[\{4\int_0^L Pw_{xx}\delta w dx\} + \overline{EA}\{-2\int_0^L u_{xx}\delta u dx - \int_0^L \frac{\partial}{\partial x}(w_x^2)\delta u dx$$

$$- 2\int_0^L \frac{\partial}{\partial x}(u_x w_x)\delta w dx - \int_0^L \frac{\partial}{\partial x}(w_x^3)\delta w dx\} + 2\overline{EI}\{\int_0^L w_{xxxx}\delta w dx\} \quad (4.9)$$

$$+ A_1\{2e_1(-\int_0^L u_{xx}\delta\varphi dx - \int_0^L \varphi_{xx}\delta u dx - \int_0^L \frac{\partial}{\partial x}(\varphi_x w_x)\delta w dx$$

$$- \int_0^L \frac{\partial}{2\partial x}(w_x^2)\delta\varphi dx) + 2k_1(\int_0^L \varphi_{xx}\delta\varphi dx)\}]dt$$

The kinetic energy is the summation of the energy corresponding to each layer and the tip mass

$$T = \frac{1}{2}\int_0^L \rho_1 A_1(w_t^2 + u_t^2)\,dx + \frac{1}{2}\int_0^L \rho_2 A_2(w_t^2 + u_t^2)\,dx\frac{1}{2}m(w_t^2 + u_t^2)\Big|_{x_m} \quad (4.10)$$

where ρ_1 and ρ_2 are the density of piezoelectric layer and inner carbon nanotube, respectively. Defining $\overline{\rho A} = \rho_1 A_1 + \rho_2 A_2$, the kinetic energy variations are

$$\int_{t_1}^{t_2} \delta T dt = \int_{t_1}^{t_2} \{ \int_0^L \overline{\rho A}(w_x \delta w_x + u_x \delta u_x) dx + m(w_x \delta w_x + u_x \delta u_x)\Big|_{x_m} \} dt \tag{4.11}$$

After changing the integration order and applying the integration by parts, one could reach

$$\begin{aligned} \int_{t_1}^{t_2} \delta T dt = \overline{\rho A} \int_0^L \{ w_x \delta w \Big|_{t_1}^{t_2} - \int_{t_1}^{t_2} w_{tt} \delta w dt + u_x \delta u \Big|_{t_1}^{t_2} - \int_{t_1}^{t_2} u_{tt} \delta u dt \} dx + m\{ w_x \delta w \Big|_{t_1}^{t_2} \\ - \int_{t_1}^{t_2} w_{tt} \delta w dt + u_x \delta u \Big|_{t_1}^{t_2} - \int_{t_1}^{t_2} u_{tt} \delta u dt \} \Big|_{x_m} \end{aligned} \tag{4.12}$$

And at t_1, t_2 the variations $\delta w, \delta u$ are equal to zero. Thus

$$\int_{t_1}^{t_2} \delta T dt = \int_{t_1}^{t_2} \{ -\overline{\rho A} \int_0^L (w_{tt} \delta w + u_{tt} \delta u)\ dx - m(w_{tt} \delta w + u_{tt} \delta u)\Big|_{x_m} \} dt \tag{4.13}$$

And the work of external force $F(x,t)$ is considered as written in Eq. (4.15). Substituting the equations found for the variations of the strain energy, kinetic energy and the external force work into the main equation of variational principle leads to

$$\begin{aligned} &\delta w [\int_0^L \{ -\overline{\rho A} w_{tt} - 2P w_{xx} + \overline{EA}(u_{xx} w_x + u_x w_{xx} + \frac{3}{2} w_{xx} w_x^2) + \frac{1}{2} A_1 e_1 \frac{\partial}{\partial x}(\varphi_x w_x) \\ &+ F(x,t) - \overline{EI} w_{xxxx} - m w_{tt} \Delta(x - x_m) \} dx] + \\ &\delta u [\int_0^L \{ -\overline{\rho A} u_{tt} + \overline{EA}(u_{xx} + w_x w_{xx}) - m u_{tt} \Delta(x - x_m) + \frac{1}{2} A_1 e_1 \varphi_{xx} \} dx] \\ &+ \delta \varphi [A_1 \int_0^L \{ e_1 u_{xx} + e_1 \frac{\partial}{2 \partial x}(w_x^2) - k_1 \varphi_{xx} \} dx] = 0 \end{aligned} \tag{4.14}$$

Setting the coefficients of δw, δu and $\delta \varphi$ zero and apply the relations of Eq. (4.3), yields

$$\begin{aligned} \overline{M}_{xx} = \overline{\rho A} w_{tt} + m w_{tt} \Delta(x - x_m) + 2P w_{xx} - \overline{EA}(u_{xx} w_x + u_x w_{xx} + \frac{3}{2} w_{xx} w_x^2) \\ - A_1 e_1 \frac{\partial}{\partial x}(\varphi_x w_x) + F(x,t) \end{aligned} \tag{4.15}$$

$$\frac{\partial D_1}{\partial x} = A_1 \{ e_1 (u_{xx} + w_x w_{xx}) - k_1 \varphi_{xx} \} = 0 \tag{4.16}$$

Again the effect of small scale size on the governing equation of system is taken into account. Therefore, the bending moment for each nanotube including inner and outer layer are written according to the Eringen's theory as[32]

$$\overline{M}_i - (e_0 a)^2 \overline{M}_{xx,i} = EIw_{xx,i} \quad , \; i = 1,2 \tag{4.17}$$

Using the same procedure discussed in Chapter 3 and applying equations (4.15) and (4.16) into above equation, the governing equations of motion for the piezoelectric layered nanotube with tip mass are obtained as

$$\begin{aligned} &\overline{EI} w_{xxxx} + \overline{\rho A} w_{tt} + m w_{tt} \Delta(x - x_m) + 2P w_{xx} - \overline{EA}(u_{xx} w_x + u_x w_{xx} + \frac{3}{2} w_{xx} w_x^2) \\ &- A_1 e_1 \frac{\partial}{\partial x}(\varphi_x w_x) + F(x,t) - (e_0 a)^2 \frac{\partial^2}{\partial x^2} \{ \overline{\rho A} w_{tt} + m w_{tt} \Delta(x - x_m) - 2P w_{xx} \\ &- \overline{EA}(u_{xx} w_x + u_x w_{xx} + \frac{3}{2} w_{xx} w_x^2) - A_1 e_1 \frac{\partial}{\partial x}(\varphi_x w_x) + F(x,t) \} = 0 \end{aligned} \tag{4.18}$$

$$\frac{\partial \varphi_x}{\partial x} = \frac{e_1}{k_1} \frac{\partial}{\partial x}(u_x + \frac{1}{2} w_x^2) = 0 \tag{4.19}$$

Also, $\overline{EI} = E_1 I_1 + E_2 I_2$, $\overline{EA} = E_1 A_1 + E_2 A_2$ and $\overline{\rho A} = \rho_1 A_1 + \rho_2 A_2$ where E_i, I_i A_i $\rho_i, i = 1,2$ are the modulus of elasticity, cross section moment of inertia, cross section area and density for each layer, respectively. Similar to previous Chapter and by using the inextensibility, the longitudinal displacement is approximated as introduced before in Eq. (3.21). Also similar to Eq. (3.22), the definitions of non-dimensional parameters seen in Appendix *B* are applied into the governing equation obtained in this section which would be helpful for better evaluations in next sections and consequently the results are presented in dimensionless forms.

4.3. VIBRATION SOLUTION OF PIEZOELECTRIC-LAYERED NANOTUBE

The Galerkin method is applied here to solve the governing equation of motion of the proposed system. In this section, the fundamental mode is considered and the orthogonality of normal modes is applied again as.

$$\int_0^l R(x,t)X_1(x)dx = 0 \tag{4.20}$$

In order to have a more detailed study, two types of external excitation is taken into the account. As the conventional case, the single frequency excitation is studied for the first case. Accordingly, the expression of the external load is assumed to be similar to Eq. (4.41) in which a harmonic point load is applied at an arbitrary distance along the nanotube. For the second case, it is assumed that the system is under multi-frequency excitation which makes the system responses more complicated and various resonance cases may occur in the structure. Also, in this Chapter it is assumed that the applied voltage and consequently the electric field of the piezoelectric layer is constant for the system[47]

4.3.1. Single Frequency Excitation

In this section the single frequency excitation is considered and the important primary resonance case is studied. As discussed before the governing equation of motion for the time response of the first mode can be obtained and solved using multiple scales method. Considering a small damping term and ordering the required coefficients of nonlinear term and applied force for analysis of primary resonance in the solution procedure[97]. The nonlinear differential equation for the time response of fundamental mode is found as

$$\ddot{Y} + \omega_1^2 Y + \varepsilon\mu\dot{Y} + \varepsilon b_1 Y^3 = \varepsilon F_0 \cos(\Omega\hat{t}) \tag{4.21}$$

where the coefficients ω_1, b_1 and F_0 are presented in Appendix *B* in as based on the system physical and geometrical properties. The solution of above Equation is written as the following series

$$Y(\hat{t}) = Y_0(T_0, T_1) + \varepsilon Y_0(T_0, T_1) + ... \tag{4.22}$$

The solution procedure for this section could be found in the literature due to the importance of derived equation known as Duffing equation [97].

Here, $T_n = \varepsilon^n t$ and the derivatives are defined as

$$\frac{d}{dt} = \frac{dT_0}{dt}\frac{\partial}{\partial T_0} + \frac{dT_1}{dt}\frac{\partial}{\partial T_1} + ... = D_0 + \varepsilon D_1 + \varepsilon^2 D_2 + .. \tag{4.23}$$

$$\frac{d^2}{dt^2} = D_0^2 + 2\varepsilon D_0 D_1 + \varepsilon^2 (D_1^2 + 2D_0 D_1) + ... \tag{4.24}$$

Applying above definitions into the main equation and separating the terms with same power of perturbation parameter, gives

$$\varepsilon^0 : D_0^2 Y_0 + \omega_1^2 Y_0 = 0 \tag{4.25}$$

$$\varepsilon^1 : D_0^2 Y_1 + \omega_1^2 Y_1 = -2D_0 D_1 Y_0 - 2\mu D_0 Y_0 - b_1 Y_0^3 + F_0 \cos(\Omega T_0) \tag{4.26}$$

For this case, it is assumed that a primary resonance occur in the system when the excitation frequency is close to the natural frequency of the system as $\Omega \approx \omega_1$. Hence, the relationship between two frequencies can be expressed as

$$\Omega = \omega_1 + \varepsilon\sigma \tag{4.27}$$

where σ, is the detuning parameter as explained in the previous Chapter. Using the solution of Eq. (4.25) i.e., $Y_0 = A(T_1)\exp(i\omega_1 T_0) + \overline{A}(T_1)\exp(-i\omega_1 T_0)$ into Eq. (4.26) and separating the secular terms, yields

$$-2i\omega_1(A' + \mu A) - 3b_1 A^2 \overline{A} + \frac{1}{2}F_0 \exp(i\sigma T_1) = 0 \tag{4.28}$$

The polar form $A = \frac{1}{2}\alpha \exp(i\theta)$ is substituted to the above equation and the real and imaginary parts are separated as

$$\begin{cases} (\sigma - \gamma')\omega_1\alpha - \frac{3}{8}b_1\alpha^3 + \frac{1}{2}F_0\cos\gamma = 0 \\ -\omega_1\alpha' - \mu\omega_1\alpha + \frac{1}{2}F_0\sin\gamma = 0 \end{cases} \tag{4.29}$$

where $\gamma = \sigma T_1 - \theta$. For the steady-state motion considering primary resonance, one should have $\gamma' = \alpha' = 0$. Thus

$$\begin{cases} \sigma\omega_1\alpha - \frac{3}{8}b_1\alpha^3 + \frac{1}{2}F_0\cos\gamma = 0 \\ -\mu\omega_1\alpha + \frac{1}{2}F_0\sin\gamma = 0 \end{cases} \tag{4.30}$$

So by finding solving the above equation, the first approximate solution for the steady state motion is

$$Y(\hat{t}) = \alpha\cos(\Omega\hat{t} - \gamma) + O(\varepsilon) \tag{4.31}$$

where $O(\varepsilon)$ shows the higher order terms. Also, the frequency amplitude relationship can be obtained by simplifying Eq. (3.30) as

$$\sigma = \left(\frac{3}{8} b_1 \alpha^3 \pm (\frac{1}{4} {F_0}^2 - (\mu \omega_1 \alpha)^2)^{1/2} \right) \Big/ (\omega_1 \alpha) \tag{4.32}$$

Also, the nonlinear natural frequency of the system is equal to

$$\widehat{\omega}_1 = \omega_1 [1 + (\frac{3b_1}{8{\omega_1}^2}) \alpha^2] + O(\varepsilon^2) \tag{4.33}$$

4.3.2. Multi-Frequency Excitation

In order to investigate important resonance cases known as simultaneous resonances, which may happen in the structure forced, vibration, the multi-frequency excitation is considered to be applied to the system and the corresponding terms of the force are not ordered. So the expression of the general external force in lateral direction is taken as the following form

$$F(\hat{x}, \hat{t}) = F_1 \cos(\Omega_1 \hat{t}) Dirac(\hat{x} - \hat{x}_1) + F_2 \cos(\Omega_2 \hat{t}) Dirac(\hat{x} - \hat{x}_2) \tag{4.34}$$

Above equation denotes that two point load harmonic forces with asymmetric frequencies are inserted to the nanotube. $\hat{x}_{j,\, j=1,2}$ indicates the position of each excitation along the structure. Thus after performing the Galerkin procedure, the differential equation of motion is obtained as the following form

$$\ddot{Y} + \omega_1^2 Y + \varepsilon \mu \dot{Y} + \varepsilon b_1 Y^3 = F_1 \cos(\Omega_1 \hat{t}) + F_2 \cos(\Omega_2 \hat{t}) \tag{4.35}$$

Using the approximate solution of Eq. (4.22) in Eq. (4.35) and setting the same power of perturbation parameter equal as

$$\varepsilon^0 : D_0^2 y_0 + \omega_1^2 Y_0 = F_1 \cos(\Omega_1 T_0) + F_2 \cos(\Omega_2 T_0) \tag{4.36}$$

$$\varepsilon^1 : D_0^2 Y_1 + \omega_1^2 Y_1 = -2 D_0 D_1 Y_0 - 2 \mu D_1 Y_0 - b_1 Y_0^3 \tag{4.37}$$

The general solution of Eq. (4.36) having both homogenous and private parts is

$$Y_0 = A(T_1)\exp(i\omega_1 T_0) + \sum_{h=1}^{2} B_j \exp(i\Omega_j T_0) + C.C. \tag{4.38}$$

where *C.C* denotes the complex conjugate of the terms as before and B_j equals to

$$f_{j,\, j=1,2} = \frac{F_j}{2(\omega_1^2 - \Omega_j^2)} \tag{4.39}$$

Substituting Eq. (4.38) into Eq. (4.37), one can find

$$\begin{aligned}
&D_0^2 Y_1 + \omega_1^2 Y_1 = \\
&-(2i\omega_1(A' + \mu A) + 3b_1 A(A\bar{A} + 2f_1^{\,2} + 2f_2^{\,2}))\exp(i\omega_1 T_0) - b_1(A^3\exp(3i\omega_1 T_0) \\
&+ f_1^{\,3}\exp(3i\Omega_1 T_0) + f_2^{\,3}\exp(3i\Omega_2 T_0)) - f_1(2i\mu\Omega_1 + 3b_1(2A\bar{A} + f_1^{\,2} + 2f_2^{\,2}))\exp(i\Omega_1 T_0) \\
&- f_2(2i\mu\Omega_2 + 3b_1(2A\bar{A} + f_2^{\,2} + 2f_1^{\,2}))\exp(i\Omega_2 T_0) - 3b_1 A^2(f_1\exp(i(2\omega_1 + \Omega_1)T_0) \\
&+ f_2\exp(i(2\omega_1 + \Omega_2)T_0) + f_1\exp(i(2\omega_1 - \Omega_1)T_0) + f_2\exp(i(2\omega_1 - \Omega_2)T_0)) \\
&- 3b_1 A(f_1^{\,2}\exp(i(\omega_1 + 2\Omega_1)T_0) + f_2^{\,2}\exp(i(\omega_1 + 2\Omega_2)T_0) + f_1^{\,2}\exp(i(\omega_1 - 2\Omega_1)T_0) + \\
&f_2^{\,2}\exp(i(\omega_1 - 2\Omega_2)T_0)) - 6b_1 A f_1 f_2(\exp(i(\omega_1 + \Omega_1 + \Omega_2)T_0) + \exp(i(\omega_1 + \Omega_1 - \Omega_2)T_0) \\
&+ \exp(i(\omega_1 - \Omega_1 + \Omega_2)T_0) + \exp(i(\omega_1 - \Omega_1 - \Omega_2)T_0)) - 3b_1 f_1^{\,2} f_2(\exp(i(2\Omega_1 + \Omega_2)T_0) \\
&+ \exp(i(2\Omega_1 - \Omega_2)T_0)) - 3b_1 f_1 f_2^{\,2}(\exp(i(2\Omega_2 + \Omega_1)T_0) + \exp(i(2\Omega_2 - \Omega_1)T_0)) + C.C
\end{aligned} \tag{4.40}$$

From Eq. (4.40) various cases of resonances including subharmonic $\omega_1 \approx \frac{1}{3}\Omega_{j,\, j=1,2}$ superharmonic $\omega_1 \approx 3\Omega_{j,\, j=1,2}$ and combination resonances such that $\omega \approx \frac{1}{2}(\Omega_j \pm \Omega_k), \omega \approx \left|\pm 2\Omega_j \pm \Omega_k\right|$, with $j = 1,2 \,\&\, k = 1,2$ can occur [97]. For the two first cases, the system can be treated similar to one frequency excitation as done in the references [97]. In this work the combination resonance is targeted and by assuming $\Omega_1 < \Omega_2$ the following combination resonance cases may happen [97].

$$\omega_1 \approx 2\Omega_2 \pm \Omega_1, \omega_1 \approx 2\Omega_1 \pm \Omega_2 \; or \; \omega_1 \approx \Omega_2 - 2\Omega_1, \omega_1 \approx \frac{1}{2}(\Omega_2 \pm \Omega_1) \tag{4.41}$$

Moreover, the effect of multi-frequencies can appear in simultaneous resonances of the nano structure vibration meaning that two resonances can occur in the system at the same time[97].For example, simultaneous superharmonic and subharmonic resonances such that $\omega \approx 3\Omega_1 \approx \frac{\Omega_2}{3}$ or simultaneous sub/superharmonic resonance with one of the combination resonances may be seen in the system. The first case i.e., simultaneous superharmonic and subharmonic resonances has been studied in literature [97]. The purpose of this study is to investigate the simultaneous resonance between sub/superharmonic resonance and one of the combination resonances as follows.

- *Case A*: $\omega \approx 3\Omega_1 \approx 2\Omega_2 - \Omega_1$

This case shows the simultaneous resonance between superharmonic and a combination of external frequencies resonances in the system forced vibration.

Accordingly, the two detuning parameters and the related equations are set as

$$\begin{cases} 3\Omega_1 = \omega_1 + \varepsilon\sigma_1 \Rightarrow \Omega_1 T_0 = \frac{\omega_1}{3} T_0 + \frac{\sigma_1}{3} T_1, \\ 2\Omega_2 - \Omega_1 = \omega_1 + \varepsilon\sigma_2 \Rightarrow (2\Omega_2 - \Omega_1) T_0 = \omega_1 T_0 + \sigma_2 T_1 \end{cases} \tag{4.42}$$

Using above equation into Eq. (4.40) and eliminating the secular terms, gives

$$2i\omega_1(A' + \mu A) + 3b_1 A(A\overline{A} + 2f_1^2 + 2f_2^2) + b_1 f_1^3 \exp(i\sigma_1 T_1) + 3b_1 f_1 f_2^2 \exp(i\sigma_2 T_1) = 0 \tag{4.43}$$

Employing the polar definition for A same as before into the above equation, yields

$$i\omega_1\alpha' - \alpha\omega_1\theta' + i\mu\alpha\omega_1 + \frac{3}{8}b_1\alpha^3 + 3b_1\alpha(f_1^2 + f_2^2) + b_1 f_1^3 \exp(i\sigma_1 T_1 - \theta) + 3b_1 f_1 f_2^2 \exp(i\sigma_2 T_1 - \theta) = 0 \tag{4.44}$$

and by separating the real and imaginary parts, one can find

$$\omega_1\alpha' + \mu\alpha\omega_1 + b_1 f_1^3 \sin(\gamma_1) + 3b_1 f_1 f_2^2 \sin(\gamma_2) = 0 \tag{4.45}$$

$$-\alpha\omega_1\theta' + \frac{3}{8}b_1\alpha^3 + 3b_1\alpha(f_1^2 + f_2^2) + b_1 f_1^3 \cos(\gamma_1) + 3b_1 f_1 f_2^2 \cos(\gamma_2) = 0 \tag{4.46}$$

where $\gamma_1 = \sigma_1 T_1 - \theta$ and $\gamma_2 = \sigma_2 T_1 - \theta$. The steady state motions i.e. $\alpha' = 0$ occurs when each $\gamma'_{j,\, j=1,2}$ be zero. Thus

$$\begin{cases} \gamma_1' = \sigma_1 - \theta' = 0 \Rightarrow \sigma_1 = \theta', \\ \gamma_2' = \sigma_2 - \theta' = 0 \Rightarrow \sigma_2 = \theta', \end{cases} \Rightarrow \sigma_1 = \sigma_2 = \sigma \,\&\, \gamma = \sigma T_1 - \theta \tag{4.47}$$

From Eq. (4.47) one can have $\Omega_2 = 2\Omega_1$. So for steady state motion, equations (4.45) and (3.46) become

$$-\mu\alpha = (B_1 + B_2)\sin(\gamma) \tag{4.48}$$

$$(\sigma - B_4)\alpha - B_3\alpha^3 = (B_1 + B_2)\cos(\gamma) \tag{4.49}$$

where

$$B_1 = \frac{b_1 f_1^3}{\omega_1}, B_2 = \frac{3b_1 f_1 f_2^2}{\omega_1}, B_3 = \frac{3b_1}{8\omega_1}, B_4 = \frac{3b_1}{\omega_1}(f_1^2 + f_2^2) \tag{4.50}$$

After some mathematical simplifications on above equations, the frequency-amplitude response of the piezoelectric carbon nanotube under multi-frequency force with the considered simultaneous resonances is computed as

$$\sigma = B_4 + B_3\alpha^2 \pm \sqrt{\frac{(B_1+B_2)^2}{\alpha^2} - \mu^2} \tag{4.51}$$

where the value $\alpha_p = (B_1+B_2)/\mu$ shows the peak of amplitude of vibration. Also, the first approximate solution for the time response of the system is found as

$$Y(\hat{t}) = \alpha\cos(3\Omega_1\hat{t} - \gamma) + \frac{F_1}{2(\omega_1^2 - \Omega_1^2)}\cos(\Omega_1\hat{t}) + \frac{F_2}{2(\omega_1^2 - 4\Omega_1^2)}\cos(2\Omega_1\hat{t}) + O(\varepsilon) \tag{4.52}$$

- *Case B*: $\omega_1 \approx \frac{\Omega_1}{3} \approx 2\Omega_2 - \Omega_1$

For this case it is assumed that the subharmonic and combination resonances occur simultaneously and the corresponding detuning parameters are defined as

$$\begin{cases} \Omega_1 = 3\omega_1 + \varepsilon\sigma_1 \Rightarrow \Omega_1 T_0 = 3\omega_1 T_0 + \sigma_1 T_1, \\ \Omega_2 - 2\Omega_1 = \omega_1 + \varepsilon\sigma_2 \Rightarrow (\Omega_2 - 2\Omega_1)T_0 = \omega_1 T_0 + \sigma_2 T_1 \end{cases} \tag{4.53}$$

Applying above definitions into Eq. (4.40) and elimination of secular terms, leads

$$2i\omega_1(A' + \mu A) + 3b_1 f_1 A(A\bar{A} + 2f_1^2 + 2f_2^2) + 3\bar{A}^2\exp(i\sigma_1 T_1) + 3b_1 f_2 f_1^2\exp(i\sigma_2 T_1) = 0 \tag{4.54}$$

The polar form for *A* is utilized again in Eq. (4.54) and the real and imaginary parts is separated. Therefore

$$\omega_1\alpha' + \mu\alpha\omega_1 + \frac{3}{4}b_1 f_1\alpha^2\sin(\gamma_3) + 3b_1 f_2 f_1^2\sin(\gamma_4) = 0 \tag{4.55}$$

$$-\alpha\omega_1\theta' + \frac{3}{8}b_1\alpha^3 + 3b_1\alpha(f_1^2 + f_2^2) + b_1 f_1\alpha^2\cos(\gamma_3) + 3b_1 f_2 f_1^2\cos(\gamma_4) = 0 \tag{4.56}$$

where $\gamma_3 = \sigma_1 T_1 - 3\theta$ and $\gamma_4 = \sigma_2 T_1 - \theta$. For the steady state motion it requires to have $\gamma_3' = \gamma_4' = 0$. Thus

$$\sigma_1 = 3\theta', \sigma_2 = \theta', \Rightarrow \sigma_1 = 3\sigma_2 = 3\sigma \tag{4.57}$$

which follows that $3\Omega_2 = 7\Omega_1$. So the corresponding frequency-amplitude relation could be found from the system of equations as follows

$$\begin{cases} \mu\alpha + B_5\alpha^2 \sin(3\gamma) + B_6 \sin(\gamma) = 0 \\ (B_4 - \sigma)\alpha + B_3\alpha^3 + B_5\alpha^2 \cos(3\gamma) + B_6 \cos(\gamma) = 0 \end{cases} \tag{4.58}$$

where

$$B_5 = 3b_1 f_1 / 4\omega_1, \quad B_6 = 3b_1 f_2 f_1^2 / \omega_1 \tag{4.59}$$

And the first approximate solution of the problem for the simultaneous resonances of this section is equal to

$$Y(\hat{t}) = \alpha \cos(\frac{\Omega_1}{3}\hat{t} - \gamma) + \frac{F_1}{2(\omega_1^2 - \Omega_1^2)} \cos(\Omega_1 \hat{t}) + \frac{F_2}{2[\omega_1^2 - (\frac{7\Omega_1}{3})^2]} \cos(\frac{7\Omega_1}{3}\hat{t}) \tag{4.60}$$

Thus, two important simultaneous resonances due to the multi-frequency excitation were studied in this section. It should be noted that other cases can also be analyzed by using the same procedure which explained in this section.

4.4. RESULTS AND DISCUSSION

In this section obtained solutions for different resonance cases are computed and effects of various parameters such as nonlocal parameter, piezoelectric thickness, applied voltage on the frequency ratio and the frequency responses of forced vibration are studied. The physical and geometrical properties of the nanotube are chosen similar to the previous

Chapter and the properties of the piezoelectric layer are selected for ZnO piezoelectric material coated on the nanotube according to the references[47].

As shown in figures 4-2 to 4-4, the ratio is very dependent to the initial amplitude due to the system nonlinearity. Effect of nonlocal parameter is depicted in Figure 4-2 which increases the ratio. Also, the thickness of piezoelectric layer is an important parameter in the frequency behavior of the system as seen in Figure 4-3 and for higher thickness, the linear frequency increases and makes the ratio smaller. Also, the influence of applied voltage is shown in Figure 4-4 and accordingly the growth on the magnitude of voltage causes an increase on the ratio while for the selected piezoelectric material the negative voltages increase the nonlinear frequency unlike the positive voltages which increase the linear frequency of the system.

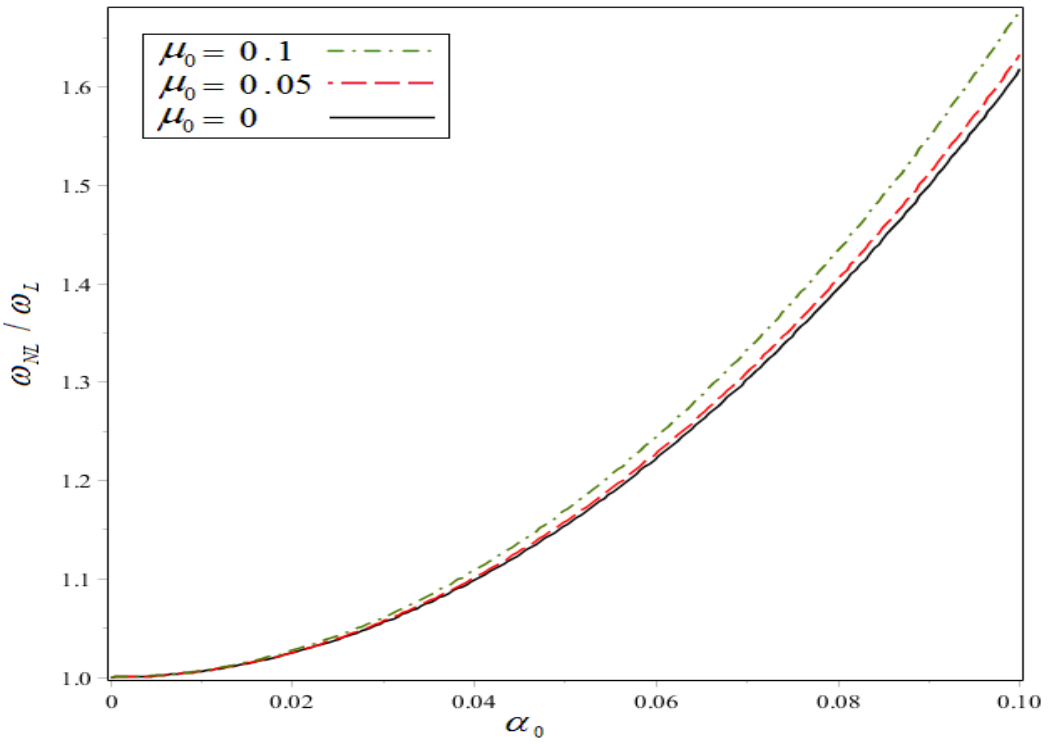

Figure 4-2 Frequency ratio vs. initial condition for different non-local parameter μ_0

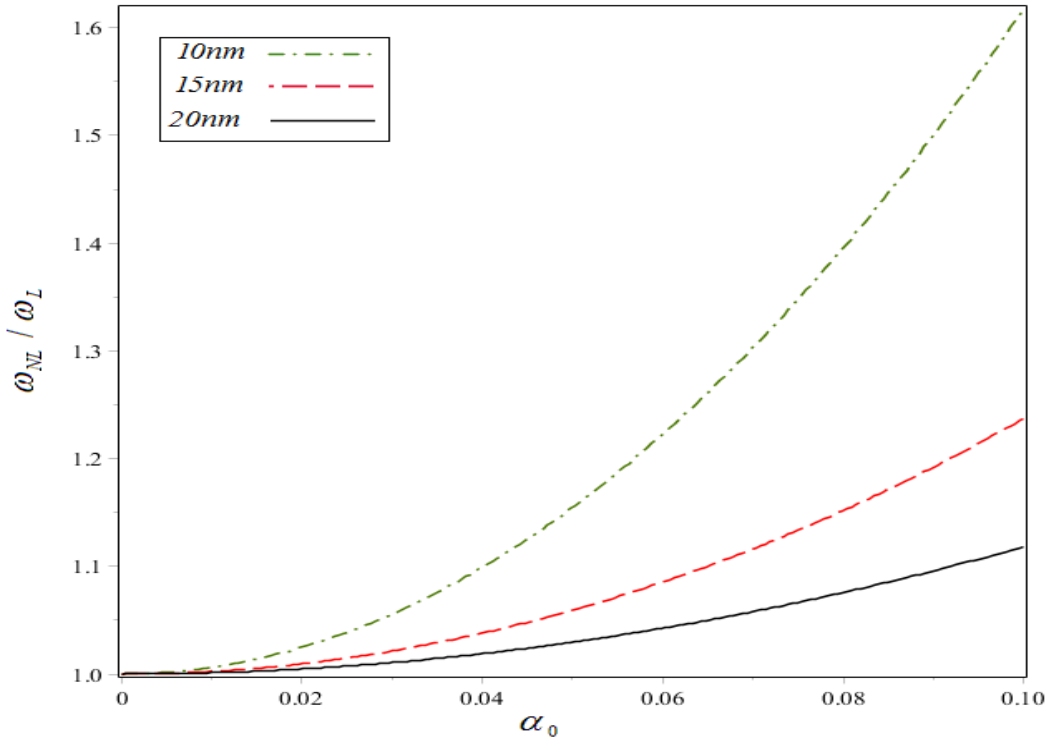

Figure 4-3 Frequency ratio vs. initial condition for different piezoelectric thickness.

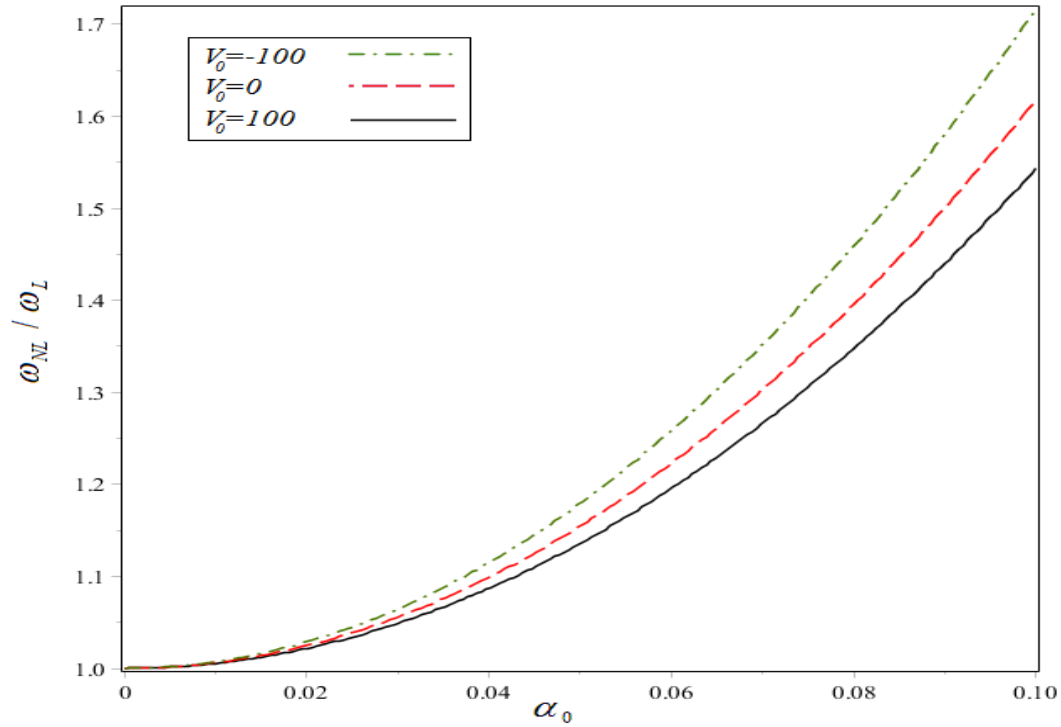

Figure 4-4 Frequency ratio vs. initial condition for different voltages V_0.

To check the validity of obtained solutions, variation of frequency ratio with piezoelectric thickness for a nanobeam having piezoelectric layer around it is shown in Figure 4-5 done by Yan and Jiang [87]. As shown, increase of the piezoelectric thickness results in the lower ratio as found in the results of presented work. Also increase on the magnitude of applied voltage leads to higher changes of the frequency ratio similar to the results of this study. In another work, vibration of a piezoelectric nanobeam is investigated by Ke, et al. is taken into the account [89]. Effects of non-local parameter on the frequency ratio of the structure is represented in Figure 4-6 and as it is obvious, an agreement is found between their results and this study [89].

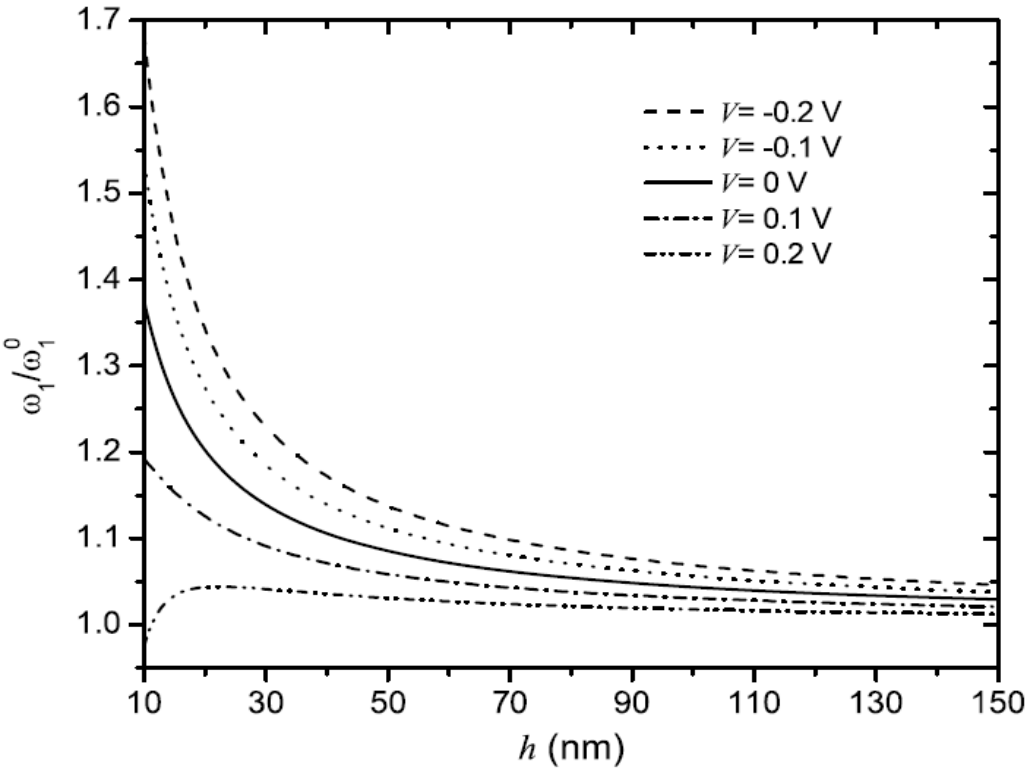

Figure 4-5 Variation of frequency ratio with piezoelectric thickness for different voltages V for piezoelectric-layered nanobeam [87].

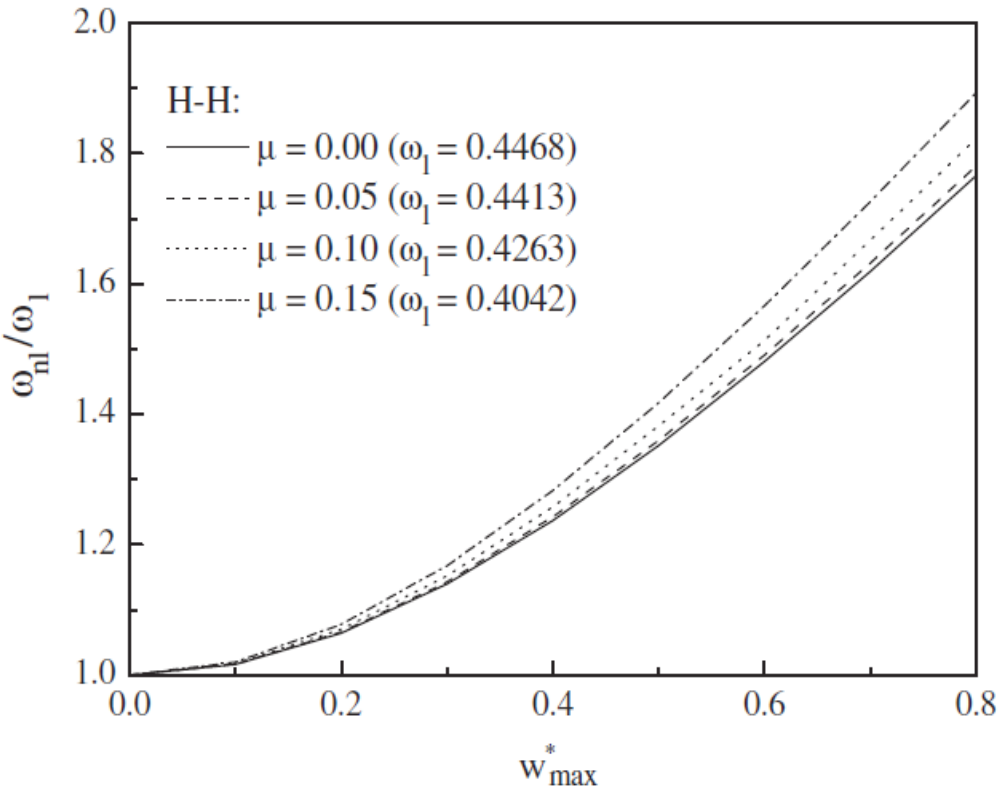

Figure 4-6 Frequency ratio vs. initial condition for different non-local parameter μ of H-H boundaries for piezoelectric nanobeam [89].

The steady state frequency responses due for primary resonance of the system due to the single frequency external excitation are represented in Figures 4-7 to 4-9. A parameter study is carried out for three parameters including nonlocal parameter, applied voltage and piezoelectric thickness.

It is obvious, the effect of nonlocal parameter on the amplitude of vibration and hardening behaviour of the system is considerable comparing to the case that this parameters is zero. Also, the increase on the piezoelectric thickness remarkably reduces the amplitude of vibration. The negative applied voltage increases the amplitudes of vibration unlike the positive one and the voltage shows not large impact on the system hardening.

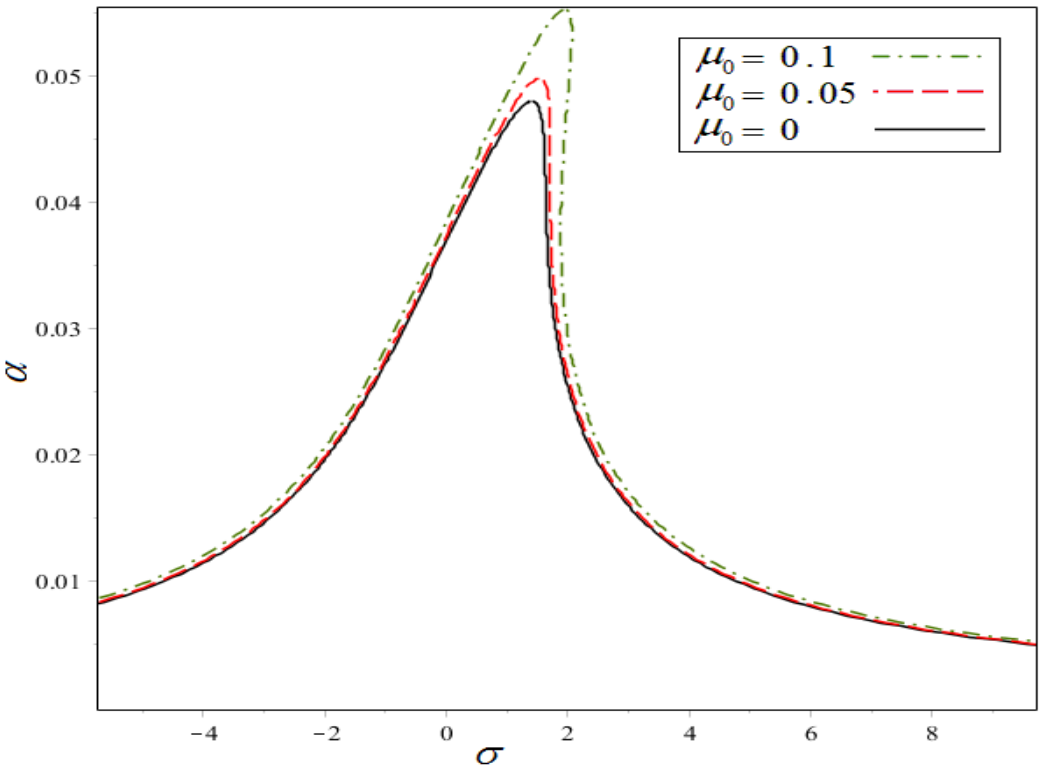

Figure 4-7 Non-local parameter μ_0 effect on frequency response for primary resonance.

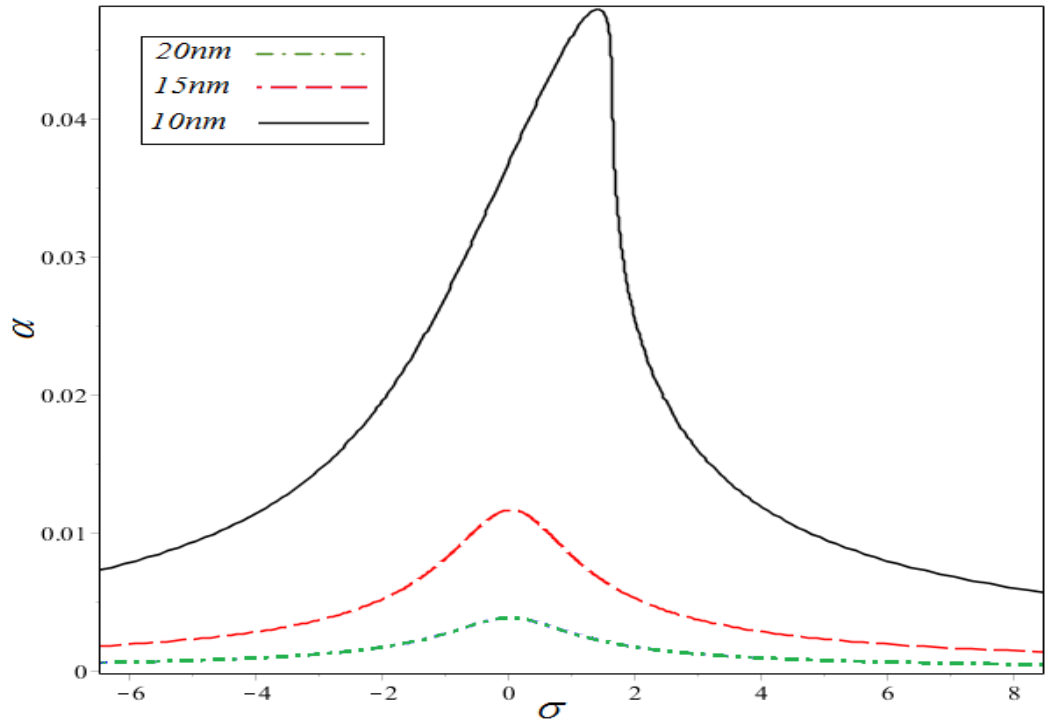

Figure 4-8 Piezoelectric thickness effect on frequency response of primary resonance.

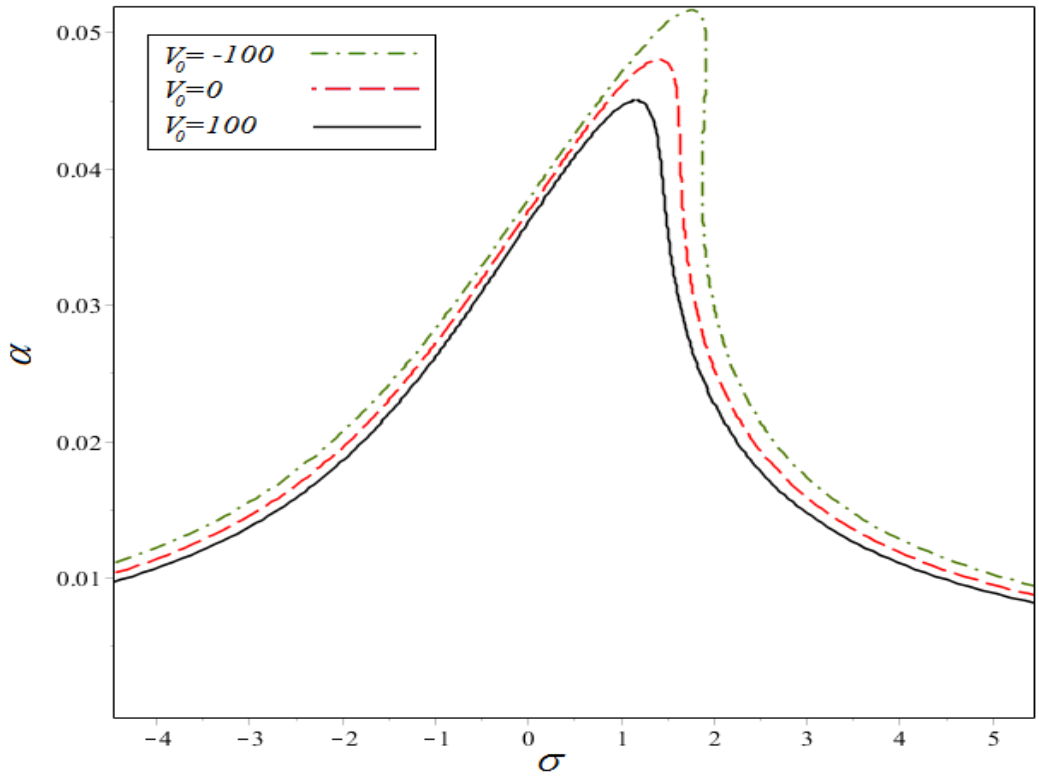

Figure 4-9 Voltage V_0 effect on frequency response for primary resonance.

The first simultaneous resonance due to the multi-frequency excitation has been examined in figures 4-10 and 4-11 for different small scale parameters and applied voltages. The positions of applied forces are taken to be in 0.5 and 0.75 of the nanotube length from the left end of the structure. These two distances are chosen typically and show the positions that maximum amplitudes of first and second modes of vibration are located. As predicted, the small scale parameter is very effective on the frequency response similar to previous case. In this case the effect of applied voltage is much considerable both in amplitudes of vibration and hardening behavior and as seen, a great shift would happen in the response curves by changing the voltage which should be considered when such systems are under multi-frequency excitation.

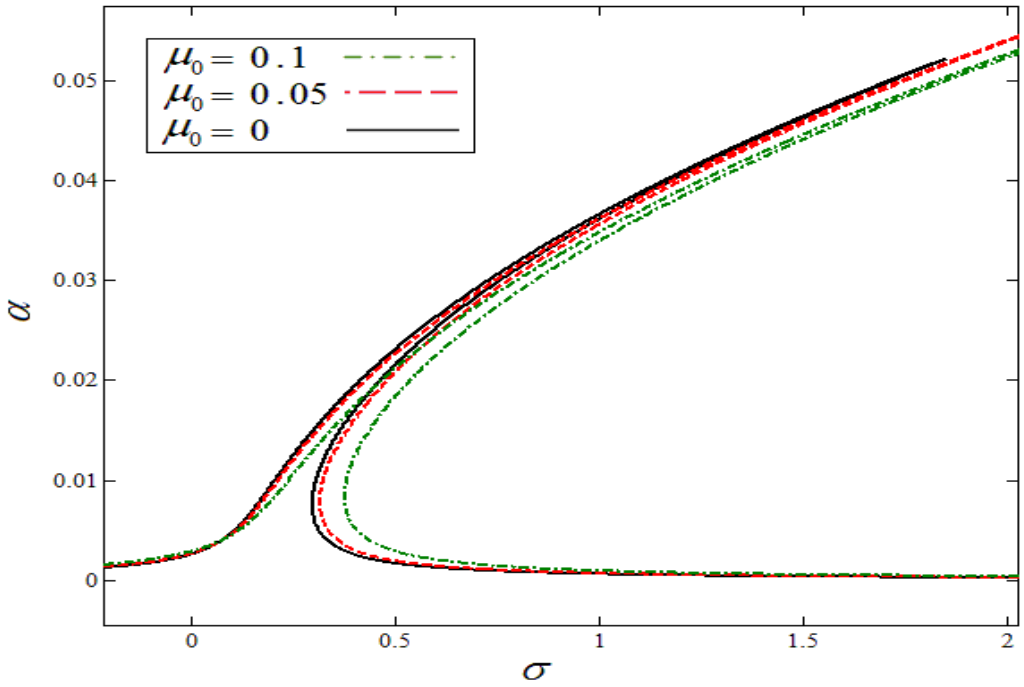

Figure 4-10 Non-local parameter μ_0 effect on frequency response of simultaneous resonance case A ($\omega \approx 3\Omega_1 \approx 2\Omega_2 - \Omega_1$).

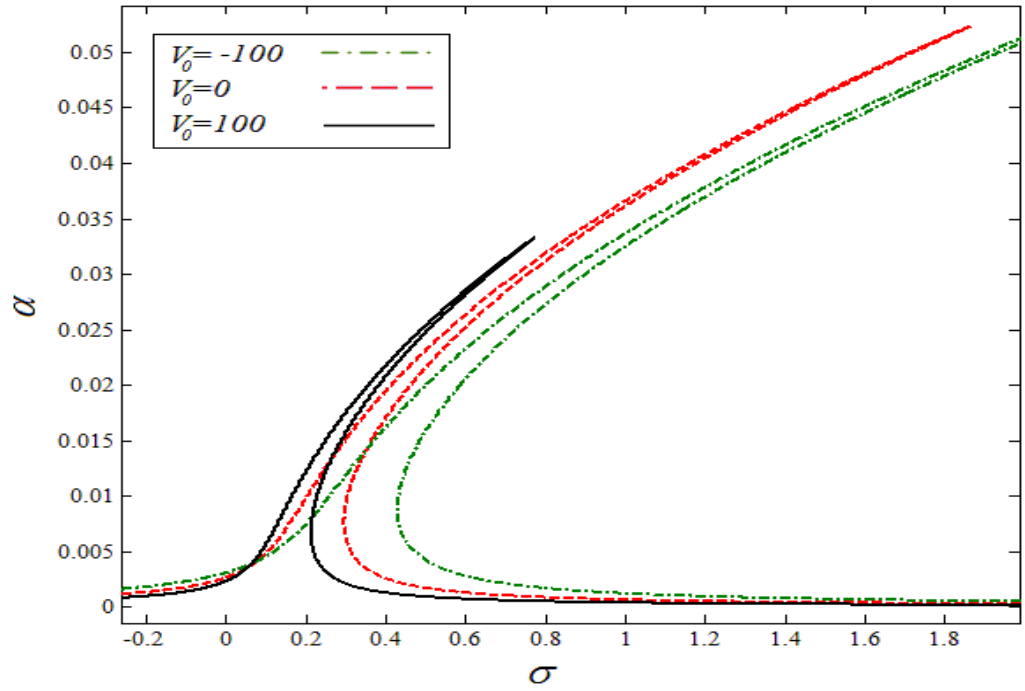

Figure 4-11 Effect of voltage V_0 on the frequency response of simultaneous resonance case A ($\omega \approx 3\Omega_1 \approx 2\Omega_2 - \Omega_1$).

The second simultaneous resonances caused by the multi-frequency excitation has been investigated in figures 4-12 to 4-14. A typical response for this case has been depicted in Figure 4-13 and as can be found, the response contains solid and dashed lines that indicate the stable and unstable solutions, respectively. Here, the two black branches resemble the subharmonic resonance and the red line denotes the combination one.

There are different possible solutions such as one nontrivial solution, three non-trivial solutions none or one of which are unstable, four non-trivial solutions one of which unstable and five non-trivial solutions one or two of which are unstable. For the possible solutions with more than one stable solutions, the initial conditions would identify which one is actually the physical solution for the structure vibration[97].

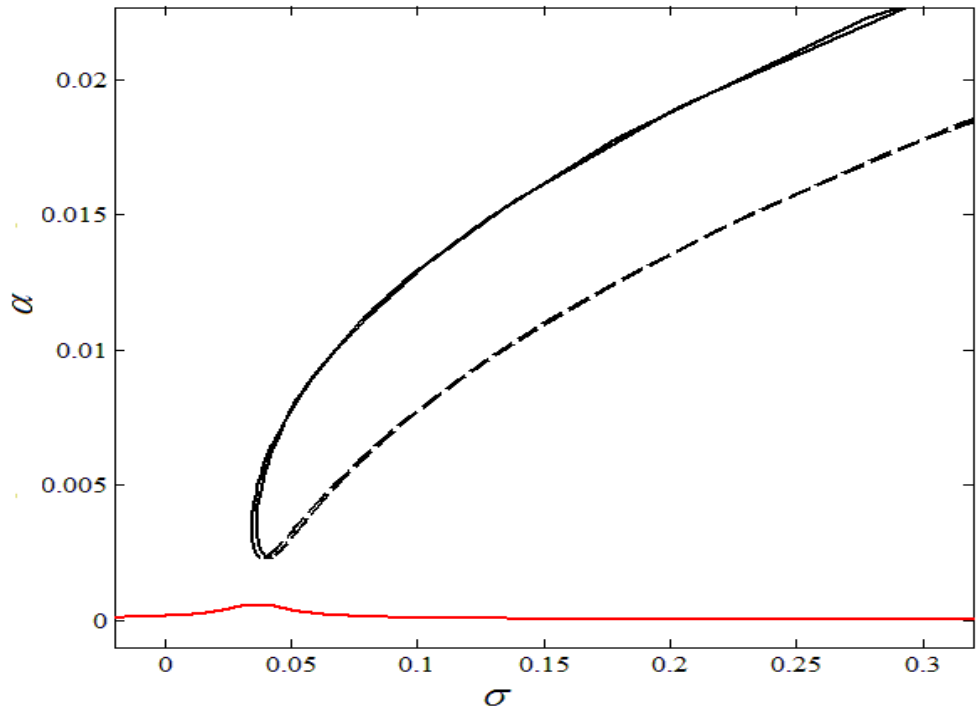

Figure 4-12 frequency response of simultaneous subharmonic-combination resonances.

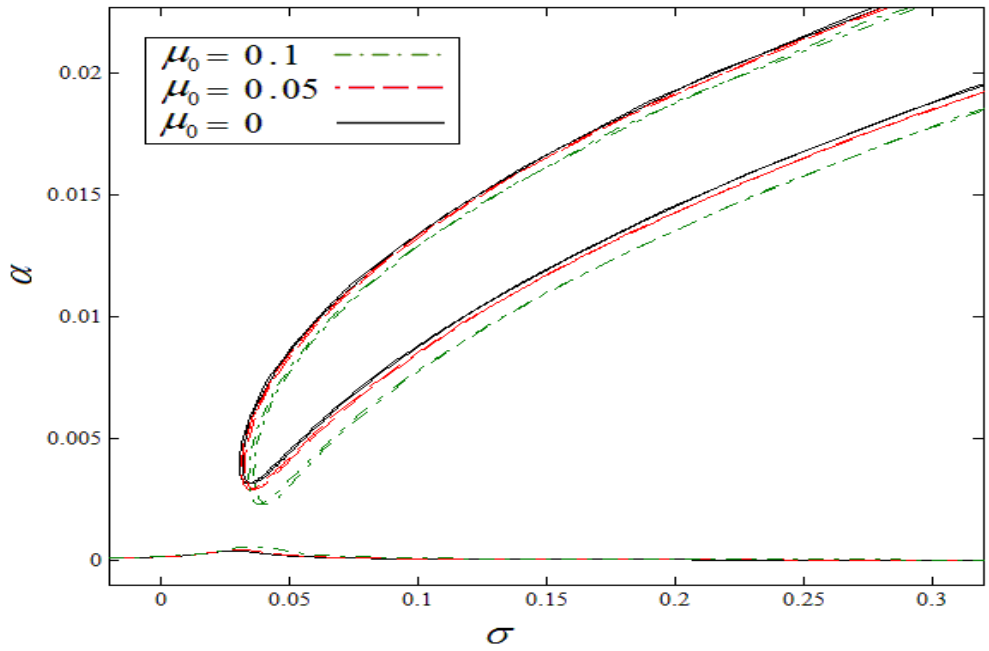

Figure 4-13 Non-local parameter μ_0 effect on frequency response of simultaneous resonance case B ($\omega_1 \approx \frac{\Omega_1}{3} \approx 2\Omega_2 - \Omega_1$).

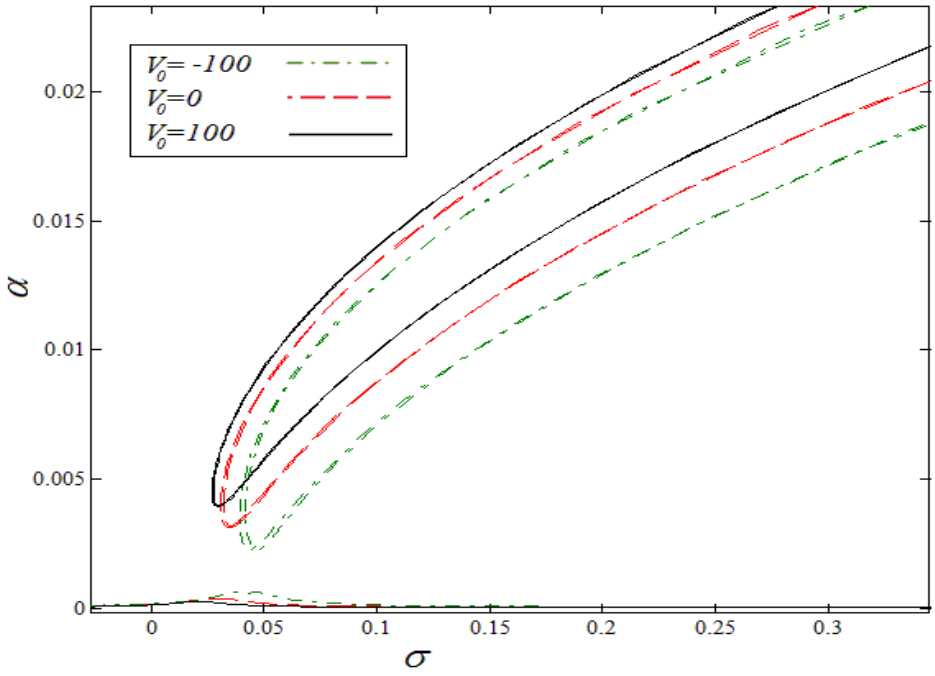

Figure 4-14 Effect of voltage V_0 on the frequency response of simultaneous resonance case B ($\omega_1 \approx \frac{\Omega_1}{3} \approx 2\Omega_2 - \Omega_1$).

The nonlocal parameter effect on the system response is investigated in Figure 4-13 and increase of this parameter shifts the solutions to the right side and for larger nonlocal parameter, the two top curves are more separated while both approach the bottom curve.

Figure 4-14 shows the effect of applied voltage on the shift and bend of the frequency response and how the branches separated or get closer for higher magnitude of voltages. Hence, the vibration of proposed model and different resonance cases for the structure force vibration have been analyzed in this section and a variety of responses under the effects of different parameters were studied.

Chapter 5: **Vibration analysis of fluid-conveying piezoelectric-layered nanotubes**

5.1. INTRODUCTION

Nonlinear vibration of a nanotube with a piezoelectric layer around it and conveying fluid flow is investigated in this Chapter. The mathematical modeling of the structure is developed by means of energy method and nonlocal theory similar to the procedure used in previous Chapters. The piezoelectric layer is taken to be slender and the fluid motion has a constant velocity. Effects of fluid motion arise in the kinetic energy and external energy of the Lagrangian equation and consequently further terms are derived and added to the governing equation due to this motion. In this Chapter the applied voltage is considered to have both constant and time variable terms and accordingly different conditions appear in the system model and corresponding solutions including parametric excitation. The forced vibration of system under external load and parametric excitation is analyzed and three different resonance conditions such as primary, parametric and simultaneous primary-parametric resonances are studied employing multiple scales method. Eventually, effects of various parameters such as applied voltage, piezoelectric layer, nonlocal parameter and fluid flow on the frequency-amplitude relation and frequency responses of the system is carried out and discussed in detail.

5.2. MATHEMATICAL MODELING

In this section the governing equation of motion for a nanotube having a piezoelectric layer and carrying a fluid is modeled. The concept of the structure is similar to what we discussed in previous Chapter which means that the structure is modeled as a double-walled nanotube in which the layers are attached to each other and there is no friction in between. The outer layer is made by a piezoelectric material and the inner one is a carbon nanotube and Euler-Bernoulli beam theory is associated with nonlocal non-classical theories for the nano system. However, it is considered that a fluid flow with constant velocity appears inside the system and consequently the analysis of fluid-solid interaction should be accomplished here. According to the literature, the reason of this consideration is that carbon nanotubes have almost frictionless interface at their walls and fluids [21]. So, they are appropriate for high flow velocities and the rate of velocity change is very small. The schematic model for the proposed system (Figure 5.1.a) and an element of fluid-conveying nanotube (Figure 5.2.b) are shown here.

To implement the energy method, the strain energy, kinetic energy and external force work relationships should be developed. Effect of fluid motion appears in two terms. First in the kinetic energy of the whole system caused by the fluid motion, and second in the work caused by the forces that the fluid flow applies to the solid structure. So, in this section the equations of these two terms are developed and added to the corresponding terms of the former model proposed in Chapter 4. As seen in the figure, the velocity vector is written as

$$\vec{V} = (v\cos(\alpha) + u_t)\vec{i} + (w_t - v\sin(\alpha))\vec{j} \tag{5.1}$$

where v is the value of fluid flow velocity and also u and w respectively show the longitudinal and transversal displacement of the structure same as before. $\vec{i}$ and $\vec{j}$ are the unit vectors in horizontal and vertical directions, respectively.

The kinetic energy due the motion of fluid is expressed as

$$T_f = \int_0^L \int_{A_f} \rho_f \vec{V}.\vec{V}\, dA_f\, dx \tag{5.2}$$

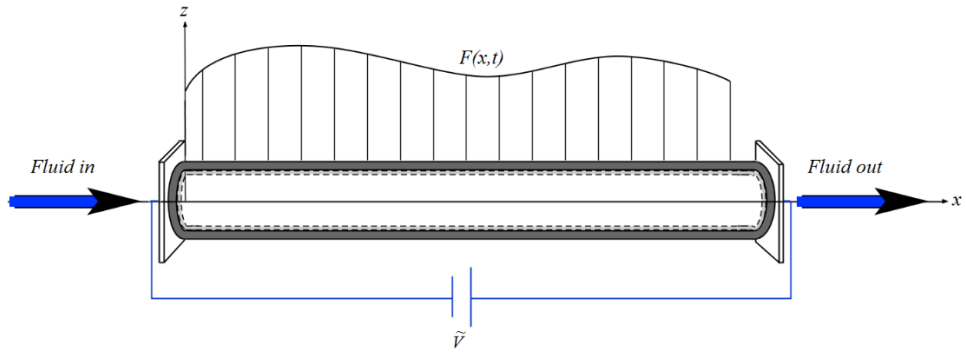

(*a*)

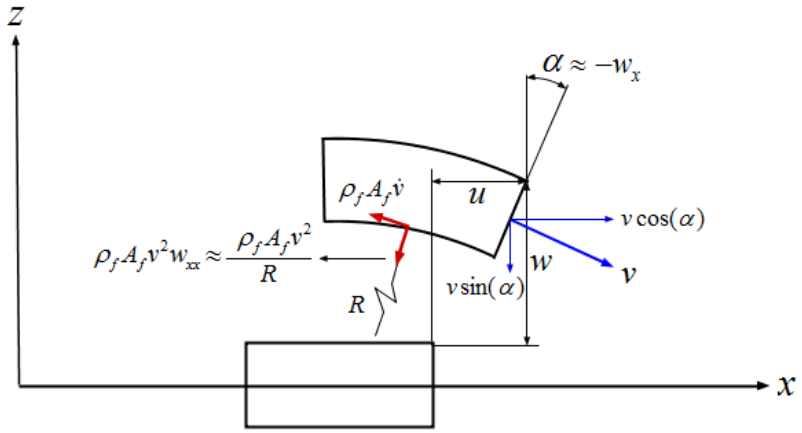

(*b*)

Figure 5-1 (*a*) Schematic model of the piezoelectric-layered nanotube conveying fluid, (*b*) An element of fluid-conveying beam under deformation [99].

In Eq. (5.2) ρ_f is the fluid density and A_f denotes the cross-sectional area of the fluid. Note that the effect of rotary inertia has been neglected in the energy due to the small size. Using the definition $\alpha \approx -w_x$, the variation of fluid kinetic energy equals

$$\begin{aligned}
\delta T_f &= \rho_f A_f \int_{t_1}^{t_2} \int_0^L \vec{V}.\delta\vec{V} dx dt \\
&= \rho_f A_f \int_{t_1}^{t_2} \int_0^L \{[(v\cos(\alpha)+u_t)\vec{i} + (w_t - v\sin(\alpha))\vec{j}].[\delta(v\cos(\alpha)+u_t)\vec{i} \\
&\qquad + \delta(w_t - v\sin(\alpha))\vec{j}]\} dx dt \\
&= \rho_f A_f \int_{t_1}^{t_2} \int_0^L \{(v\cos(\alpha)+u_t)(v\sin(\alpha)\delta w_x + \delta u_t) + (w_t - v\sin(\alpha))(\delta w_t \\
&\qquad + v\cos(\alpha)\delta w_x)\} dx dt
\end{aligned} \tag{5.3}$$

After some mathematical simplifications and by applying the boundary conditions knowing that at t_1, t_2 the variations $\delta w, \delta u$ are zero, the solution of above integral by means of integration by parts is obtained as

$$\begin{aligned}
\delta T_f = \rho_f A_f \int_{t_1}^{t_2} \int_0^L \{[&-v\sin(\alpha) w_{xt}\delta u - v\sin(\alpha) u_{xt}\delta w + v\cos(\alpha) w_{xx} u_t \delta w - u_{tt}\delta u \\
&- w_{tt}\delta w - 2v\cos(\alpha) w_{xt}\delta w - v\sin(\alpha) w_{xx} w_t \delta w]\} dx dt
\end{aligned} \tag{5.4}$$

Finally, the variations of kinetic energy due to the presence of fluid flow, by factorizing the coefficients of $\delta w, \delta u$, is

$$\begin{aligned}
\delta T_f = \rho_f A_f \int_{t_1}^{t_2} \int_0^L \{&-[v\sin(\alpha) u_{xt} - v\cos(\alpha) w_{xx} u_t + w_{tt} + 2v\cos(\alpha) w_{xt} + v\sin(\alpha) w_{xx} w_t]\delta w \\
&-[v\sin(\alpha) w_{xt} + u_{tt}]\delta u\} dx dt
\end{aligned} \tag{5.5}$$

The external work of the forces that the fluid exerted on the structure should be found. As seen in Figure 5.1.b, the centrifugal and tangential forces are generally applied to the system. However, by considering the fluid velocity constant, the latter would be

vanished and it is only needed to find the work done by centrifugal force F_c. Using the displacement vector $u\vec{i} + w\vec{j}$, the force vector and the corresponding external work are expressed as

$$F_c = -\rho_f A_f v^2 w_{xx}(\sin(\alpha)\vec{i} + \cos(\alpha)\vec{j}) \tag{5.6}$$

$$W_f = \int_0^L \{[-\rho_f A_f v^2 w_{xx}(\sin(\alpha)\vec{i} + \cos(\alpha))\vec{j}].[u\vec{i} + w\vec{j}]\}dx \tag{5.7}$$

And the variation of corresponding external work is

$$\begin{aligned}\delta W_f &= \int_{t_1}^{t_2}\int_0^L \{[-\rho_f A_f v^2 w_{xx}(\sin(\alpha)\vec{i} + \cos(\alpha))\vec{j}].[\delta u\vec{i} + \delta w\vec{j}]\}dxdt \\ &= -\rho_f A_f v^2 \int_{t_1}^{t_2}\int_0^L \{\sin(\alpha)w_{xx}\delta u + \cos(\alpha)w_{xx}\delta w\}dxdt\end{aligned} \tag{5.8}$$

Now the equations (5.5) and (5.8) are combined with the variation equations of eternal work, strain and kinetic energies obtained for piezoelectric-layered nanotube in previous Chapters which are equations (3.15), (4.9) and (4.13), respectively. Therefore, by setting the coefficients of the variations equal to zero, one can obtain

$$\begin{aligned}\delta w: \overline{M}_{xx} &= \overline{\rho A} w_{tt} + m w_{tt}\Delta(x - x_m) - \overline{EA}(u_{xx}w_x + u_x w_{xx} + \frac{3}{2}w_{xx}w_x^2) \\ &+ 2Pw_{xx} + \rho_f A_f[v\sin(\alpha)u_{xt} - v\cos(\alpha)w_{xx}u_t + w_{tt} + 2v\cos(\alpha)w_{xt} \\ &+ v\sin(\alpha)w_{xx}w_t + v^2\cos(\alpha)w_{xx}] - A_1 e_1 \frac{\partial}{\partial x}(\varphi_x w_x) - F(x,t)\end{aligned} \tag{5.9}$$

$$\delta\varphi: \frac{\partial D_1}{\partial x} = 0 \tag{5.10}$$

Substituting Eq. (5.10) into Eq. (5.9) and using the definition of shear forces of inner layer and piezoelectric material from previous Chapter, the equation corresponding

to the bending moments can be obtained. Finally, by combining above equation with the nonlocal theory and using the governing equation for the moments considering small scale effect, the equations of motion for the proposed system are achieved as

$$\begin{aligned}
&\overline{EI}w_{xxxx} + \overline{\rho A}w_{tt} + mw_{tt}\Delta(x-x_m) - \overline{EA}(u_{xx}w_x + u_x w_{xx} + \frac{3}{2}w_{xx}w_x^2) \\
&+ 2Pw_{xx} + \rho_f A_f[v\sin(\alpha)u_{xt} - v\cos(\alpha)w_{xx}u_t + w_{tt} + 2v\cos(\alpha)w_{xt} \\
&+ v\sin(\alpha)w_{xx}w_t + v^2\cos(\alpha)w_{xx}] - A_1 e_1 \frac{\partial}{\partial x}(\varphi_x w_x) - F(x,t) \\
&-(e_0 a)^2 \frac{\partial^2}{\partial x^2}\{\overline{\rho A}w_{tt} + mw_{tt}\Delta(x-x_m) - \overline{EA}(u_{xx}w_x + u_x w_{xx} + \frac{3}{2}w_{xx}w_x^2) \\
&+ 2Pw_{xx} + \rho_f A_f[v\sin(\alpha)u_{xt} - v\cos(\alpha)w_{xx}u_t + w_{tt} + 2v\cos(\alpha)w_{xt} \\
&+ v\sin(\alpha)w_{xx}w_t + v^2\cos(\alpha)w_{xx}] - A_1 e_1 \frac{\partial}{\partial x}(\varphi_x w_x) - F(x,t)\} = 0
\end{aligned} \tag{5.11}$$

$$\frac{\partial \varphi_x}{\partial x} = \frac{e_1}{k_1}[\frac{\partial}{\partial x}(u_x + \frac{1}{2}w_x^2)] = 0 \tag{5.12}$$

Again for above equations, the non-dimensional forms are applied as before and the solutions will be obtained according to the dimensionless parameters as defined in Appendix *C*.

5.3. VIBRATION SOLUTION OF PIEZOELECTRIC LAYERED NANOTUBE CONVEYING FLUID

Similar to previous Chapters, the Galerkin method is employed to simplify the obtained partial differential equation in the previous section considering fundamental mode of vibration. For simplicity, it is assumed that $\sin(\alpha) \approx \alpha \approx -w_x$ and $\cos(\alpha) \approx 1$ [99]. Also, reviewing the literature shows that it is common to neglect the effect of higher order terms arising from the fluid motion on the system [99, 100]. In addition, for this Chapter the

applied voltage and corresponding electric field are taken to have both constant and time variable terms and therefore more detailed cases can be investigated due to this consideration. So, by taking the function of transversal and longitudinal displacements as Eq. (3.21) and applying the idea of orthogonality of normal modes for the fundamental mode of vibration, the nonlinear ordinary differential equation governing to the time response of the system transversal vibration including small damping parameter is obtained as follows

$$\ddot{Y}(\hat{t}) + (\omega_0^2 + \varepsilon c_1 \cos(\Omega_1 \hat{t}))Y(\hat{t}) + 2\varepsilon\mu\dot{Y}(\hat{t}) + \varepsilon c_2 Y^3(\hat{t}) = \varepsilon F_0 \cos(\Omega_2 \hat{t}) \tag{5.13}$$

where the relations of ω_0^2, c_1, c_2 and F_0 are represented in Appendix *C*. Note that the external load is taken as Eq. (4.41) which is a harmonic point load with the frequency Ω_2 and the applied voltage includes a constant value and a harmonic time function with the frequency Ω_1 as seen Appendix *C* which causes parametric excitation in the proposed system. Also, the required coefficients of above equation are ordered with respect to ε and inserted their effects on the solution procedure based on multiple scales method[97]. Now by substituting Eq. (5.22) as the solution of Eq. (5.13) and separating the same power of ε, gives

$$\varepsilon^0 : D_0^2 Y_0 + \omega_0^2 Y_0 = 0 \tag{5.14}$$

$$\varepsilon^1 : D_0^2 Y_1 + \omega_0^2 Y_1 = -2D_0 D_1 Y_0 - 2\mu D_0 Y_0 - c_1 Y_0 \cos(\Omega_1 T_0) - c_2 Y_0^3 + F_0 \cos(\Omega_2 T_0) \tag{5.15}$$

Similarly, the solution of Eq. (5.14) equals to

$$Y_0 = A(T_1)\exp(i\omega_0 T_0) + CC \tag{5.16}$$

Applying Eq. (5.16) into Eq. (5.15), one can reach

$$D_0^2 Y_1 + \omega_0^2 Y_1 =$$
$$-[2i\omega_0(A' + \mu A) + 3c_2 A^2 \bar{A}]\exp(i\omega_0 T_0) - \frac{c_1}{2}[A\exp(i(\Omega_1 + \omega_0)T_0) \quad (5.17)$$
$$+ \bar{A}\exp(i(\Omega_1 - \omega_0)T_0)] - c_2 A^3 \exp(3i\omega_0 T_0) + \frac{F_0}{2}\exp(\Omega_2 T_0) + CC$$

From above equation it is obvious that three resonance cases including primary, parametric and simultaneous primary-parametric resonances may occur in the system as discussed one by one here

- *Case A:* $\Omega_2 = \omega_0 + \varepsilon\sigma_2$

This case shows the primary resonance as seen in previous Chapters. Thus, the secular terms of Eq. (5.17)

$$-2i\omega_0(A' + \mu A) - 3c_2 A^2 \bar{A} + \frac{1}{2}F_0 \exp(i\sigma_2 T_1) = 0 \quad (5.18)$$

The aim is not to repeat the solution procedure as it was done in previous Chapter for single frequency excitation. Using the polar form $A = \frac{1}{2}\alpha\exp(i\theta)$, the steady state motion of the system for this resonance case can be explained by the following frequency-amplitude relationship

$$\sigma_2 = \left(\frac{3}{8}c_2\alpha^3 \pm (\frac{1}{4}F_0{}^2 - (\mu\omega_0\alpha)^2)^{1/2}\right) \Big/ (\omega_0\alpha) \quad (5.19)$$

and first approximate solution is

$$Y(\hat{t}) = \alpha\cos(\Omega_2\hat{t} - \gamma_2) + O(\varepsilon) \quad (5.20)$$

where $\gamma_2 = \sigma_2 T_1 - \theta$ and $O(\varepsilon)$ shows the higher order terms. Also, for all cases the nonlinear natural frequency of the system is equal to which can be used to find the ratio of nonlinear to linear frequency.

$$\hat{\omega}_0 = \omega_0 [1 + (\frac{3c_2}{8\omega_0^{\ 2}})\alpha^2] + O(\varepsilon^2) \tag{5.21}$$

- *Case B:* $\Omega_1 = 2\omega_0 + \varepsilon\sigma_1$

For this case namely parametric resonance, it is assumed that the frequency of parametric excitation caused by the applied voltage is near to the system natural frequency. Taking this condition, the elimination of secular terms from Eq. (5.17) gives

$$-2i\omega_1(A' + \mu A) - 3c_2 A^2 \overline{A} + \frac{1}{2} c_1 \overline{A} \exp(i\sigma_1 T_1) = 0 \tag{5.22}$$

Applying the polar form $A = \frac{1}{2}\alpha \exp(i\theta)$ and taking out the real and imaginary parts

$$\begin{cases} \frac{1}{2}(\gamma_1' - \sigma_1)\omega_0 \alpha + \frac{3}{8} c_2 \alpha^3 + \frac{1}{4} c_1 \alpha \cos\gamma_1 = 0 \\ \omega_0 \alpha' + \mu\omega_0 \alpha + \frac{1}{4} c_1 \alpha \sin\gamma_1 = 0 \end{cases} \tag{5.23}$$

where $\gamma_1 = \sigma_1 T_0 - 2\theta$.

For the steady-state motion of parametric resonance, one should set $\gamma_1' = \alpha' = 0$. Thus

$$\begin{cases} -\frac{1}{2}\sigma_1 \alpha + \frac{3}{8\omega_0} c_2 \alpha^3 = -\frac{1}{4\omega_0} c_1 \alpha \cos\gamma_1 \\ \mu\alpha = -\frac{1}{4\omega_0} c_1 \alpha \sin\gamma_1 \end{cases} \tag{5.24}$$

Solving the above system for α, the frequency-amplitude relationship of the steady-state motion is obtained as

$$\alpha = \left\{ \frac{8\omega_0}{3c_2} \left[\frac{\sigma_1}{2} \pm \left((\frac{c_1}{4\omega_0})^2 - \mu^2 \right)^{1/2} \right] \right\}^{1/2} \tag{5.25}$$

Form the above equation it can be found that the first condition of having solution is when $\frac{c_1}{4\omega_0} \geq \mu$. Also for positive σ_1, requires $\sigma_1 \geq 2((\frac{c_1}{4\omega_0})^2 - \mu^2)^{1/2}$ and when it is negative, requires $|\sigma_1| \leq 2((\frac{c_1}{4\omega_0})^2 - \mu^2)^{1/2}$ to have the solution. Thus, the response of system has been obtained for this case of resonance and to be discussed in next sections.

- *Case C*: $\omega_0 \approx \Omega_1 \approx \frac{1}{2}\Omega_2$

For this case it is assumed that the primary and parametric resonances occur simultaneously and the corresponding detuning parameters are introduced as

$$\begin{cases} \Omega_1 = 2\omega_0 + \varepsilon\sigma_1 \Rightarrow \Omega_1 T_0 = \omega_0 T_0 + \sigma_1 T_1 \\ \Omega_2 = \omega_0 + \varepsilon\sigma_2 \Rightarrow \Omega_2 T_0 = \omega_0 T_0 + \sigma_2 T_1 \end{cases} \tag{5.26}$$

Using the above definitions and eliminating the secular terms from Eq. (5.17), leads

$$2i\omega_0(A' + \mu A) + 3c_2 A^2 \overline{A} + \frac{1}{2} c_1 \overline{A} \exp(i\sigma_1 T_1) + \frac{1}{2} c_1 F_0 \exp(i\sigma_2 T_1) = 0 \tag{5.27}$$

Applying the polar form for *A* and separating the real and imaginary parts, one can have

$$\omega_0 \alpha' + \mu\alpha\omega_0 + \frac{1}{4} c_1 \alpha \sin(\gamma_1) - \frac{1}{4} F_0 \sin(\gamma_2) = 0 \tag{5.28}$$

$$-\alpha\omega_0\theta' + \frac{3}{8} c_2 \alpha^3 + \frac{1}{4} c_1 \alpha \cos(\gamma_1) - \frac{1}{4} F_0 \cos(\gamma_2) = 0 \tag{5.29}$$

where $\gamma_1 = \sigma_1 T_1 - 2\theta$ and $\gamma_2 = \sigma_2 T_1 - \theta$. For the steady state motion one should have $\gamma_1' = \gamma_2' = 0$. Thus

$$\sigma_1 = 2\theta', \sigma_2 = \theta', \Rightarrow \sigma_1 = 2\sigma_2 = 2\sigma \tag{5.30}$$

Thus, the frequency-amplitude relation could be obtained from the system of equations as

$$\begin{cases} \alpha + \dfrac{c_1}{4\mu\omega_0}\alpha\sin(2\gamma) - \dfrac{F_0}{2\mu\omega_0}\sin(\gamma) = 0 \\ -\sigma + \dfrac{3c_2}{8\omega_0}\alpha^2 + \dfrac{c_1}{4\omega_0}\cos(2\gamma) - \dfrac{F_0}{2\omega_0\alpha}\cos(\gamma) = 0 \end{cases} \tag{5.31}$$

Therefore, the solution of steady state motion could be found for this case as well and to be calculated for numerical values in next section.

5.4. RESULTS AND DISCUSSION

The aim of this section is to examine the obtained solutions of previous section and to perform parameter studies to investigate the effects of various physical and mechanical parameters on the vibration behavior of the developed structure. The physical properties of the structure and fluid flow have been chosen according to the references [8, 47, 76]. The frequency ratio and frequency responses are plotted for different resonance cases due the presence of applied harmonic voltage, external excitation and the influence of piezoelectric layer, fluid motion and small scale parameter are considered for the obtained results.

Figures 5-2 to 5-5 represent the variations of frequency ratio with respect to the initial amplitude of vibration and for all of them the increase on the initial amplitude leads to a nonlinear increase on the frequency ratio. Effect of the fluid velocity on the ratio is

shown in Figure 5-2 and accordingly for higher velocity, the ratio becomes larger as well. Hence, the fluid velocity is a considerable parameter for adjusting the structure natural frequency. Also, the variations of applied voltage makes a great change on the frequency ratio. It should be noted that the amplitudes of both constant and harmonic voltages have been changed for this study however the amplitude of harmonic one has no effect on the nonlinear natural frequency but on the forced vibration to be investigated later. Again the growth on the magnitude of the voltage has a direct impact on enhancing the ratio while the positive and negative voltages have opposite effects vs. each other.

Figures 5-4 and 5-5 have been plotted for different nonlocal parameters and piezoelectric thickness respectively. Similar to previous Chapters, the effect of nonlocal parameter should be taken into the account for the frequency analysis of such systems due to its effect on the frequency ratio. Also, the growth on the piezoelectric layer thickness would reduce the ratio by increasing the linear frequency.

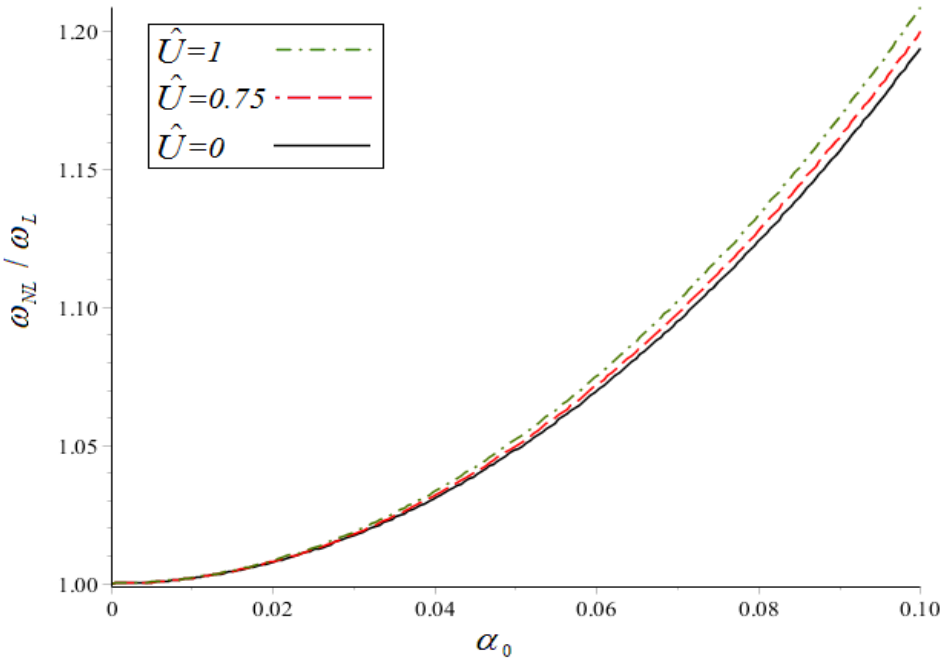

Figure 5-2 Frequency ratio vs. initial condition for different fluid velocities $\hat{U}$

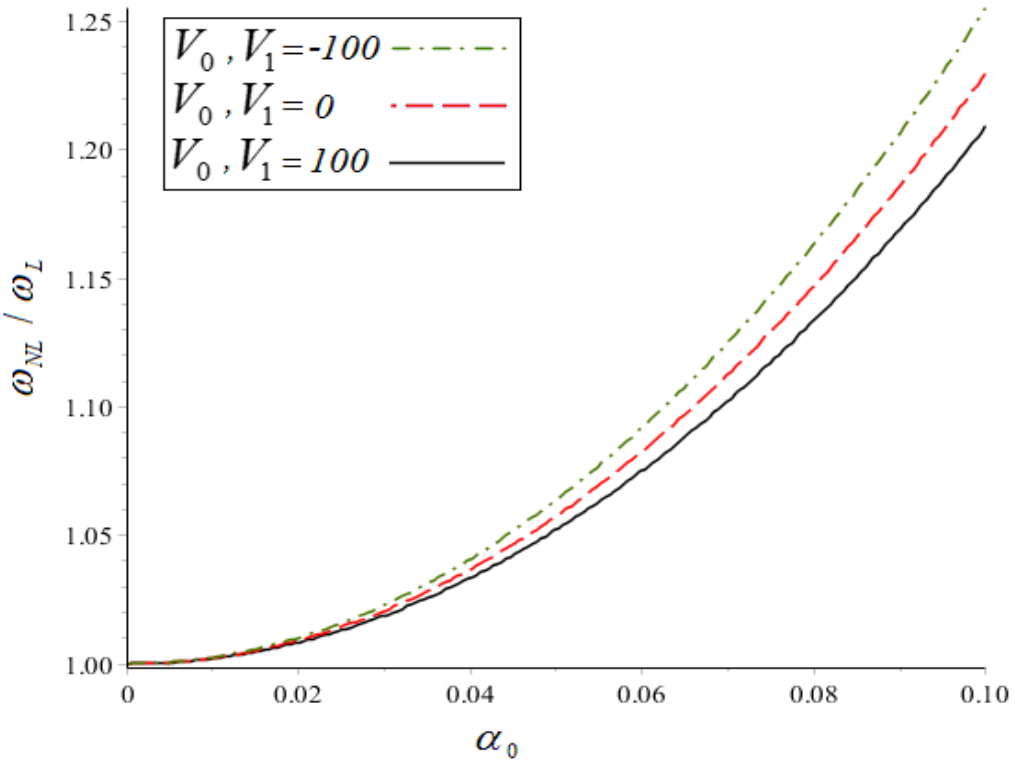

Figure 5-3 Frequency ratio vs. initial condition for different voltages V_0, V_1.

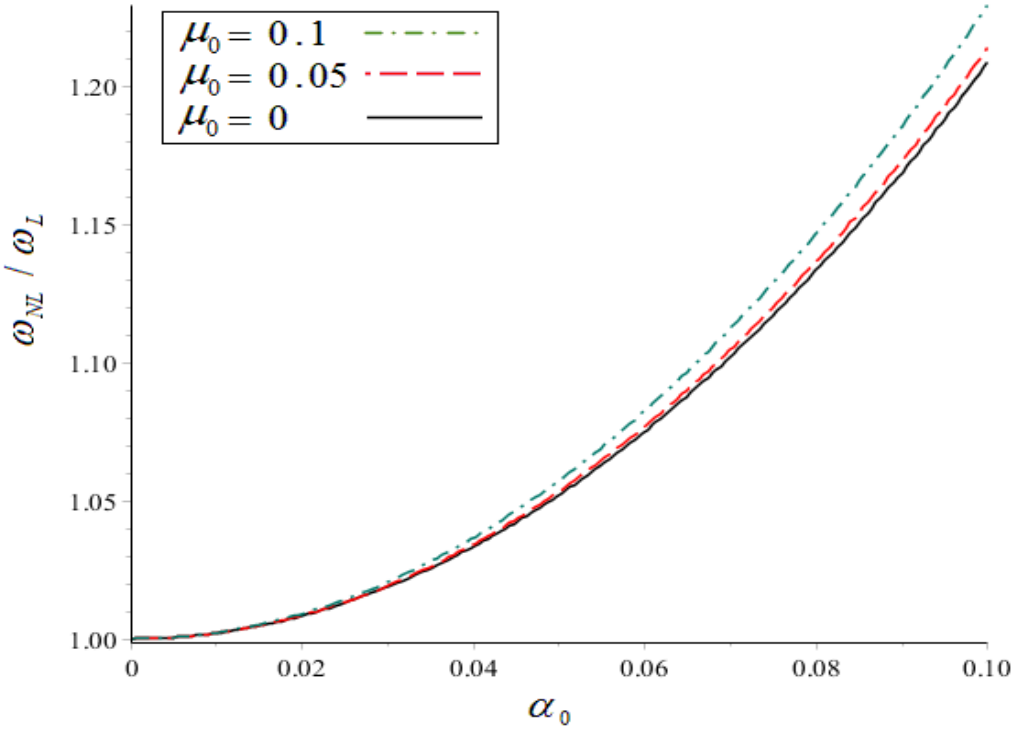

Figure 5-4 Frequency ratio vs. initial condition for different non-local parameter μ_0

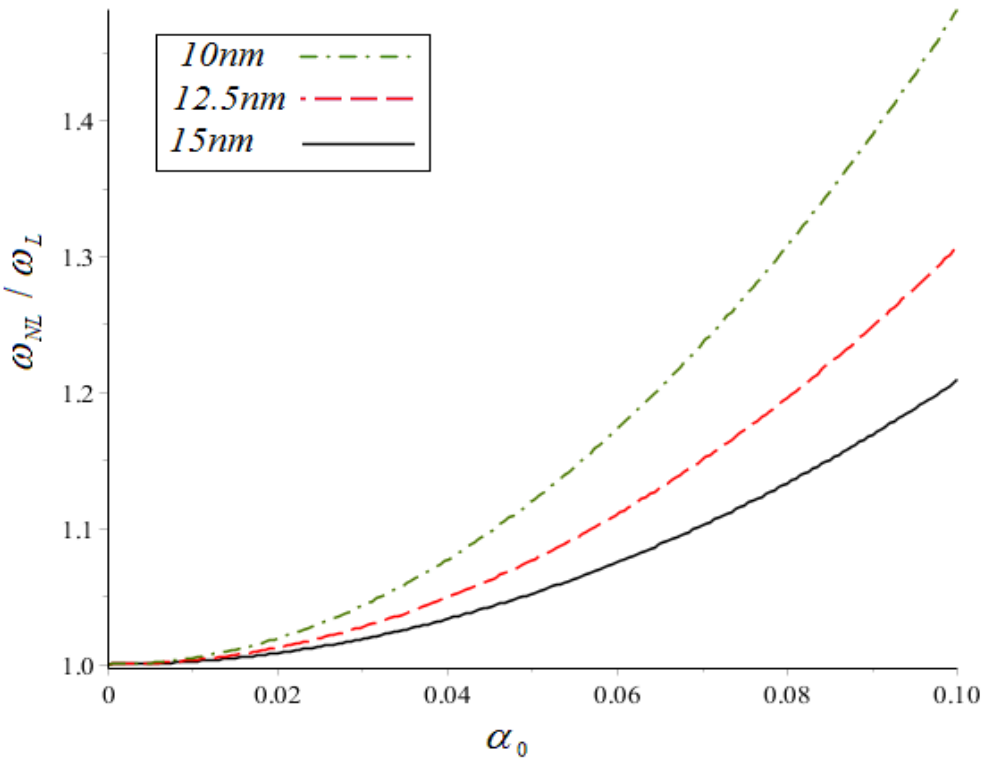

Figure 5-5 Frequency ratio vs. initial condition for different Piezoelectric thickness.

Variation of the linear frequency with respect to the fluid velocity of the system has been investigated in Figures 5-6 to 5-8 by testing different parameters such as intermediate mass, nonlocal parameter and applied voltages, respectively. As shown in the figures, the increase on the fluid velocity reduces the frequency with a nonlinear rate. The stable region for the system vibration is for the positive frequencies and when the frequency reaches to zero the system moves to the unstable region which happens at a specific fluid velocity known as critical velocity.

Also, the maximum frequency is when the fluid is not moving inside the system. From Figure 5-6 it can be understood that the intermediate mass does not have any effect on the critical velocity of the system and the increase on the mass would lead to lower maximum frequency which could be taken as a control parameter just for this purpose. It

should be noted that the position of the intermediate mass is taken to be at the middle of the structure length. Effect of nonlocal parameter is shown in Figure 5-7 and it is seen that the increase on this parameter would lead to smaller maximum linear frequency and critical fluid velocity. As it is obvious by considering the classical model in which the nonlocal parameter is zero, larger critical velocity is obtained which causes an error in predicting the vibrational behaviour and stability of proposed structure due to the influence of nano scale dimensions of the system. Effect of applied constant voltage is also depicted in figure 4-8 and accordingly the higher positive voltage, the higher maximum frequency and higher critical velocity obtain for the system vibration. It means an increase on the voltage would result in greater stable area of the system vibration which is very important and can be taken as a design and control parameter for modeling and analysis of the proposed system.

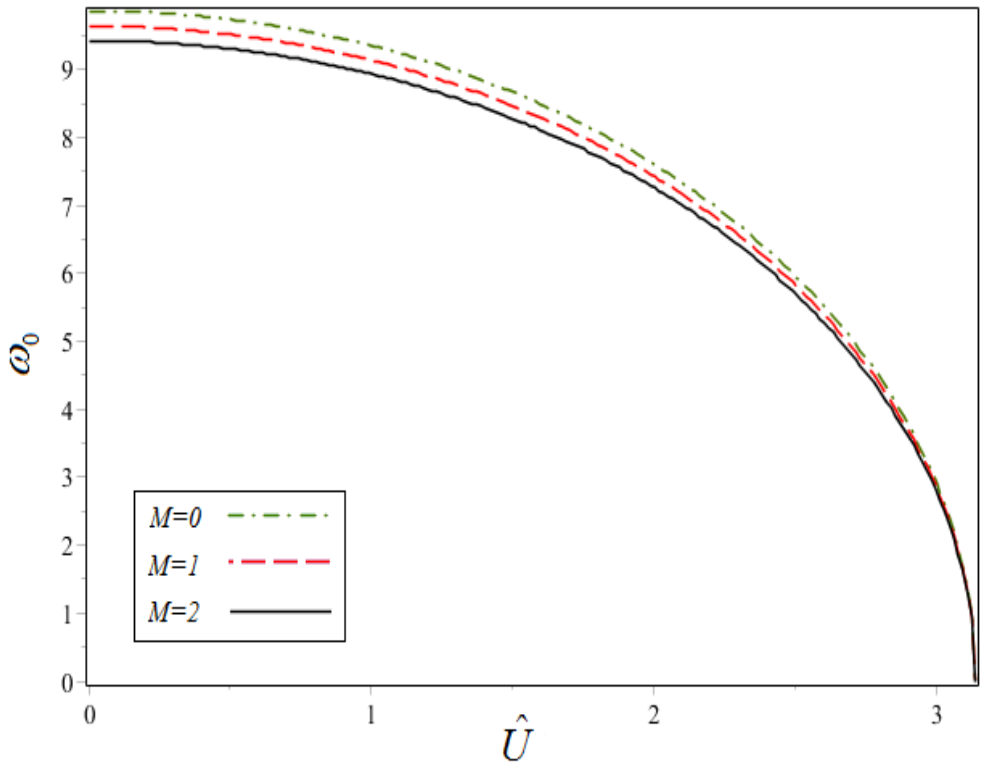

Figure 5-6 Linear frequency vs. fluid velocity for different intermediate masses M .

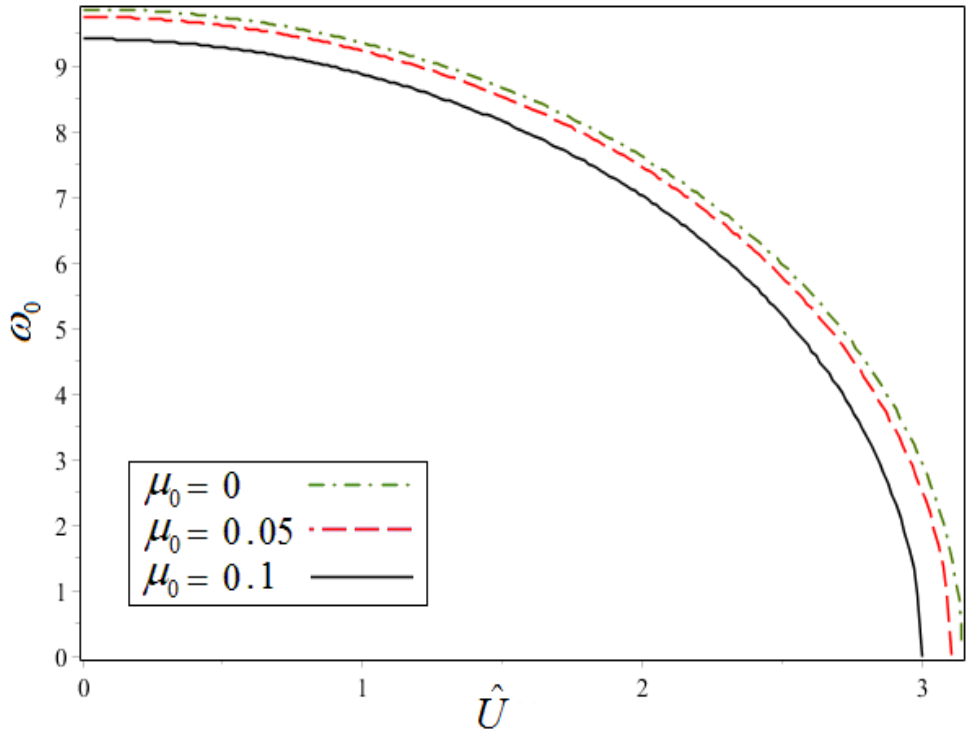

Figure 5-7 Linear frequency vs. fluid velocity for different non-local parameters μ_0

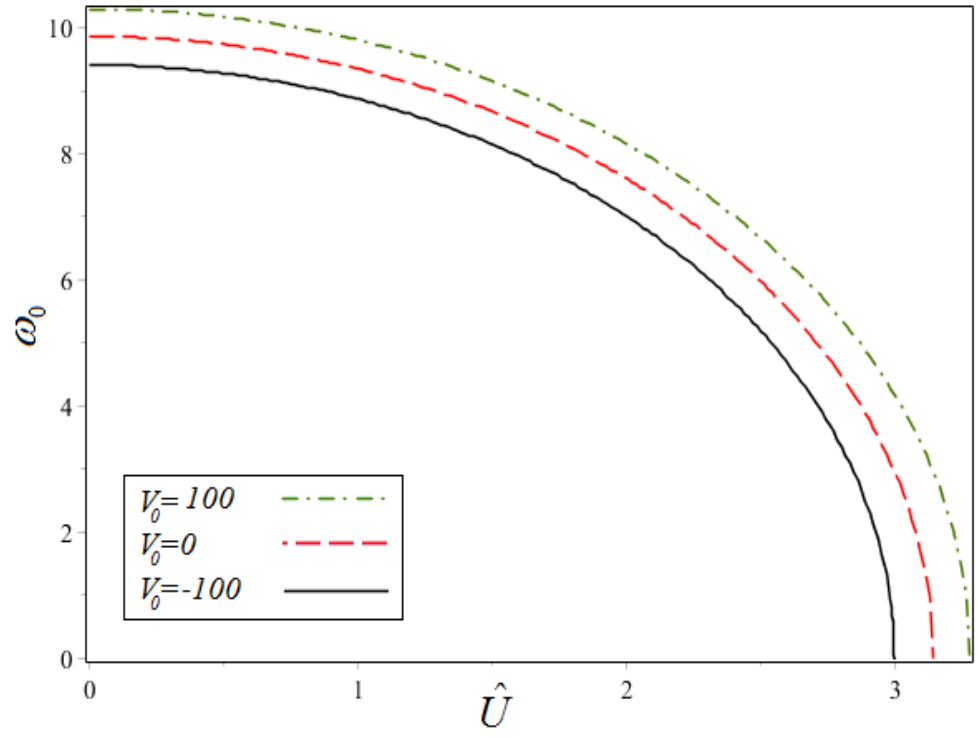

Figure 5-8 Linear frequency vs. fluid velocity for different voltages V_0

The validity of obtained solutions are examined by comparing some results of presented study with the similar works. Accordingly, the effect of fluid flow velocity on the frequency ratio of a nanotube is presented in Figure 5-9 [67]. As shown the increase of fluid velocity makes considerable growth on the ratio similar to this study. It should be noted that they considered classical theories for modeling the structure vibration unlike the presented work [67]. Also, the linear frequency variation with fluid velocity is shown in Figure 5-10 for a fluid-conveying carbon nanotube vibration [73]. Effect of fluid velocity on the frequency and non-local parameter on the stability region are shown in this work which have good agreements with the presented results of this study. Note that the results of their work were obtained for actual system dimensions while the results of presented work is in non-dimensional form [73].

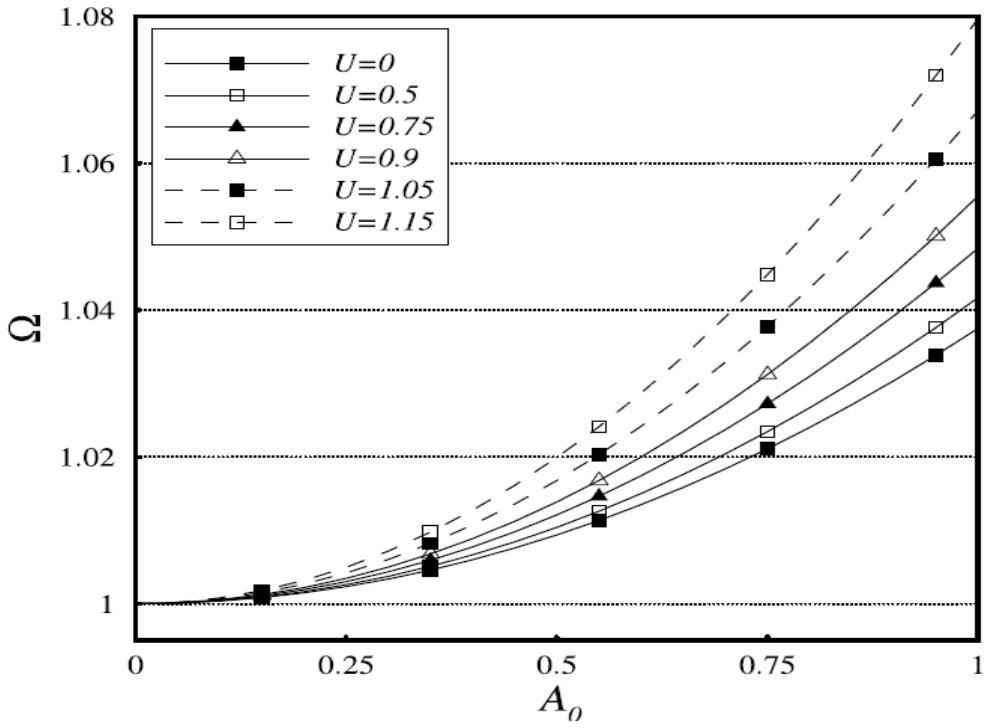

Figure 5-9 Frequency ratio vs. initial condition for different fluid velocities *U* for fluid-conveying nanotube [67].

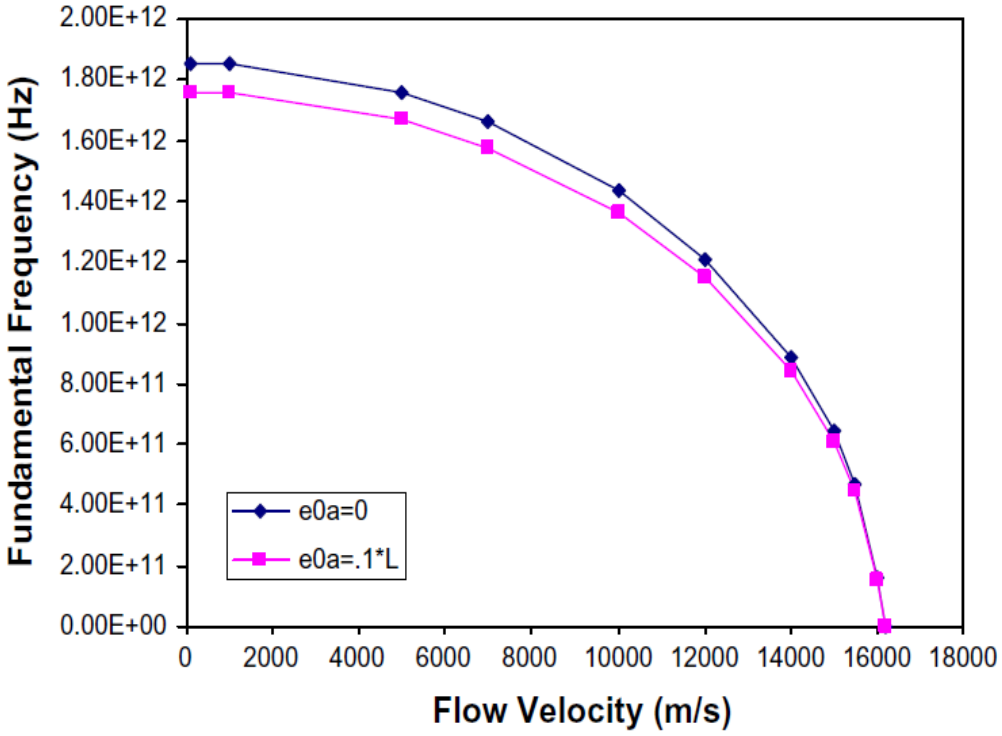

Figure 5-10 Linear frequency vs. fluid velocity for different non-local parameters e_0a for fluid-conveying nanotube [73].

The results of primary resonance due to the external excitation have been depicted in figures 5-11 to 5-13. Effect of changing the fluid velocity on the frequency responses has been shown in Figure 5-11 and as seen here, the more fluid velocity, the higher amplitude of vibration and harder behaviour would happen in the system vibration and consequently by adjusting the fluid velocity the desirable amplitude and hardening behaviour could be obtained for the system.

The effects of piezoelectric thickness and nonlocal parameters are presented in Figures 5-12 and 5-14, respectively and as seen in previous models, the frequency response is very sensitive to both parameters in terms of nonlinear hardening behaviour and amplitude of vibration.

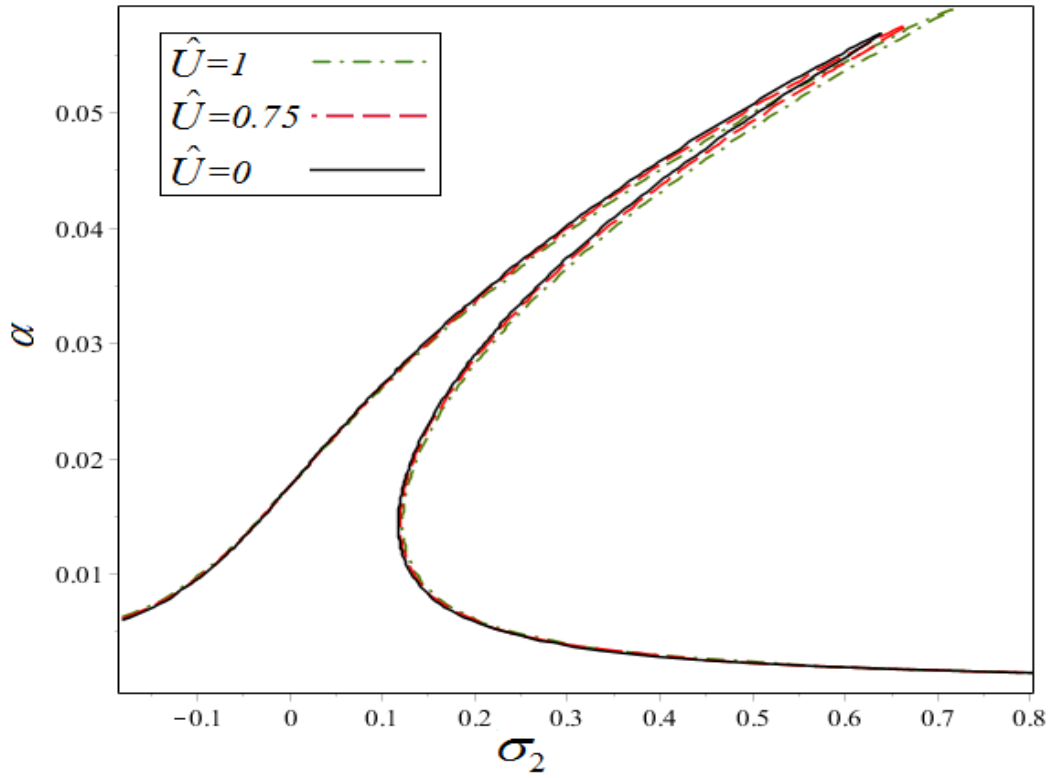

Figure 5-11 Fluid velocity $\hat{U}$ effect on the frequency response of primary resonance.

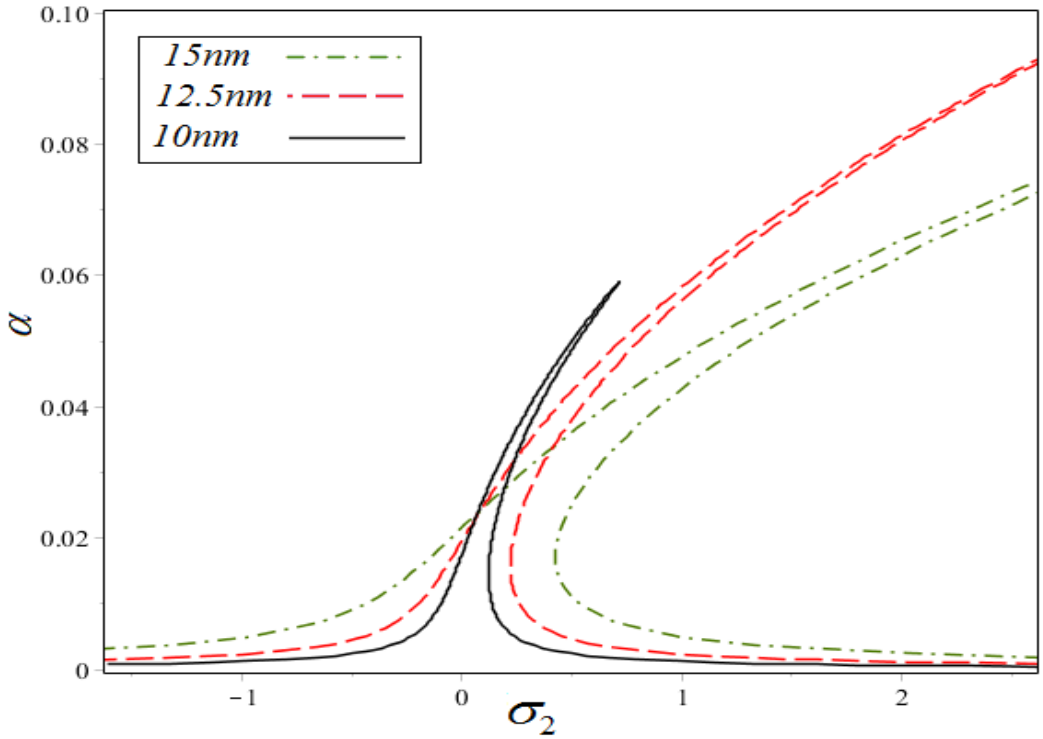

Figure 5-12 Piezo-layer thickness effect on frequency response of primary resonance

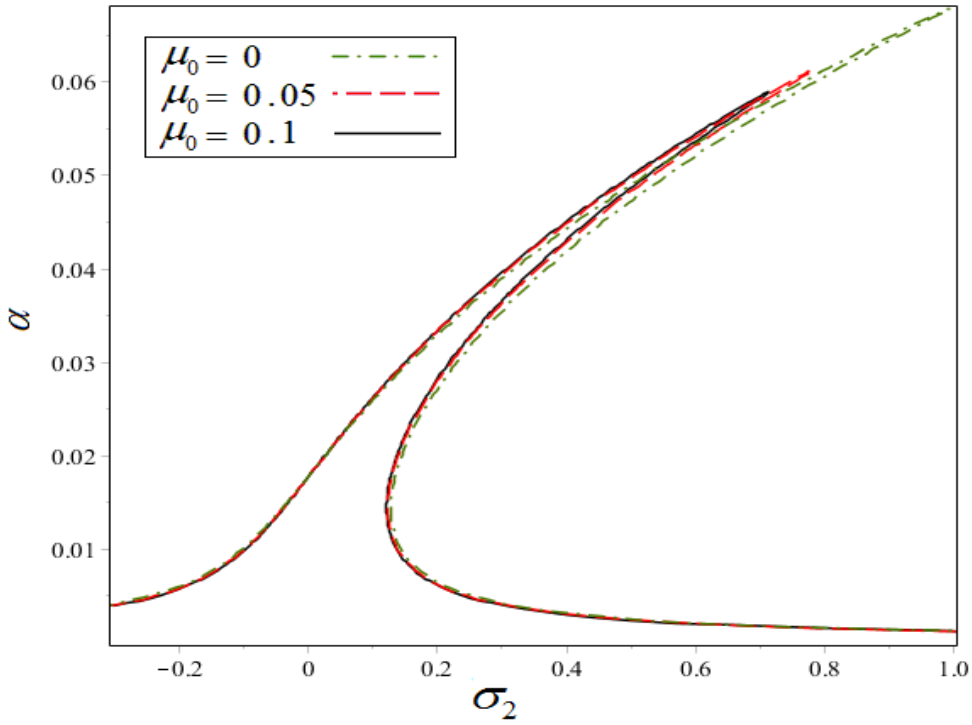

Figure 5-13 Nonlocal parameter μ_0 effect on frequency response of primary resonance

The vibrational behaviours of the structure under parametric excitation which is caused by the applied harmonic voltage are represented in figures 5-14 to 5-21. Figure 5-14 shows a typical frequency-amplitude response of the system in which the dashed lines show the unstable solution which does not happen in the physical view of the system[97]. As shown by the arrows, the jump phenomena may occur on the system when the voltage frequency approaches to the natural frequency from the right side and by reducing the detuning parameter and accordingly a sudden shift happens in the amplitude of vibration to the upper curve and the system response is divided to three regions[97]. Figure 5-15 namely response curve shows the effect of changing the amplitude of parametric excitation which can be done by changing the amplitude of applied harmonic voltage on the vibration amplitude. The dashed line shows the unstable solution and again the jump phenomena is seen as the red arrows follow depending on increasing or decreasing the excitation

amplitude. Further information regarding such behaviours can be found in the references[97]. Effects of nonlocal parameter, piezoelectric thickness, fluid velocity and amplitude of applied voltages are represented in figures 5-16 to 5-19, respectively. As shown, the nonlocal parameter is effective on the hardening behavior but the system response is much more sensitive to the piezoelectric thickness both in hardening behavior and changing the jump amplitude and increase of this parameter results in larger middle region in the system response. The fluid velocity has also some impact on the nonlinear hardening behavior as well as some effects on the middle region. The increase on the applied voltage amplitudes does not change the hardening bends but create a greater middle region which influences on the points that jump occurs as well as the amplitude of jump phenomena. As two typical system parameters, the effect of piezoelectric thickness and applied voltages on the response curve have been plotted in figures 5-20 and 5-21, respectively. As shown increase on the applied voltage changes the point in which the jump would occur and leads to higher amplitudes for the system.

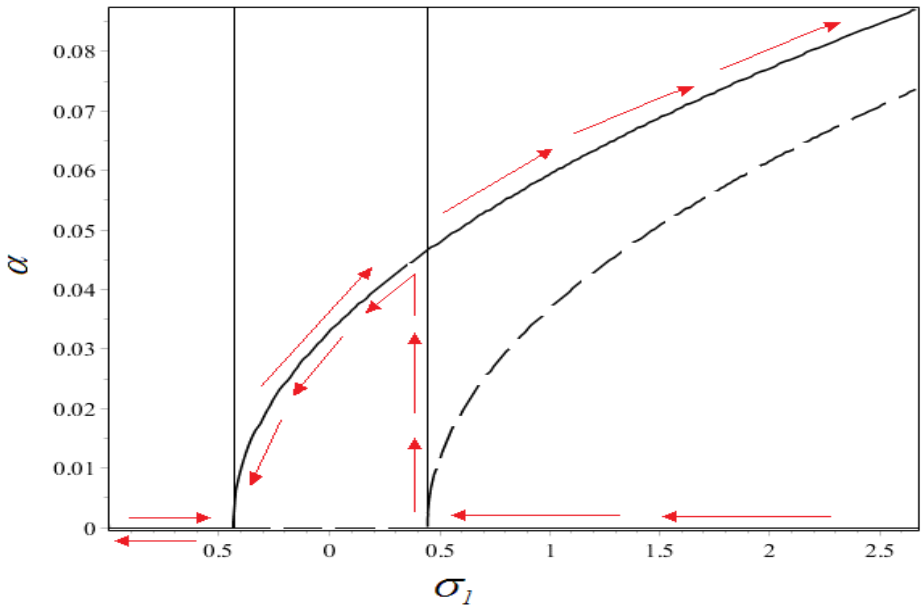

Figure 5-14 Frequency response of the system for parametric resonance.

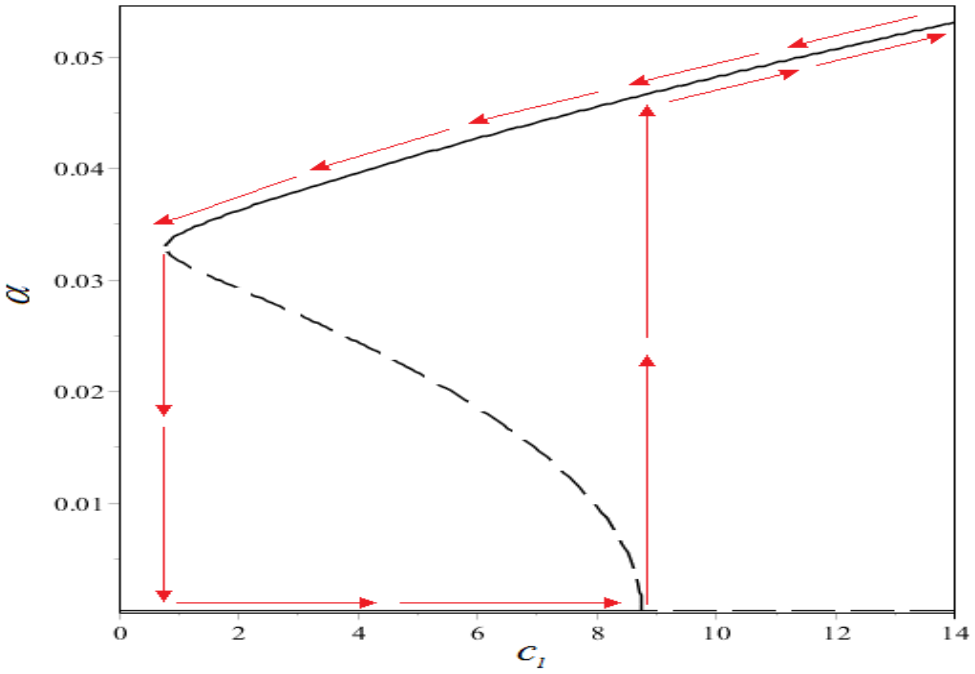

Figure 5-15 Response curve of the system for parametric resonance.

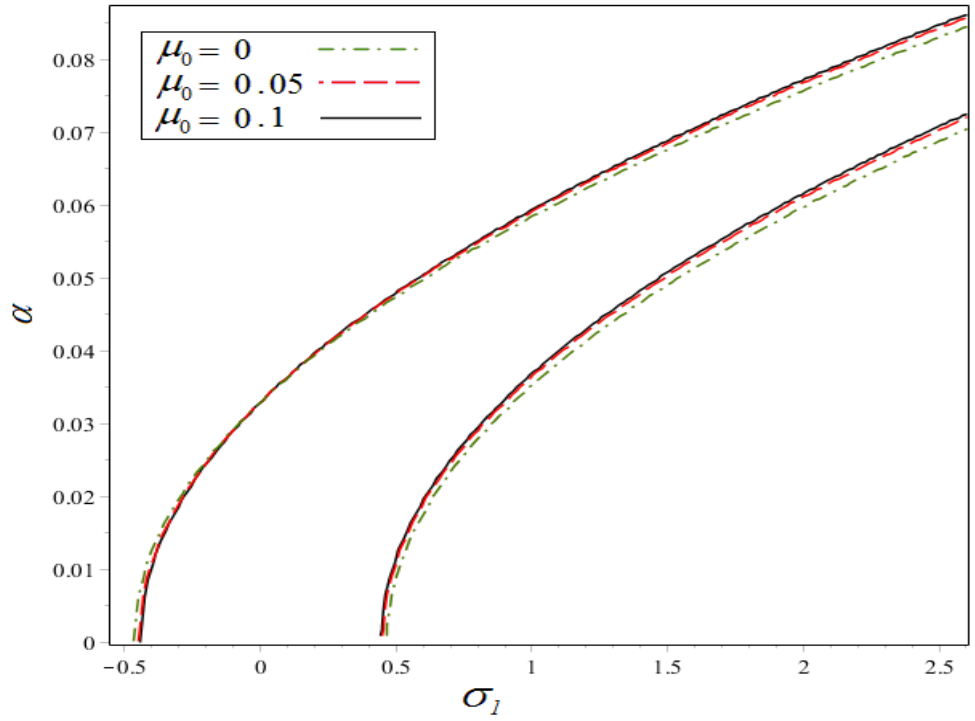

Figure 5-16 Non-local parameter μ_0 effect on frequency response for parametric resonance.

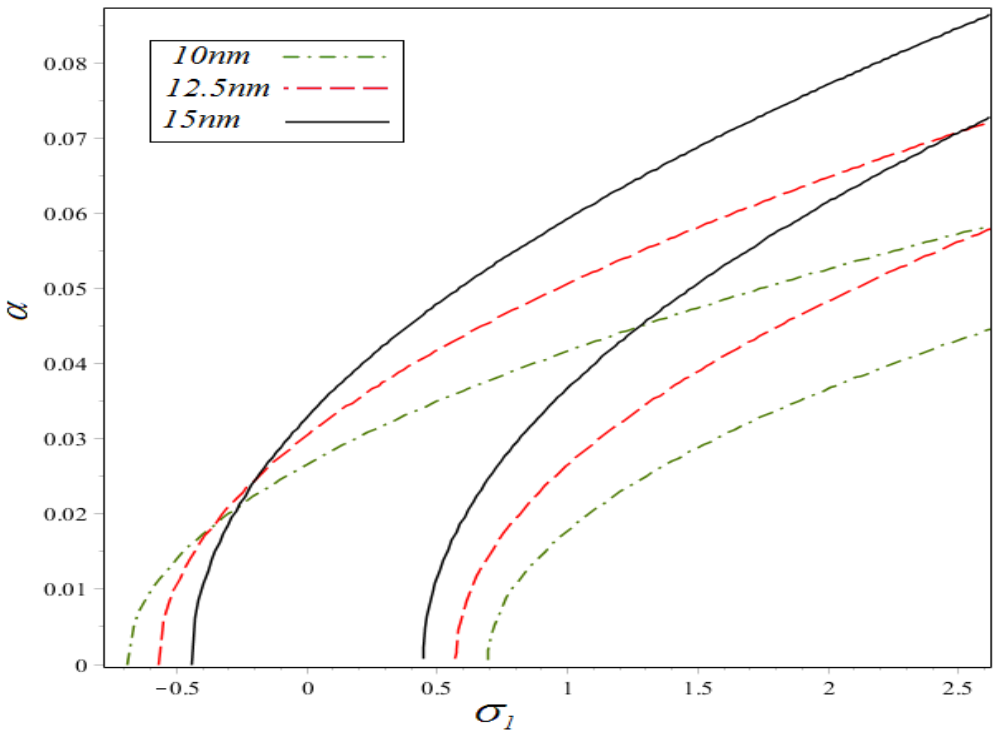

Figure 5-17 Piezo thickness effect on frequency response of parametric resonance.

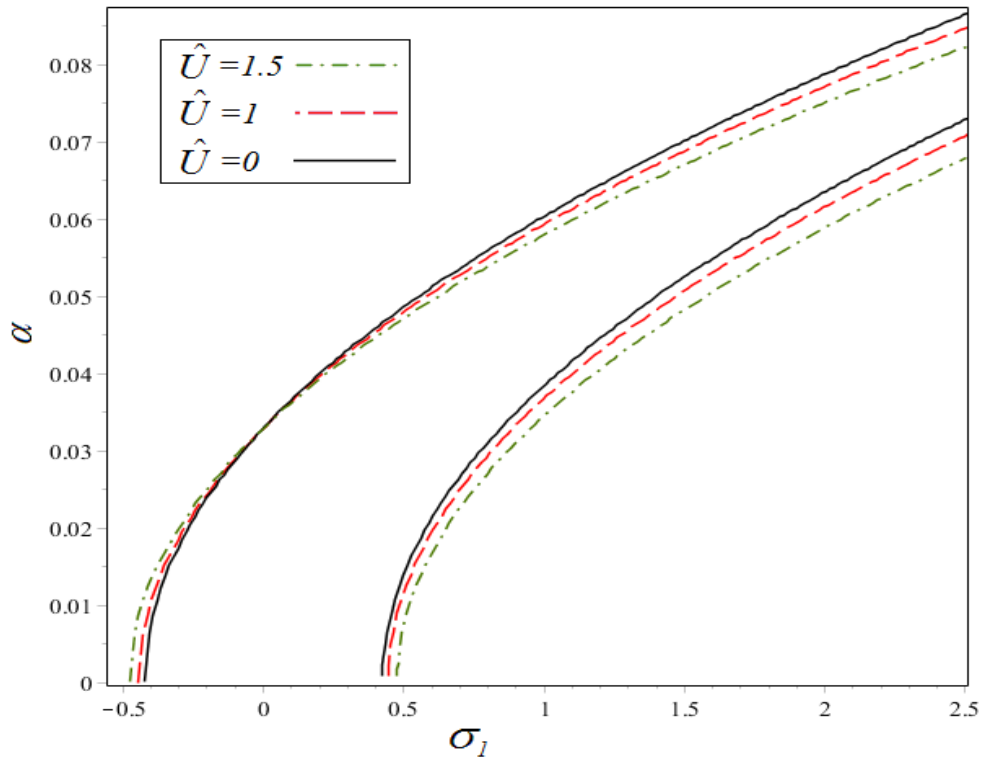

Figure 5-18 Fluid velocity $\hat{U}$ effect on frequency response for parametric resonance.

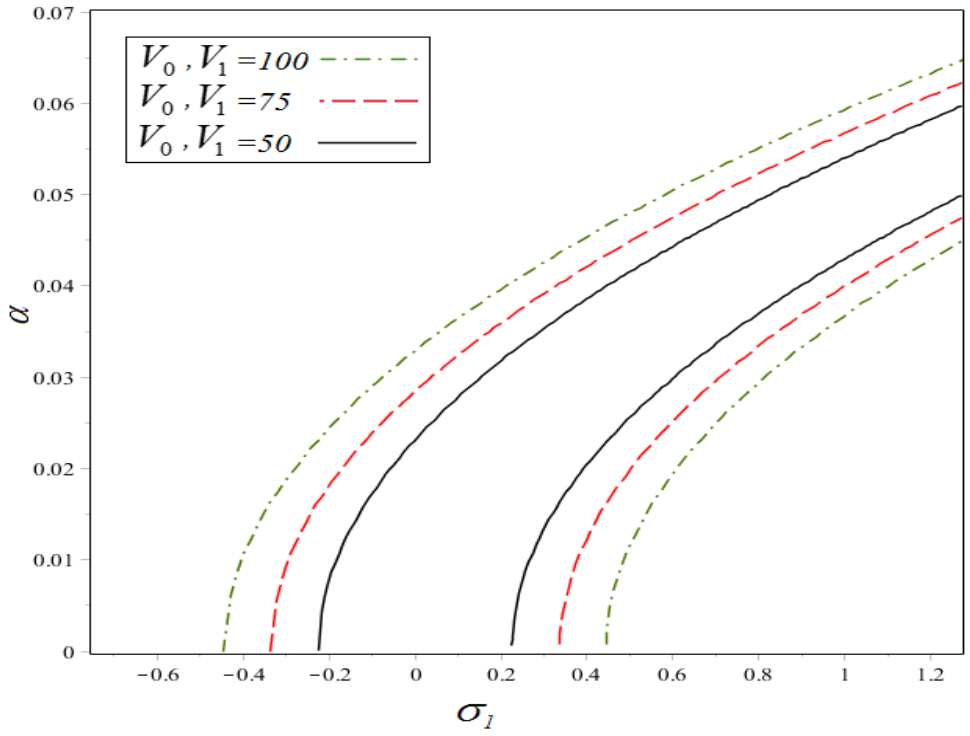

Figure 5-19 Voltages V_0, V_1 effect on frequency response for parametric resonance.

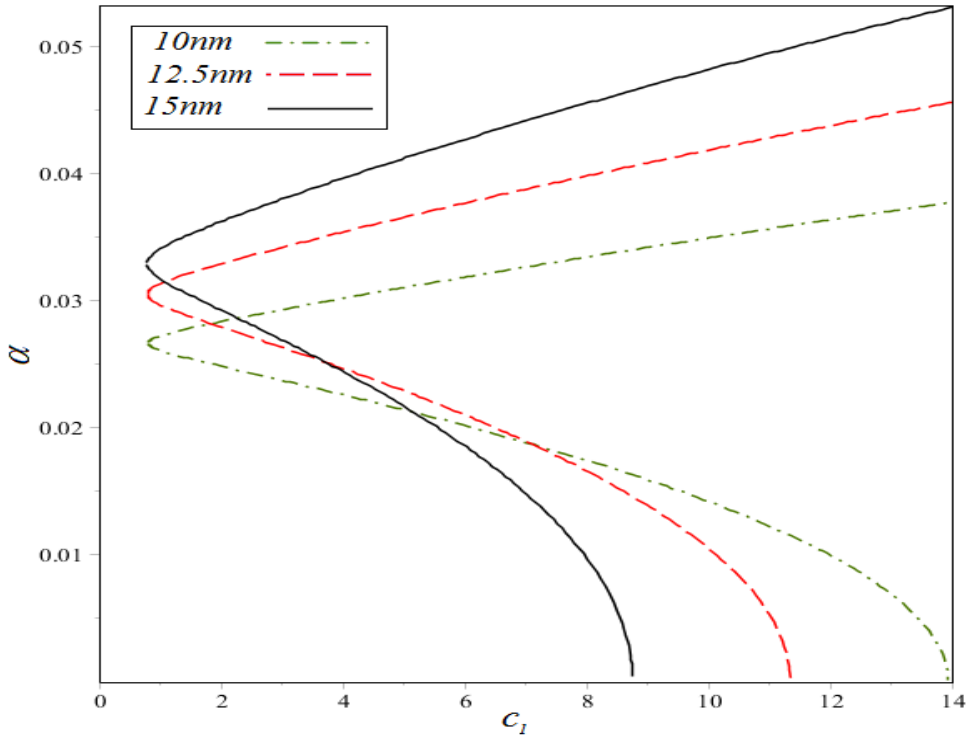

Figure 5-20 Piezoelectric thickness effect on response curve of parametric resonance.

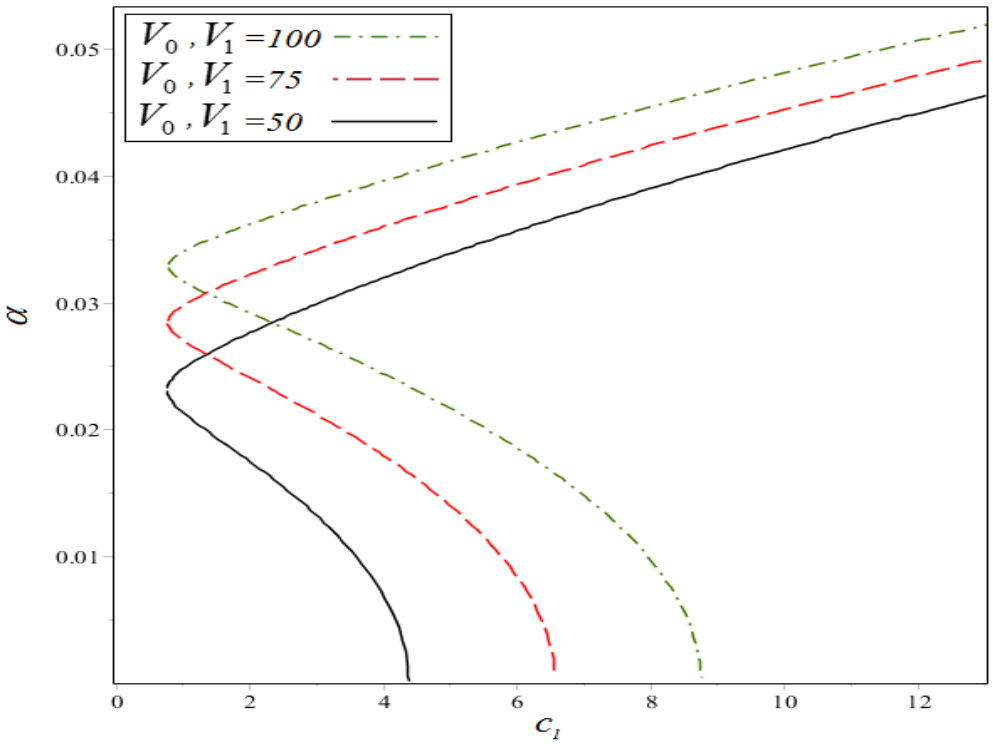

Figure 5-21 Voltages V_0, V_1 effect on response curve of parametric resonance.

The frequency responses of the system for simultaneous resonances when both parametric and external excitation resonances may occur at the same time are analyzed in figures 5-22 to 5-26. Figure 5-22 shows a typical frequency response curve obtained for the proposed model under aforementioned resonance case. Accordingly, the curve includes solid and dashed lines indicating stable and unstable solutions, respectively. As seen in this figure, three curves of the frequency response including right, left and middle branches and consequently various solutions may occur depending the value of detuning parameter which is the nearness of natural frequency and excitation frequency. The solution can be observed in three distinct cases including: a) one stable periodic solution, b) three periodic solutions containing two stable and one unstable solutions and c) five solutions holding three stable and two unstable solutions[101]. It should be noted that in physical view, either of these stable solutions can occur depending on the initial conditions of the system[97].

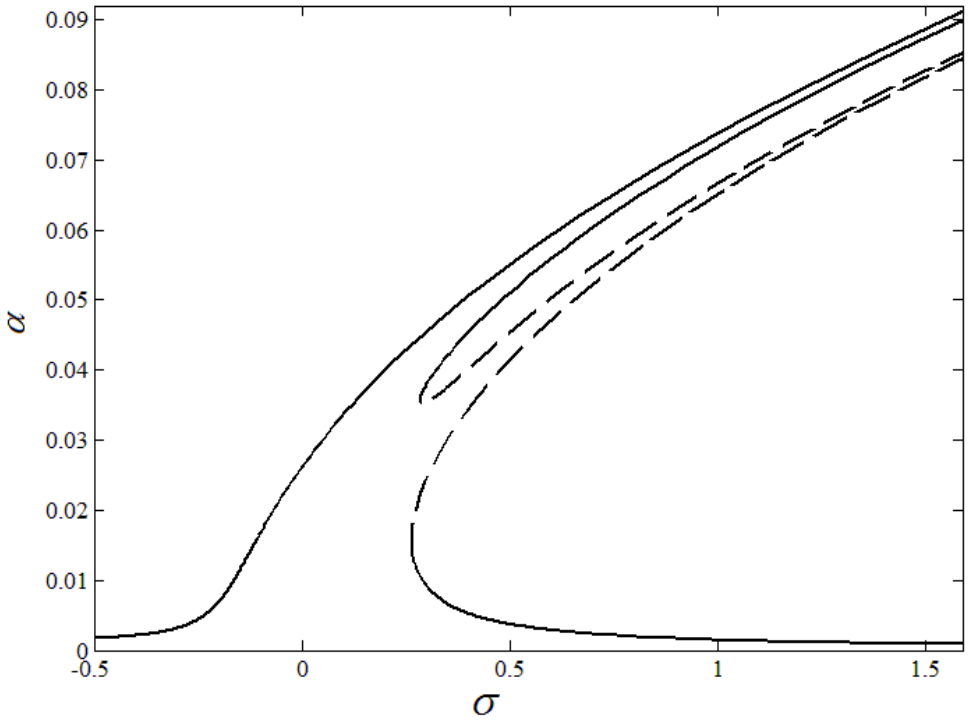

Figure 5-22 Frequency response of the system for simultaneous resonance.

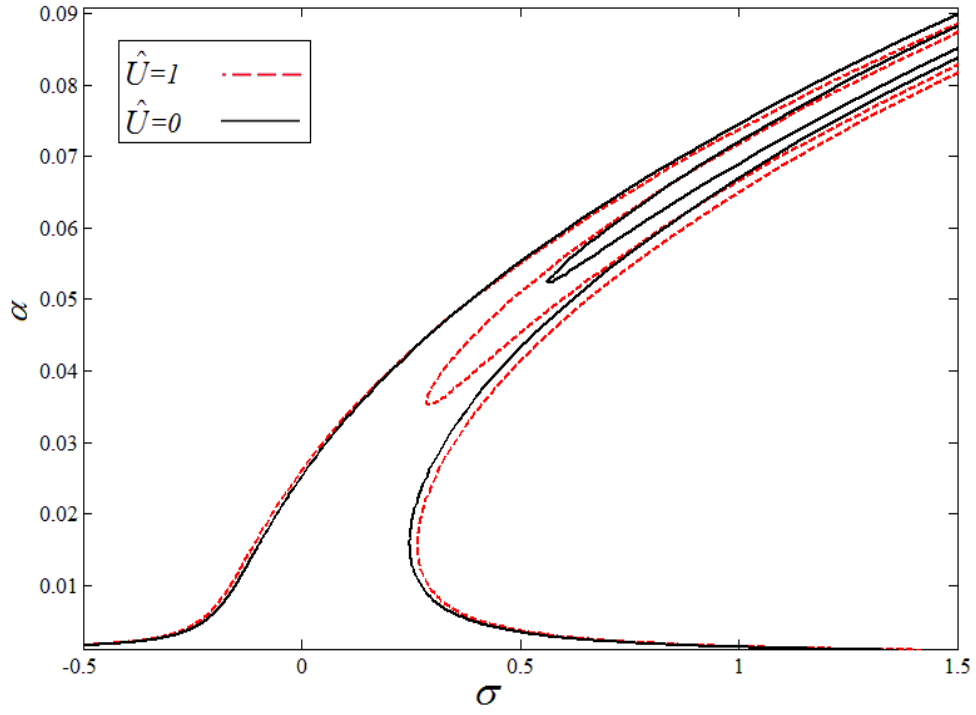

Figure 5-23 Fluid velocity $\hat{U}$ effect on frequency response for simultaneous resonance

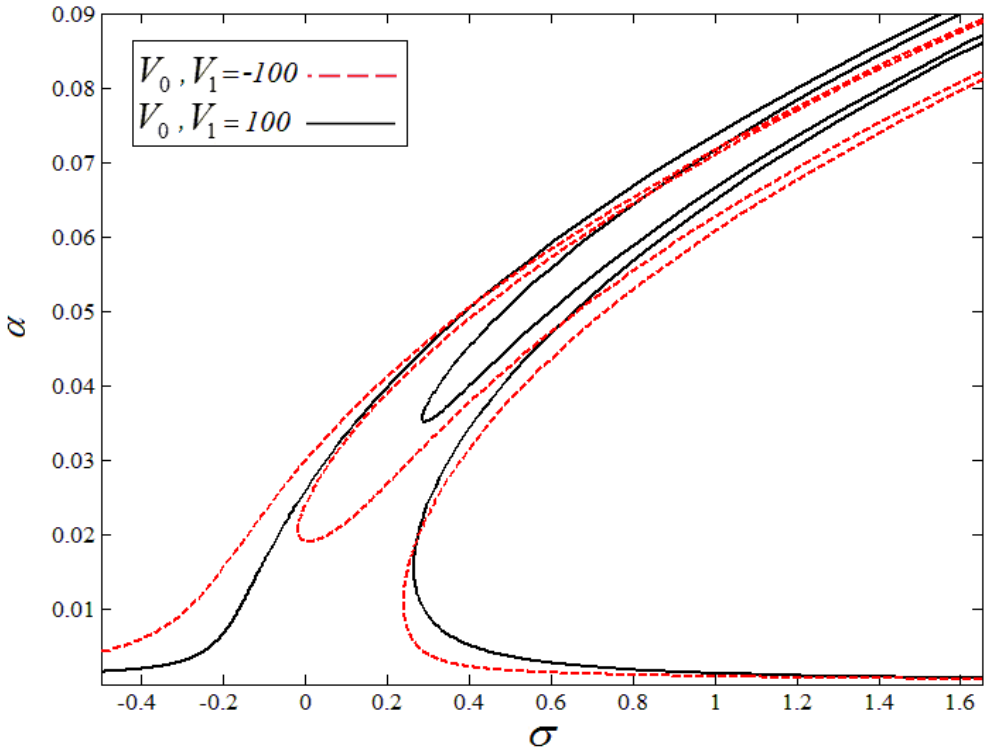

Figure 5-24 Voltages V_0,V_1 effect on frequency response for simultaneous resonance.

Effects of fluid velocity and applied voltage on the frequency responses of this simultaneous resonance have been depicted in figures 5-23 and 5-25, respectively. As seen from both figures, increase on the fluid velocity and the negative voltages, a considerable curves shift and bend can be seen in the system which is due to the increase of the natural frequency[97].

The piezoelectric layer thickness and nonlocal parameter influence on the frequency responses have been plotted in Figures 5-25 and 5-26, respectively and shift on the hardening of the curves and area of the existing solutions can be observed by changing these two parameters which should be taken into the account in order to predict the vibration behaviour of the proposed model when it is under the resonances of parametric and external load excitations at the same time.

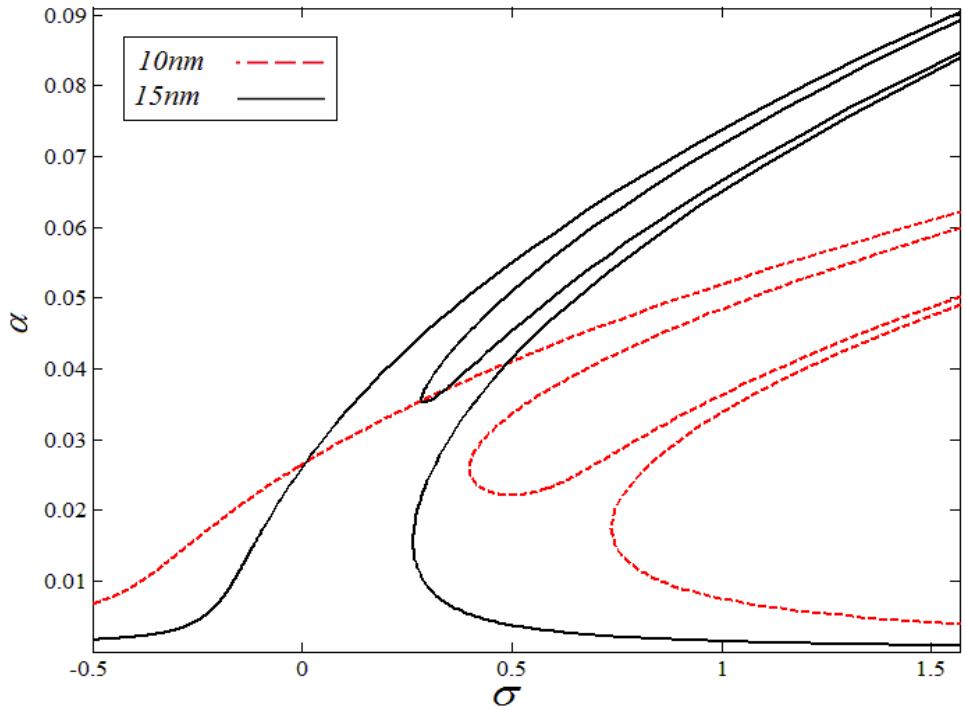

Figure 5-25 Piezo thickness effect on frequency response of simultaneous resonance.

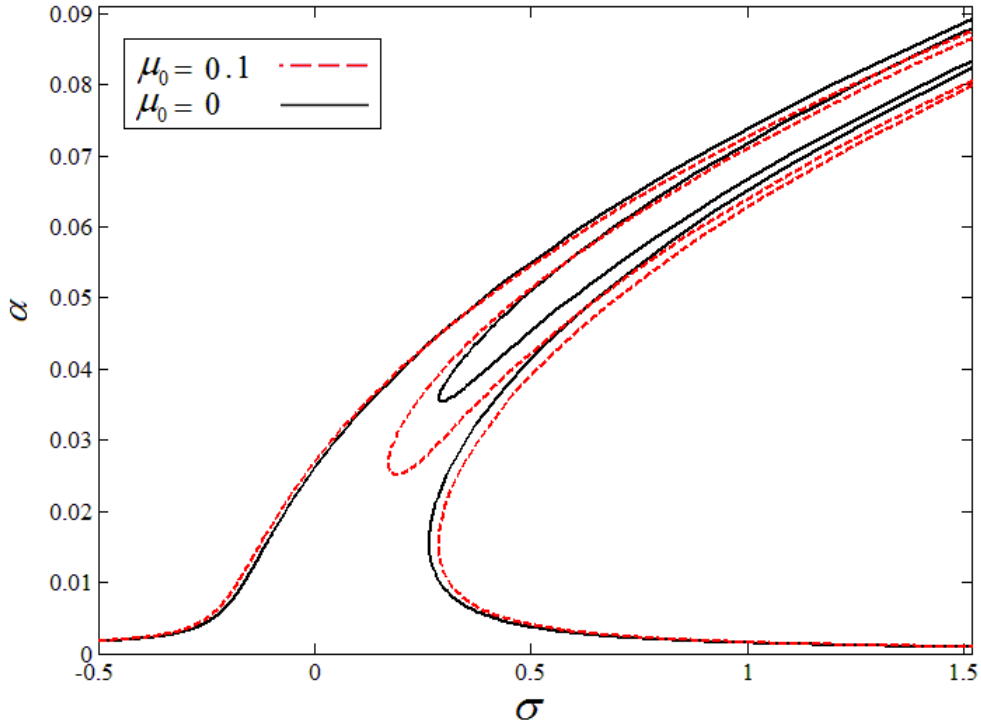

Figure 5-26 Non-local parameter μ_0 effect on frequency response for simultaneous resonance.

Thus, a variety of resonance cases have been investigated for the vibrations of the developed model and effects of different parameters on the vibration response of the system were represented and fully discussed.

Chapter 6: **Vibration analysis of curved piezoelectric-layered nanotubes**

6.1. INTRODUCTION

In this Chapter the vibration behaviour of a curved piezoelectric-layered nanotube is modeled and solved. The structure is considered to have a planer curvature in its shape and therefore effect of this shape is appeared in the obtained equations of the model. Again, by applying the energy method, Lagrangian formula and Hamiltonian principle associated with non-local theories the governing equation of motion of the corresponding system is carried out. In next step, the problem is solved using Galerkin and multiple scales method and the system responses under external excitation and parametric load are found.

The piezoelectric layer is taken to be slender as before and the applied voltage is a harmonic function of time. Two cases of resonance condition are evaluated here known as primary and parametric resonance and the frequency responses are obtained for steady state motion. Effects of different parameter such as applied voltage, piezoelectric thickness and shape of structure curvature on the system responses are investigated. For the last item, two types of curves including quadratic and cubic shapes are typically considered for the structure and the influence of changing the shape on the frequency-amplitude responses are plotted and discussed.

6.2. MATHEMATICAL MODELING

The dynamic modeling of a piezoelectric-layered nanotube having a general two dimensional curvature along the structure under external excitation is modeled here.

For better understanding of the model, a schematic representation of the system is shown in Figure 5.1. For this case and by using the Euler-Bernoulli beam theory, the displacement fields and corresponding strain are written as [102]

$$\begin{cases} w(x,z,t) = w(x,t) + \bar{Z}(x) \\ u(x,z,t) = u(x,t) - z\dfrac{\partial w(x,t)}{\partial x} \end{cases} \tag{6.1}$$

$$\varepsilon_{xx} = u_x - zw_{xx} + \frac{1}{2}\left(\frac{\partial}{\partial x}(w+\bar{Z})\right)^2 - \frac{1}{2}\bar{Z}_x \tag{6.2}$$

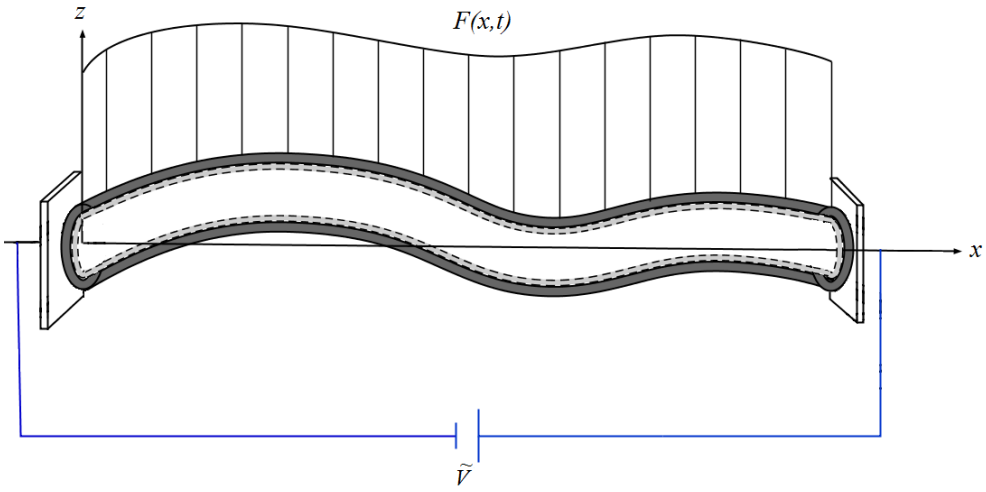

Figure 6-1 Schematic model of the curved piezoelectric-layered nanotube.

where, $\bar{Z}(x)$ represents the deflection of the beam model centroid axis along the system as a function of horizontal axis *x*. The energy method and Hamiltonian principle are implemented in order to find the governing equation of motion. Thus, the strain and kinetic

energies and external force work with their variations should be developed. Using Eq. (6.2), the strain energy and the corresponding variation using integration by part is found as

$$
\begin{aligned}
&U = \\
&\frac{1}{2}\{\int_0^L \{E_1A_1(u_{x,1}^2 + u_{x,1}w_{x,1}^2 + \frac{1}{4}w_{x,1}^4 + w_{x,1}^2\overline{Z}_x^2 + 2u_{x,1}w_{x,1}\overline{Z}_x + w_{x,1}^3\overline{Z}_x) \\
&+ e_1A_1(\varphi_x u_{x,1} + \frac{1}{2}\varphi_x w_{x,1}^2 + \varphi_x w_{x,1}\overline{Z}_x) + E_1I_1w_{xx,1}^2\}dx \\
&\int_0^L \{E_2A_2(u_{x,2}^2 + u_{x,2}w_{x,2}^2 + \frac{1}{4}w_{x,2}^4 + w_{x,2}^2\overline{Z}_x^2 + 2u_{x,2}w_{x,2}\overline{Z}_x + w_{x,2}^3\overline{Z}_x) \\
&+ E_2I_2w_{xx,2}^2\}dx + \int_0^L A_1[e_1(u_{x,1} + \frac{1}{2}w_{x,1}^2 + w_{x,1}\overline{Z}_x) - k_1\varphi_x]\varphi_x dx\}
\end{aligned}
\tag{6.3}
$$

Similar to the procedure used for the kinetic energy previously (see Chapter 3, Eqs. (3.11) to (3.14)), the variation of this energy can be easily obtained however the mass is not considered for this model and the variation of external force work is similar to Eq. (3.15). Now by applying the same procedure, obtained equations are substituted to the main equation of variational principle and by setting the coefficients of δw and δu to zero, one can obtain

$$
\begin{aligned}
&\overline{M}_{xx} = \\
&\overline{\rho A}w_{tt} - A_1e_1\frac{\partial}{\partial x}(\varphi_x(w_x + \overline{Z}_x)) - \overline{EA}\frac{\partial}{\partial x}(u_x w_x + \frac{1}{2}w_x^3 + w_x\overline{Z}_x^2 + u_x\overline{Z}_x + \frac{3}{2}w_x^2\overline{Z}_x) + F(x,t)
\end{aligned}
\tag{6.4}
$$

$$
A_1\{e_1\frac{\partial}{\partial x}(u_x + \frac{1}{2}w_x^2 + w_x\overline{Z}_x) - k_1\varphi_{xx}\} = 0 \tag{6.5}
$$

Inserting above equation to the Eringen's non-classical equation of bending moment used for nano scale systems, the governing equations of motion for the transverse vibration of nano cantilevered nanotube using Euler- Bernoulli theory associated with nan-local theory are found as

$$\overline{EI}w_{xxxx} + \overline{\rho A}w_{tt} - \overline{EA}\frac{\partial}{\partial x}(u_x w_x + \frac{1}{2}w_x^3 + w_x\overline{Z}_x^2 + u_x\overline{Z}_x + \frac{3}{2}w_x^2\overline{Z}_x)$$
$$- A_1 e_1 \frac{\partial}{\partial x}(\varphi_x(w_x + \overline{Z}_x)) - F(x,t) - (e_0 a)^2 \frac{\partial^2}{\partial x^2}\{\overline{\rho A}w_{tt} - A_1 e_1 \frac{\partial}{\partial x}(\varphi_x(w_x + \overline{Z}_x)) \quad (6.6)$$
$$- \overline{EA}\frac{\partial}{\partial x}(u_x w_x + \frac{1}{2}w_x^3 + w_x\overline{Z}_x^2 + u_x\overline{Z}_x + \frac{3}{2}w_x^2\overline{Z}_x) - F(x,t)\} = 0$$

$$\frac{\partial \varphi_x}{\partial x} = \frac{e_1}{k_1}\frac{\partial}{\partial x}(u_x + \frac{1}{2}w_x^2 + w_x\overline{Z}_x) = 0 \quad (6.7)$$

and the relationship between transversal and longitudinal displacement for the system with curvature with immovable ends is approximated as[8]

$$u = -\int_0^x (\frac{1}{2}w_{xx}^2 + \overline{Z}_x.w_x)dx + \frac{x}{L}\int_0^L (\frac{1}{2}w_{xx}^2 + \overline{Z}_x.w_x)dx \quad (6.8)$$

Thus, by defining dimensionless parameters for the obtained equations as seen in Appendix *D*, the solution procedure of the obtained model are developed for non-dimensional problem in the next section.

6.3. VIBRATION SOLUTION OF CURVED PIEZOELECTRIC-LAYERED NANOTUBE

In this section the Galerkin method is again utilized for simplifying the obtained equation of motion from the previous section. The discretized form of transversal vibration for the fundamental mode has been considered here. The applied voltage is taken to be a harmonic function of time with the frequency Ω_1 and the external load is as Eq. (4.41) indicating a harmonic point load with the frequency Ω_2 imposed at an arbitrary distance

along the structure. After applying the Galerkin method and the concept of normal modes orthogonality, the ordinary differential equation of first mode time response is obtained as

$$\ddot{Y}(\hat{t})+\omega_0^2 Y(\hat{t})+\hat{d}_1 Y(\hat{t})\cos(\Omega_1\hat{t})+\hat{d}_2 Y^2(\hat{t})+\hat{d}_3 Y^3(\hat{t})=\hat{F}_0\cos(\Omega_1)+\hat{F}_1\cos(\Omega_2\hat{t}) \tag{6.9}$$

where the constant parameters of above equation are presented in Appendix *D* Based on the physical and geometrical properties of the curved structure. As seen, due to the system curvature a quadratic nonlinearity is added to the system and the effect of harmonic voltage appears in both parametric and external excitation. The multiple scales method is now employed for solving Eq. (6.9). For this purpose a small damping term is added to the equation and in order to insert the effect of nonlinear terms and external forces, the corresponding coefficients should be ordered. So the equation is rewritten as

$$\begin{aligned}\ddot{Y}(\hat{t})+\omega_0^2 Y(\hat{t})+2\varepsilon^2\mu\dot{Y}(\hat{t})+\varepsilon^2 d_1 Y(\hat{t})\cos(\Omega_1\hat{t})+\varepsilon d_2 Y^2(\hat{t})+\varepsilon^2 d_3 Y^3(\hat{t})\\ =\varepsilon^2[F_0\cos(\Omega_1\hat{t})+F_1\cos(\Omega_2\hat{t})]\end{aligned} \tag{6.10}$$

Again the considered solution of above equation is taken as

$$Y(\hat{t})=P_0(T_0,T_1,T_2)+\varepsilon P_0(T_0,T_1,T_2)+\varepsilon^2 P_0(T_0,T_1,T_2)+... \tag{6.11}$$

Substituting Eq. (6.11) into (6.10), and equating the terms with the same power of ε , gives

$$\begin{aligned}&\varepsilon^0:\\ &D_0^2 Y_0+\omega_0^2 Y_0=0\end{aligned} \tag{6.12}$$

$$\begin{aligned}&\varepsilon^1:\\ &D_0^2 Y_1+\omega_0^2 Y_1=-2D_0D_1Y_0-d_2Y_0^2\end{aligned} \tag{6.13}$$

$$\begin{aligned}&\varepsilon^2:\\ &D_0^2 Y_2+\omega_0^2 Y_2=-2D_0D_1Y_1-D_1^2Y_0-2D_0D_2Y_0-2\mu D_0Y_0-2d_2Y_0Y_1-d_3Y_0^3\\ &\qquad -b_1Y_0\cos(\Omega_1\hat{t})-F_0\cos(\Omega_1\hat{t})-F_1\cos(\Omega_2\hat{t})\end{aligned} \tag{6.14}$$

The general solution of Eq. (6.12) can be obtained as

$$Y_0 = A(T_1, T_2)\exp(i\omega_0 T_0) + \overline{A}(T_1, T_2)\exp(-i\omega_0 T_0) \tag{6.15}$$

Substituting Eq. (6.15) into (6.13), one can have

$$D_0^2 Y_1 + \omega_0^2 Y_1 = -2i\omega_0 D_1 A\exp(i\omega_0 T_0) - d_2[A^2\exp(2i\omega_0 T_0) + A\overline{A}] + CC \tag{6. 16}$$

Elimination of secular terms from above equation requires

$$D_1 A = 0 \tag{6.17}$$

which means that the amplitude A is independent from T_1 or $A(T_1, T_2) = A(T_2)$. Then, the solution of Eq. (6.16) considering both private and homogenous solutions, equals

$$Y_1 = \frac{d_2}{\omega_0^2}(-2A\overline{A} + \frac{1}{3}A^2\exp(2i\omega_0 T_0) + \frac{1}{3}\overline{A}^2\exp(-2i\omega_0 T_0)) \tag{6.18}$$

Now equations (6.15) and (6.18) are substituted into Eq. (6.14) and after some mathematical simplification and considering the elimination of the terms correspond to D_1 , leads

$$\begin{aligned} D_0^2 Y_2 + \omega_0^2 Y_2 = & -2i\omega_0(A' + \mu A)\exp(i\omega_0 T_0) \\ & - \frac{2d_2}{\omega_0^2}[-2A^2\overline{A}\exp(i\omega_0 T_0) + \frac{A^3}{3}\exp(3i\omega_0 T_0) + \frac{A^2\overline{A}}{3}\exp(i\omega_0 T_0)] \\ & - d_3[A^2\overline{A}\exp(i\omega_0 T_0) + A^3\exp(3i\omega_0 T_0)] - \frac{d_1\overline{A}}{2}\exp(i\Omega_1 T_0) \\ & + \frac{F_0}{2}\exp(i\Omega_1 T_0) + \frac{F_1}{2}\exp(i\Omega_2 T_0) + CC \end{aligned} \tag{6.19}$$

From above equation it is known that three different resonances may occur in the system including two primary resonances when $\Omega_1 \approx \omega_0$ or $\Omega_2 \approx \omega_0$, and one parametric

resonance when $\Omega_1 \approx 2\omega_0$. Also, simultaneous resonances might be seen when $\Omega_1 \approx \Omega_2 \approx \omega_0$ or $0.5\Omega_1 \approx \Omega_2 \approx \omega_0$. Similar cases of aforementioned resonances have been studied in previous Chapters. Thus, in this Chapter two resonances are investigated for the proposed model as follows

- *Case A:* $\Omega_2 = \omega_0 + \varepsilon\sigma_2$

For this primary resonance, the elimination of secular terms from Eq. (6.19) leads to

$$2i\omega_0(A' + \mu A) + (3d_3 - \frac{10d_2^2}{3\omega_0^2})A^2\overline{A} - \frac{1}{2}F_1\exp(i\sigma_2 T_1) = 0 \tag{6.20}$$

Applying the same procedure as seen before and using the polar form $A = \frac{1}{2}\alpha\exp(i\theta)$, the frequency-amplitude relationship of the steady state motion is obtained as

$$\sigma_2 = \left(\frac{1}{8\omega_0}(3d_3 - \frac{10d_2^2}{3\omega_0^2})\alpha^3 \pm (\frac{1}{4}F_1^{\,2} - (\mu\omega_0\alpha)^2)^{1/2}\right)\Big/(\omega_0\alpha) \tag{6.21}$$

Also the first approximate solution is obtained as

$$Y(\hat{t}) = \alpha\cos(\Omega_2\hat{t} - \gamma_2) + O(\varepsilon) \tag{6.22}$$

where $\gamma_2 = \sigma_2 T_1 - \theta$. In addition, the nonlinear natural frequency of the system is

$$\hat{\omega}_0 = \omega_0[1 + \frac{1}{8\omega_0^{\,2}}(3d_3 - \frac{10d_2^2}{3\omega_0^2})\alpha^2] + O(\varepsilon^2) \tag{6.23}$$

As seen, the effects of all nonlinear terms appear on the relations of this case.

- *Case B:* $\Omega_1 = 2\omega_0 + \varepsilon\sigma_1$

Considering parametric resonance due to the harmonic applied voltage and eliminating secular terms from Eq. (6.19) gives

$$2i\omega_0(A' + \mu A) + (3d_3 - \frac{10d_2^2}{3\omega_0^2})A^2\overline{A} + \frac{1}{2}d_1\overline{A}\exp(i\sigma_1 T_1) = 0 \tag{6.24}$$

Employing the polar form of A and considering the steady state motion, one can achieve

$$\alpha = \left\{ \frac{8\omega_0}{(3d_3 - \frac{10d_2^2}{3\omega_0^2})} \left[\frac{\sigma_1}{2} \pm \left((\frac{d_1}{4\omega_0})^2 - \mu^2 \right)^{1/2} \right] \right\}^{1/2} \tag{6.25}$$

where above equation shows frequency response of the structure for the considered resonance case. Again, the conditions of having solutions for Eq. (6.25) can be easily obtained by setting the terms under square roots greater than zero similar to the previous Chapter case *B.*

6.4. RESULTS AND DISCUSSION

In this section the vibration behavior of the developed curved nano structure is analyzed by computing the obtained relations of proposed solution procedures using numerical values. As the model considered a general form of planer curvature, two types of curvature including quadratic and cubic are typically examined for this purpose. Accordingly, the frequency ratio and frequency responses owing to the external and parametric resonances are studied for both curves and effects of piezoelectric layer and the shape waviness are investigated in the results.

Figure 6-2 represents the considered quadratic curves of the piezoelectric layer nanotube developed in previous section. As shown, different waviness are taken into the account for this case. It should be noted that the waviness parameter r, indicates the ratio between the vertical position of nanotube middle point and the horizontal distance of two ends. Thus, the influence of changing r is investigated as an important parameter of the structure quadratic shape.

Also, different formations of cubic curves are represented in Figure 6-3. In order to study and compare different types of this curvature, the maximum vertical position of the structure is kept to be constant and the horizontal position of this maximum point $\bar{x}$, is varied from the left end to the middle and effect of this variation is taken into the account for the results.

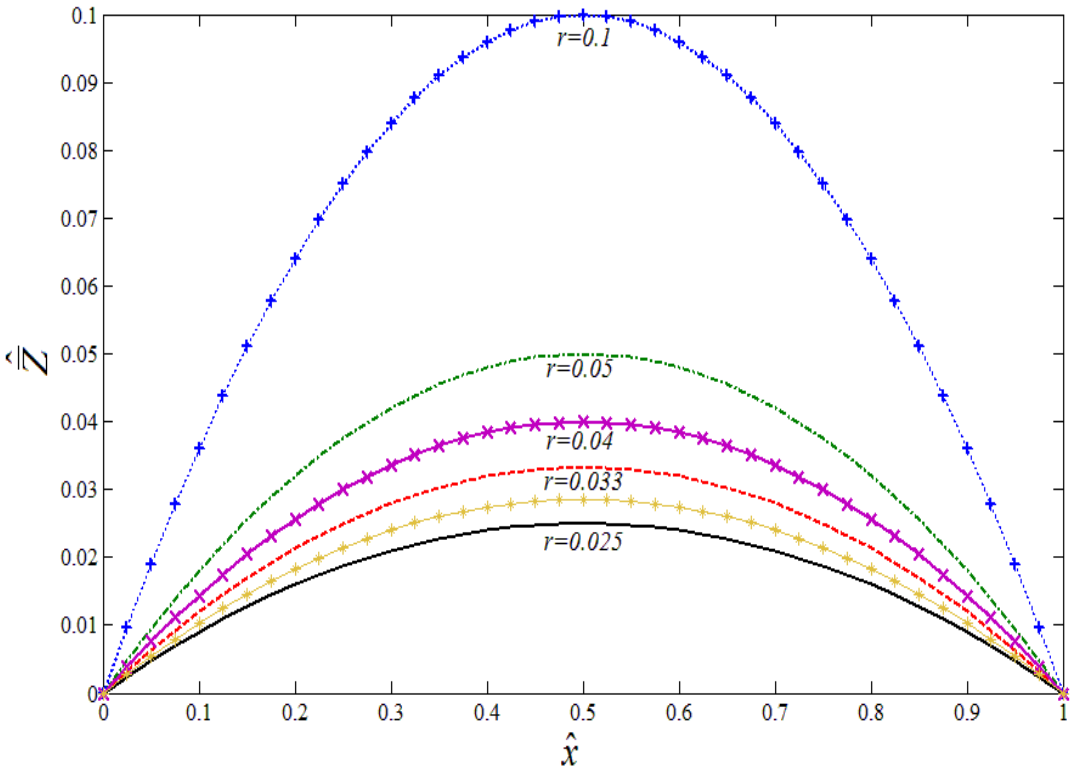

Figure 6-2 Typical quadratic curve with different waviness.

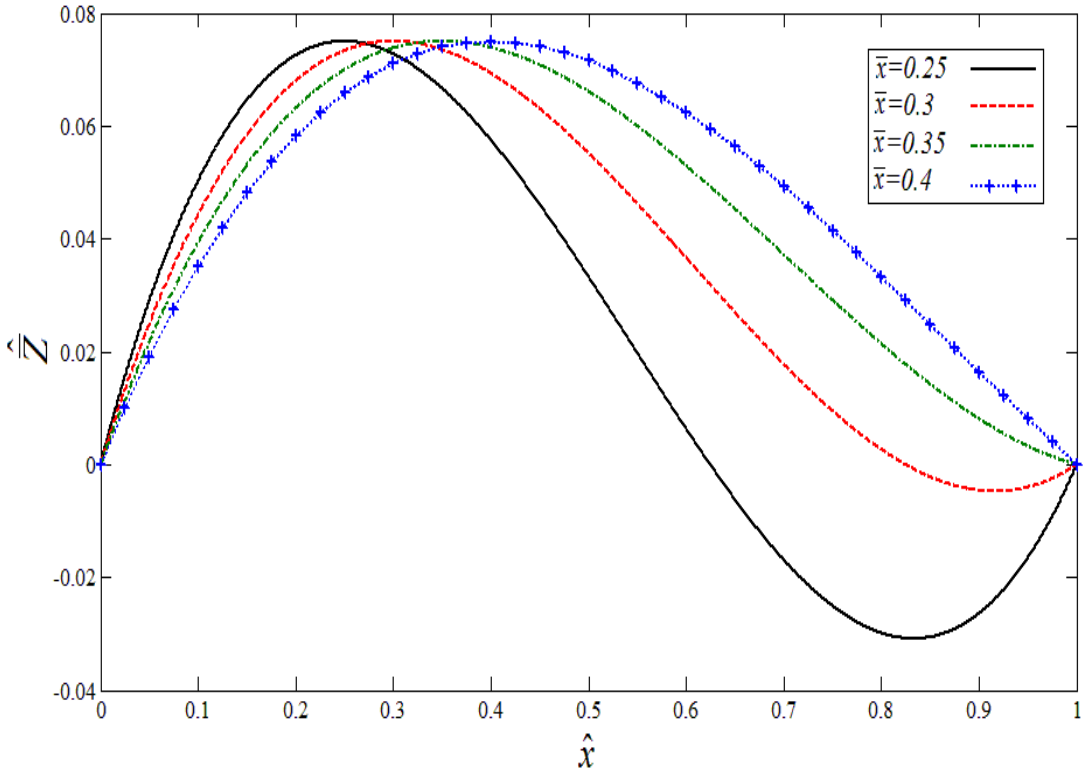

Figure 6-3 Typical cubic curve with different waviness.

Figure 6-4 shows the frequency ratio of quadratic curve with respect to the initial conditions. As shown, for small waviness the ratio is increasing and the values is greater than one while for larger waviness the ratio decreases and the value becomes less than one. So for a range of waviness, by changing from small to large values, the ratio behavior is fully changed. This is a very important characteristic which could be used to reach the required frequency behavior by setting the waviness of the structure. The reason for such behavior is that due to the presence of curvature on the structure, a quadratic nonlinear term exists in the corresponding governing equation. Hence, the coefficient of this term adds a negative term into the nonlinear frequency-amplitude. It should be noted that for further increase on the waviness, the system may show unstable behaviour due to aforementioned terms. An interesting result is when the waviness is $r = 0.044$ in which the frequency ratio

remains constant and is equal to one. For this special case namely critical curve, the system frequency is independent from the initial amplitude and consequently the system behavior is linear which is very important for design of systems.

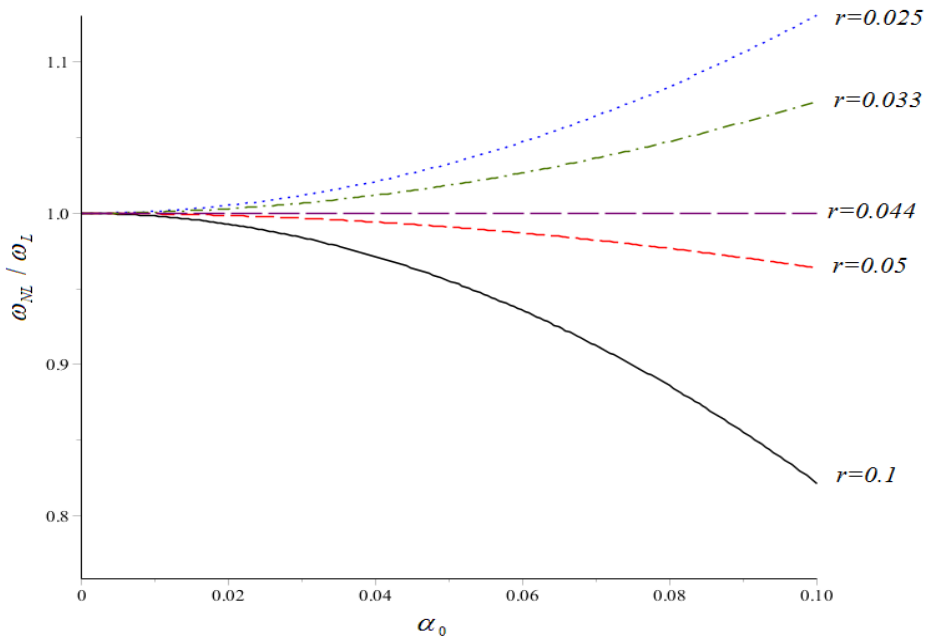

Figure 6-4 Waviness Effect r on frequency ratio for quadratic curve.

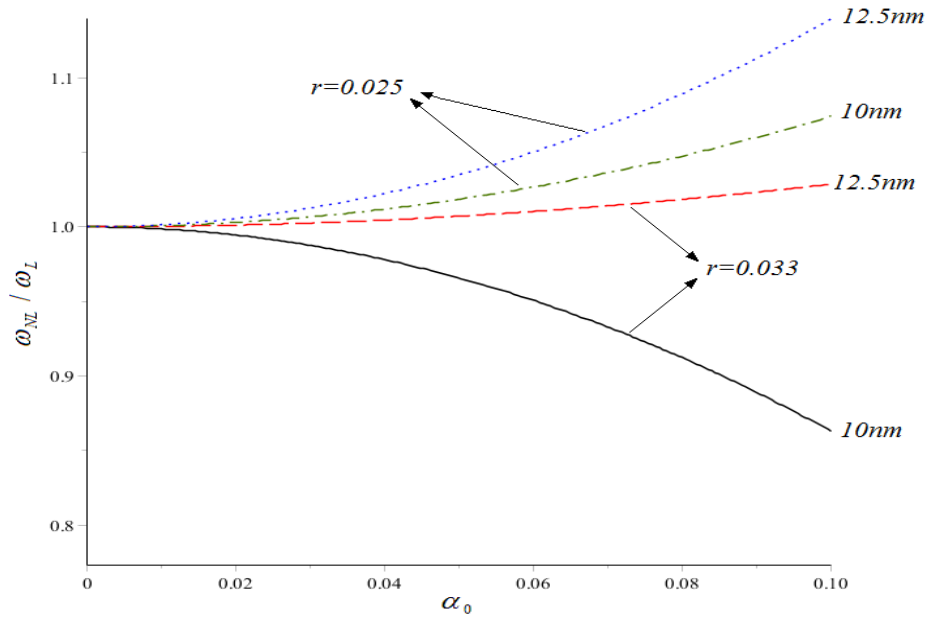

Figure 6-5 Waviness r and piezoelectric thickness effects on frequency ratio for quadratic curve.

Figure 6-5 depicts the variation of frequency ratio for different piezoelectric layer thicknesses. As seen, for the waviness in which the frequency ratio is greater than one, the growth on the thickness would result in higher frequency ratio. However, for the waviness that the change rate is negative, the increase on the thickness reduces the magnitude of ratio change rate. Figure 6-6 represents the frequency ratio of the cubic curved structure for various positions of maximum point. It is apparent that when the maximum point is very close to the structure end, the ratio is higher and as the point shifts to the middle, the ratio decreases and at a distance it would become less than one which should be considered in the system analysis. Similarly, the reason is because of the negative terms that the initial curve causes in the nonlinear frequency-amplitude relationship. For this case, the critical curvature exists when the position of maximum point is located at $\bar{x} = 0.325$. As seen in the figure, the ratio is equal to one for all initial amplitudes which means that the system has linear behaviour for this curve.

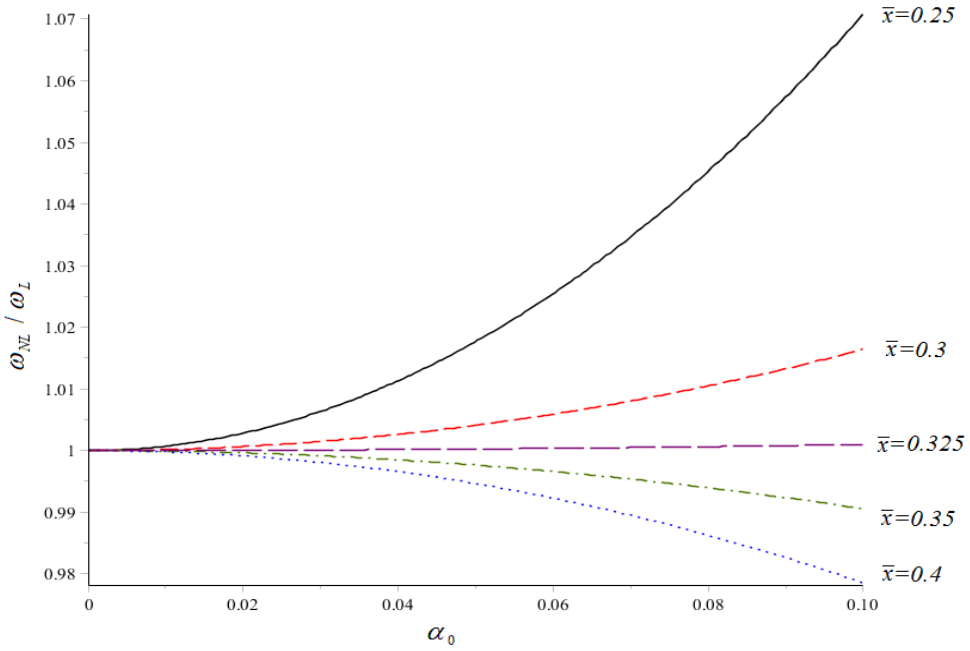

Figure 6-6 Curvature shape $\bar{x}$ effects on frequency ratio of cubic curve.

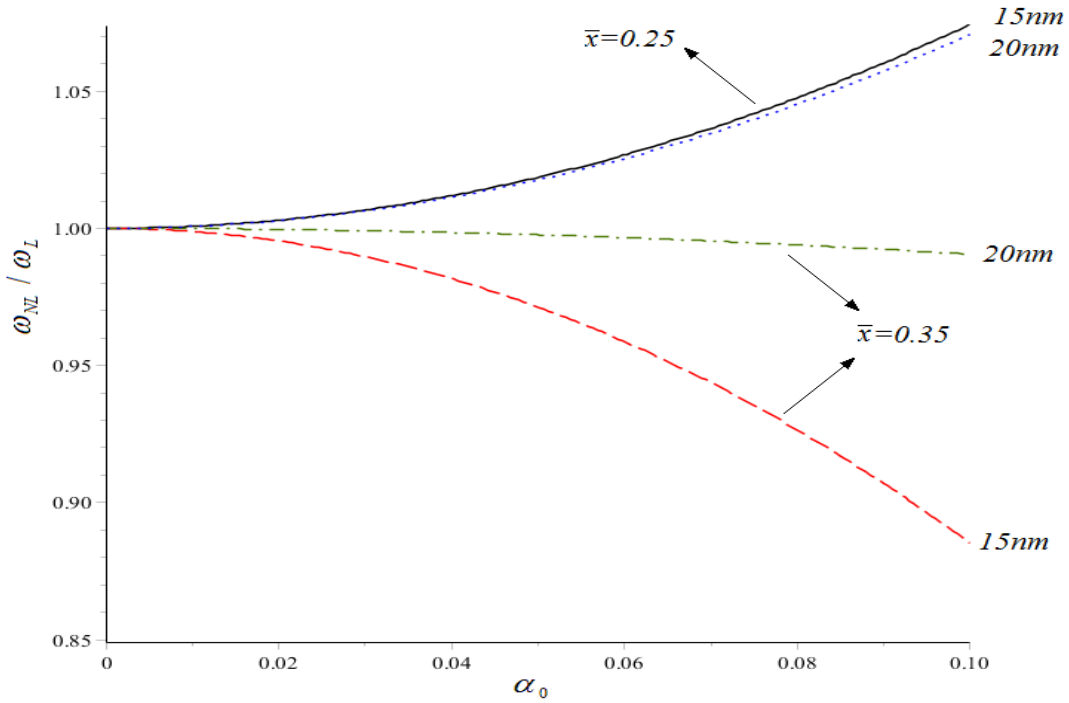

Figure 6-7 Curvature shape $\bar{x}$ and piezoelectric thickness effects on frequency ratio of cubic curve.

The piezoelectric layer thickness effect is plotted in Figure 6-7 an for this type of curvature either the maximum point position is close to the end or to the middle, the decrease on the thickness leads to greater magnitude of change rate for the frequency ratio. The frequency responses of the curved system under primary resonance are represented in figures 6-8 to 6-11 for both aforementioned curvatures. Effect of quadratic curve waviness on the hardening- softening behavior of the quadratic curve structure is seen in Figure 6-8. Accordingly, for small waviness the system behaviour is extremely hard while by increasing the waviness the system tends to be close to the linear behaviour and after that bends to the left side which results in softening behaviour. This shift also reduces the structure amplitude of vibration. So, the curve waviness can be considered as a control parameter in order to find the desirable behaviour whether it is soft, hard or even linear for

such nonlinear nano system. As shown in dashed red curves in Figure 6-8, for the critical structure curvature $r = 0.044$ the frequency-amplitude is absolutely linear which should be taken into the account. As a typical parameter study, effect of piezoelectric layer thickness on the frequency response is shown in Figure 6-9 and similar to the results of previous models, for higher thickness the amplitude of vibration considerably decreases.

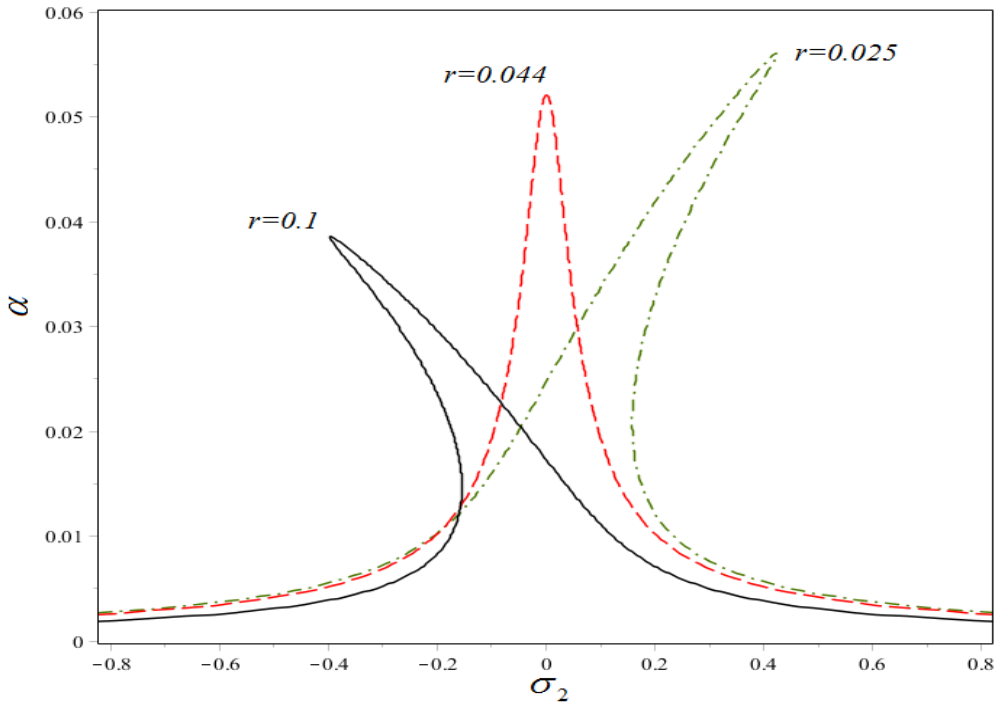

Figure 6-8 Quadratic curvature waviness r effect on response of primary resonance.

Obtained solutions are validated by comparing the results with similar models and for this purpose frequency responses of a curved nanotube is depicted in Figure 6-9 done by Askari [8]. Effects of quadratic curvature on the system response and hardening-softening behaviour of the structure is presented by changing the waviness and as shown, an agreement is found between that work which is for actual dimensions and presented non-dimensional results [8]. It should be noted that similar results were found by Saadatnia, et al. for a fluid-conveying curved nanotube using NURBS method [86].

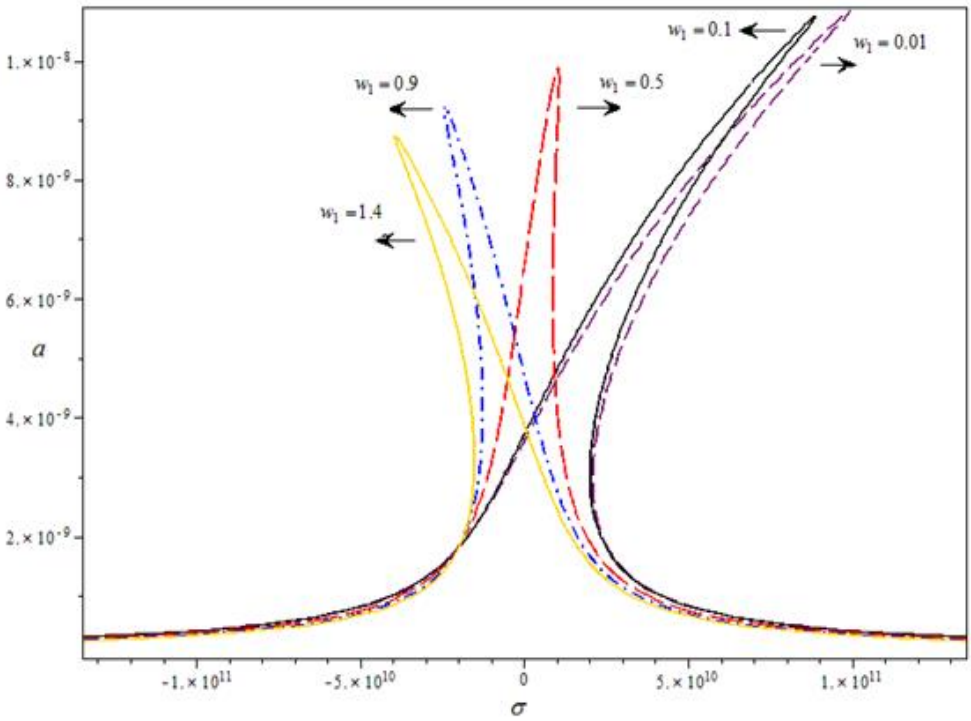

Figure 6-9 Effect of nanotube curvature shape on frequency responses [8].

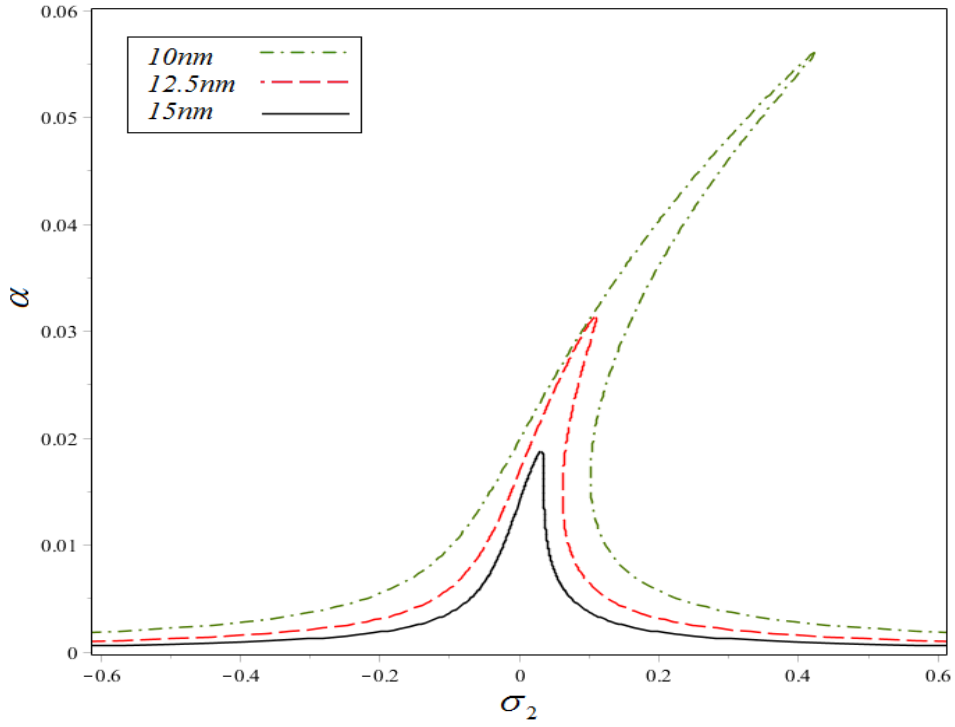

Figure 6-10 Piezoelectric thickness effect on frequency response of quadratic curve primary resonance.

Effect of the maximum point position on the frequency response of the structure with cubic curvature is investigated in Figure 6-11. When the position of this point is close to the structure end, the system nonlinear behaviour is hard and as the position moves toward the middle, not only the softening behaviour appears, but also the vibration amplitude decreases which is an interesting result which can be used in prediction and also design of such curved system.

In Figure 6-12, the piezoelectric thickness is typically analyzed when the maximum point position is close to the end or to the middle. For both hard and soft behaviours caused by the maximum point position, the thickness growth brings down the amplitude however the amplitude is smaller for softening behaviour in comparison with the harder one. Again the frequency response for the especial case of critical curvature in which $\bar{x} = 0.325$ the system shows linear vibration in spite of the presence of nonlinear terms in the general equation.

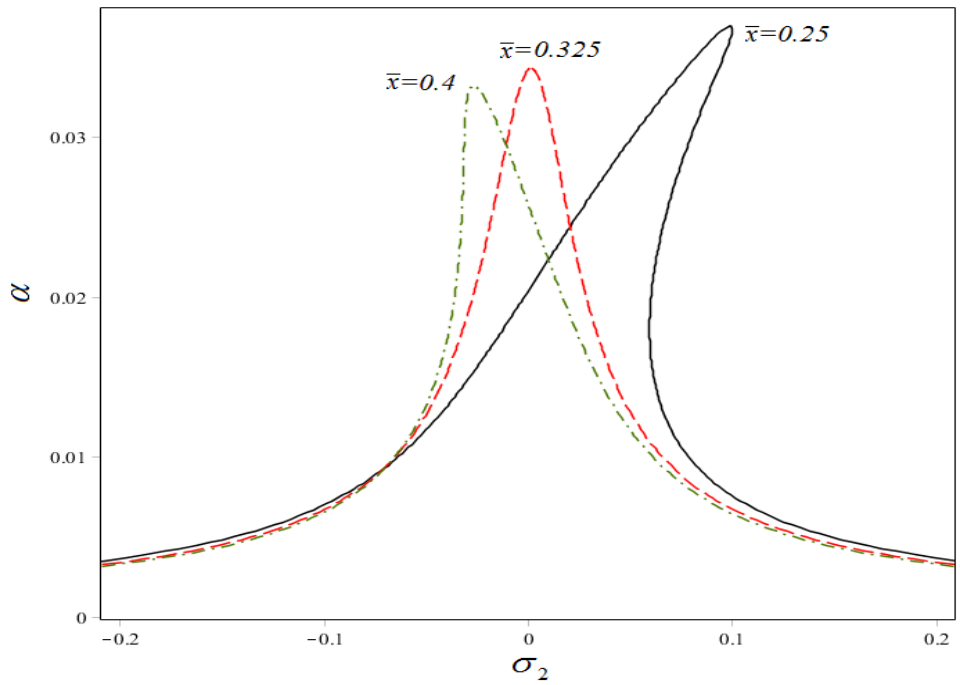

Figure 6-11 Cubic curve shape $\bar{x}$ effect on frequency response of primary resonance

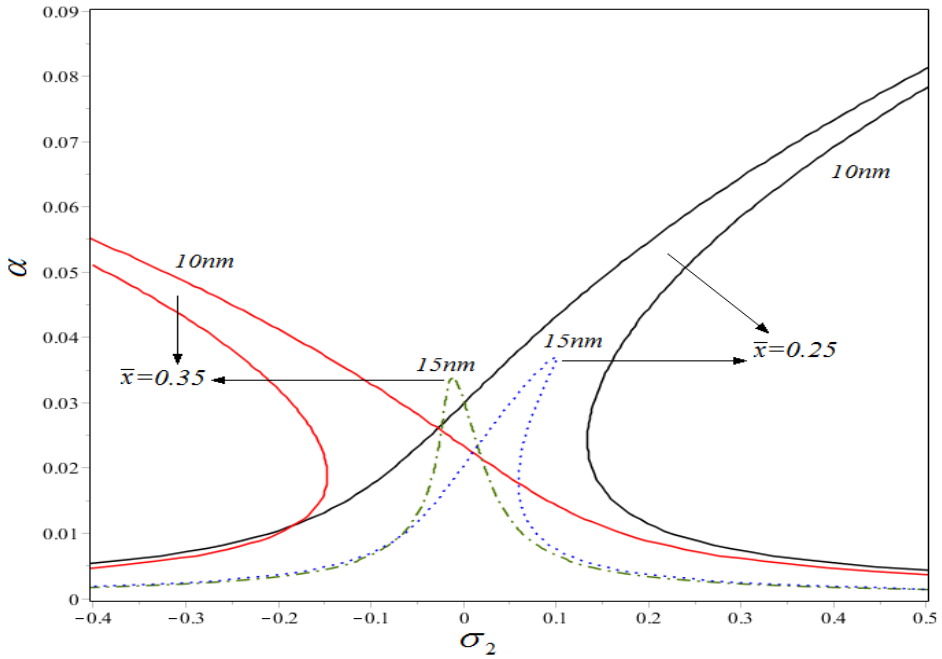

Figure 6-12 Piezoelectric thickness effect on frequency response of cubic curve primary resonance.

The responses of the structure under parametric resonance are represented in figures 6-13 to 6-16 for aforementioned quadratic and cubic curves. The frequency responses of the quadratic curve with different waviness is shown in Figure 6-13 and accordingly for lower waviness the hardening behaviour is observed and by increasing this parameter the system response moves to the left side which the system becomes soft. The system response for the critical quadratic curvature $r = 0.044$ is obvious in Figure 6-13 and as expected no nonlinearity is observed for the parametric resonance same as external one. The response curve which is the variation of vibration amplitude with respect to changing the parametric excitation amplitude is represented in Figure 6-14 for different quadratic curve waviness. It should be reminded that the amplitude of parametric excitation can be varied by changing the harmonic applied voltage and the physical understanding of such graphs has been

discussed in previous Chapter. As it is obvious, increase on the waviness reduces the amplitude of vibration as well as the jump on the system.

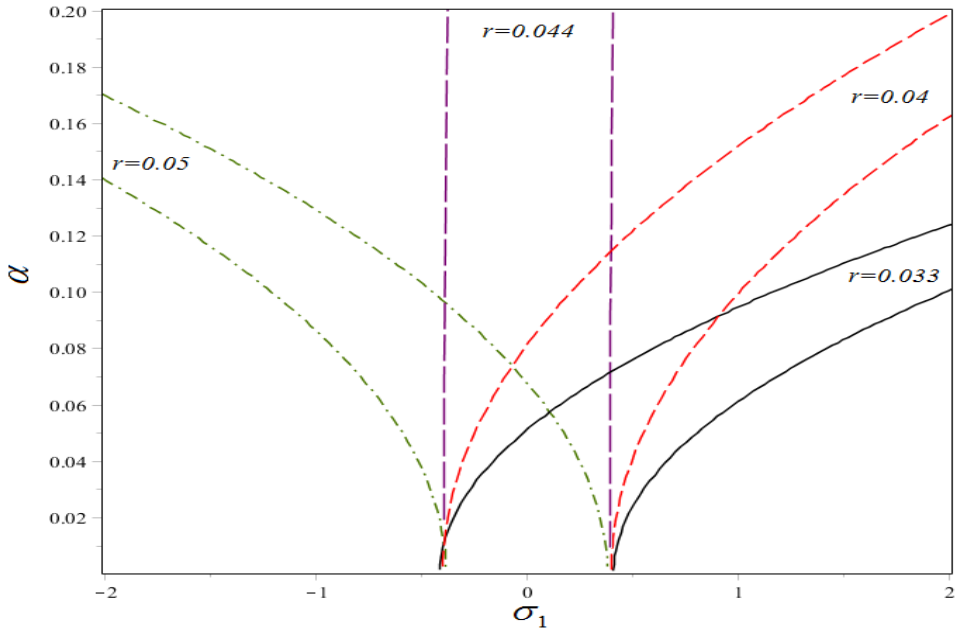

Figure 6-13 Quadratic curvature waviness r effect on frequency response of parametric resonance.

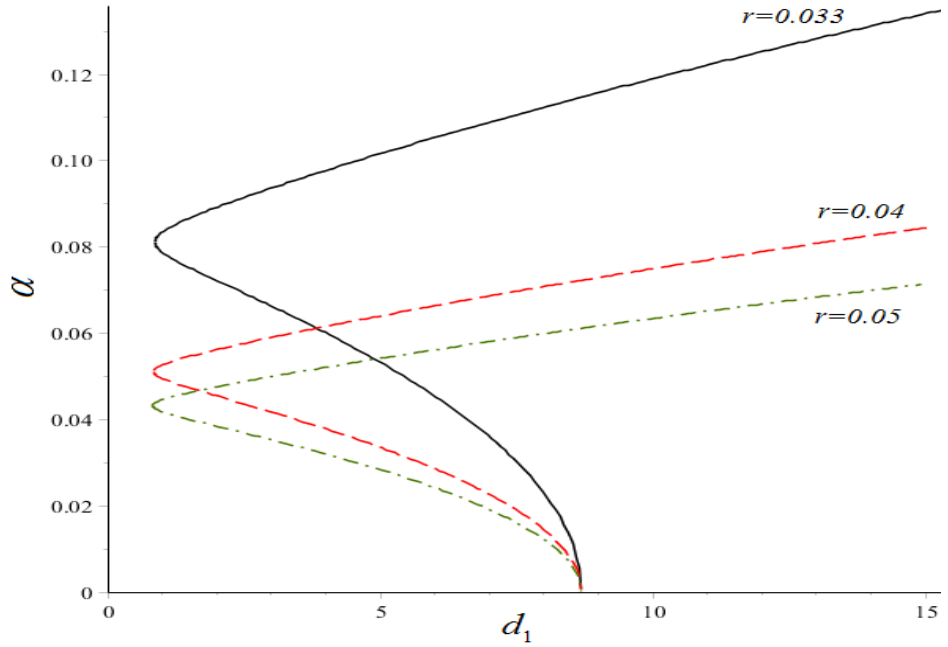

Figure 6-14 Quadratic curvature waviness r effect on response curve of parametric resonance.

Frequency response of the structure with cubic carve is depicted in Figure 6-15 due to parametric resonance and effect of maximum point position is studied. It is clear that when the position is at very end, the system is extremely hard while the position approaches the middle, the system shows softening response. It should be noted that for the critical cubic curvature, the linear behaviour of the system is represented by dashed purple lines.

The response curve of the cubic curvature and the effect of maximum point position is represented in Figure 6-16. Accordingly, the more the maximum point moves toward the middle the lower amplitude of vibration and jump occur in the system. Thus, the position can be taken as an important parameter to understand the vibration behavior and can be used to find the required response in terms of vibration amplitude, hardening-softening and even linear behavior for the proposed structure with cubic curvature.

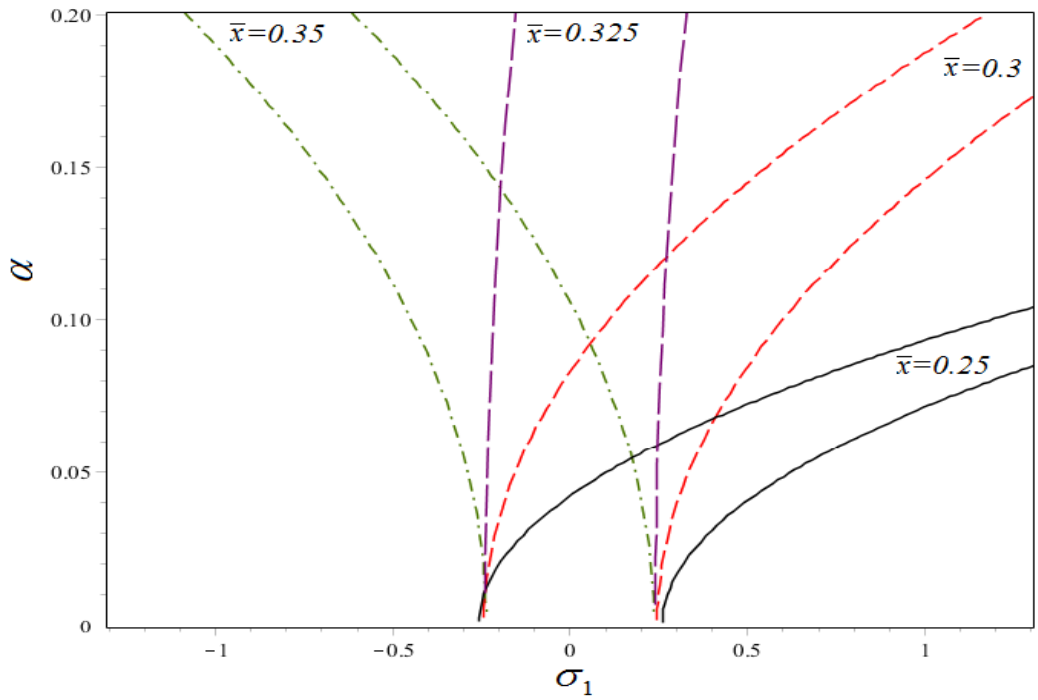

Figure 6-15 Cubic curvature shape $\bar{x}$ effect on frequency response of parametric resonance.

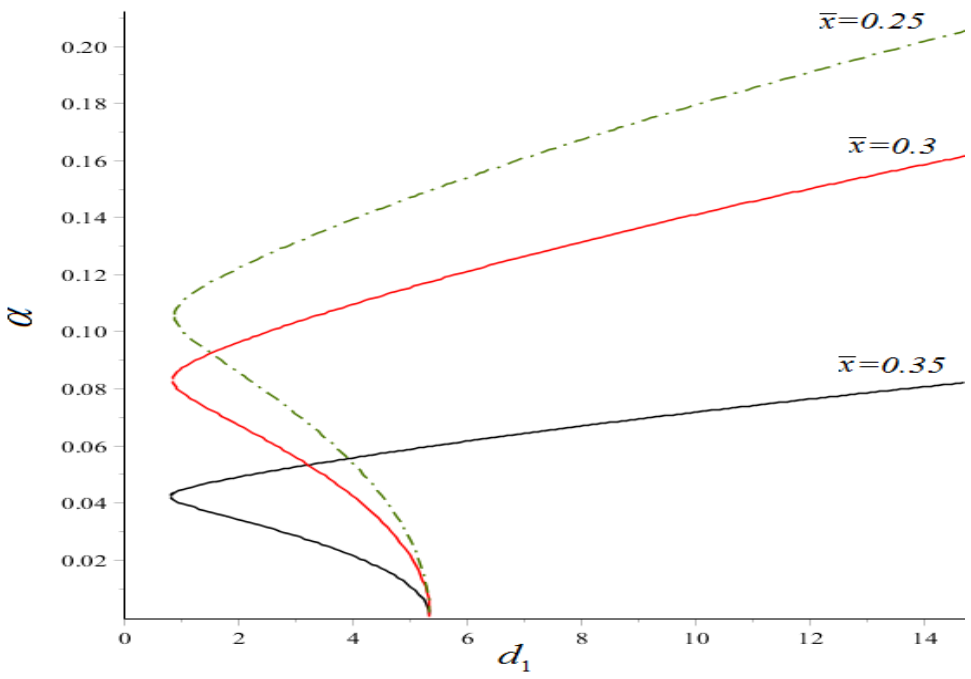

Figure 6-16 Cubic curvature shape $\bar{x}$ effect on response curve of parametric resonance

Thus, vibration behaviour of the piezoelectric-layered nanotube with a planer curvature were represented in this section. Two well-known curves were considered for the structure and frequency responses for primary and parametric resonances were obtained for different shape parameters. Also, important critical cases for the curvature shapes were found such that the system vibrations were linear.

Chapter 7: **Conclusions and future works**

7.1. CONCLUDING REMARKS

This Chapter is dedicated to summarize the overall findings of this research and to state the research original contributions. Generally, nonlinear vibration analysis of a group of nanotube-based structures were developed and fully investigated. The developed systems included multi-mode vibrations of a nanotube carrying intermediate mass, vibration of piezoelectric-layered nanotube under single frequency and multi-frequency excitations, piezoelectric-layered nanotube conveying fluid flow under constant and harmonic voltages and curved piezoelectric-layered nanotube under external excitation and harmonic voltage. Various vibrational behaviours such as frequency behaviour, internal, external, parametric, combination and simultaneous resonances were considered and analytically solved. The outcome of this thesis can be specifically explained in the following paragraphs for any of aforementioned models.

Governing equation of motion for the transversal vibration of a nanotube structure carrying intermediate mass using nonlocal theory were developed in Chapter three. The equation were discretized by means of Galerkin method applying orthogonality of normal modes and coupled nonlinear ordinary differential equations of the modes time responses were obtained. Hinged-Hinged, Clamped-Clamped and Clamped-Hinged structure ends

were considered and the corresponding equations were solved applying multiple scales method as a powerful perturbation method. The expressions of nonlinear natural frequencies of both modes were obtained and the resonance responses due to the harmonic external excitation were analytically calculated. It was shown that the coupled governing equation for clamped-hinged boundary condition is different from the two other conditions. This difference causes internal resonance as well as external one unlike the two other boundaries.

It was shown that the natural frequency of the system is very sensitive to the initial conditions due to the nonlinearity of the system which means that in studying such system the effect of nonlinearity must be taken into the account instead of linearizing the model. An important result was the effect of nonlocal parameter in the natural frequency and frequency responses of the system. Unlike classical studies of such nanostructure, this parameter must be considered in the vibration analysis of nanotubes since it caused remarkable differences in the responses. Effect of intermediate mass was another important parameter in the natural frequency and frequency responses of the system which was investigated here. This parameter can play the role of an external element in the system such as viruses, bacteria, humidity or even the sensor element and understanding the effect of this mass is very important in vibration applications such as predictions, sensing, and detections which were done in this research. The jump phenomena which may occur in the system vibration was also discussed for the model forced vibration under primary external resonance. It was shown that the structure parameters especially nonlocal parameter have noticeable effects on the amplitude and the detuning parameter in which the jump phenomena may happen for the system.

In Chapter four, the vibration modeling of a nanotube system having a slender piezoelectric layer was investigated. The piezo material was taken as ZnO material and for the proposed system, the governing equation of motion were established and solved. The frequency expressions were achieved and the system responses under single frequency and multi-frequency excitation were carried out using the perturbation method. It was shown that the presence of piezoelectric layer is very critical in the vibration response of the system. Considering constant voltages which were applied to the structure, the linear and nonlinear frequency of the system is very dependent to the magnitude of the voltage and therefore by adjusting the proper voltage, the desirable frequency behaviour could be obtained according to the demands of the mechanical application. Again, the nonlocal parameter was studied as a significant parameter in the model investigation. The results revealed that for better understanding of such small size structures, this effect is very noticeable in vibration responses and should be taken into the account for accurate vibration predictions of proposed systems.

A conventional primary resonance was investigated as before for the developed structure. However, a very important and interesting case was when the system would be under multi-frequency excitation as studied in this research. It was found that for multi-frequency external loads, the vibrational behaviour of the system could be very complicated due to the variety of resonance cases including subharmonic, superharmonic, combination and simultaneous resonances may occur in the system. Hence, two important simultaneous resonance were analytically solved and fully discussed. It was shown how the piezoelectric material presence and applied voltage influence the stable solutions of the system and make shifts on the frequency-amplitude relationships. Also, it was shown that

the hardening behaviour of the system which moves the system away from the linear one is very dependent to the applied voltage, piezo layer and also the nonlocal parameter.

Vibration modeling and analysis of piezoelectric layered nanotube with the presence of fluid flow were developed in the next Chapter. For this purpose the governing equations related to the fluid–structure interaction were established and added to the model considering various linear and nonlinear terms. The Galerkin approach was then applied for the fundamental mode of vibration and the obtained equation for the system time response was solved using multiple scales method for different cases. For this model, it was assumed that the applied voltage contains both constant and harmonic terms which inserts parametric excitation into the system as well. Afterward, frequency analysis were carried out and the system responses under primary, parametric and simultaneous primary-parametric resonances were obtained and fully discussed. It was shown that the fluid velocity reduces the linear natural frequency and for a critical velocity the system moves to unstable region due to the fluid flow. Effect of various parameter such as nonlocal parameter, applied voltage amplitude and intermediate mass on the critical velocity were represented and accordingly the two first parameters have a visible impact on the critical velocity unlike the mass. It was concluded that the amplitude of harmonic voltage has no effect on the system natural frequency unlike the constant voltage which is significantly effective on this vibrational characteristic.

In the primary resonance owing to the external excitation, the fluid velocity increases the hardening behaviour and amplitudes of vibration so this parameter should be taken into the account during the forced vibration analysis of the suggested structure. The magnitude of applied voltage and the piezoelectric thickness are two other system parameters which

change the nonlinear hardening behavior and amplitude of vibration due to this type of resonance. The parametric resonance showed new type of responses comparing to the previous cases. It was shown that the different kind of jump phenomena, stable solutions and unstable solutions exist in the vibration behavior. It was found that increase on the fluid velocity causes harder behavior unlike the increase on the amplitude of harmonic voltage but both parameter can change the jump amplitude and position. The nonlocal parameter was also influencing in this type of vibration which should be considered although in classical studies this parameter were neglected. A very interesting result was the variation of vibration amplitude with respect to the parametric excitation amplitude for a constant detuning parameter which the jump phenomena, stable and unstable solutions could be seen for the obtained results. The last important case which might occur in the system vibration was when both resonances occur at the same time and the system responses were totally different from the other previous cases. It was discussed that three type of regions could appear in the system which are dependent to the value of detuning parameter and initial conditions. For this case, changes on the fluid velocity and applied voltage shift the response curves considerably and also the nonlocal parameter is very effective on the responses of simultaneous resonance.

The vibration analysis of piezoelectric layered nanotube with a curvature was analyzed in the sixth Chapter this work. The assumption of curvature on the structure configuration was a very important consideration since in a number of real mechanical systems the structure shape is not straight or uniform. The governing equation of motion for the system with general planer curvature was developed considering nonlocal theory. Obtained partial differential equation were simplified employing Galerkin method and then solved by

means of multiple scales method under the presence of external load and harmonic voltage. It was found that extra nonlinear terms and excitations arise from the system curvature in the governing differential equation of the structure time response. Therefore, the curvature shape was considered as the main factor which was studied in this part. For this purpose, two important curves including quadratic and cubic were taken into the account as many structure curves can be approximated by the aforementioned curve types.

For the quadratic model, the curvature waviness were studied as the control parameter. It was observed that as the waviness changes from small values to larger ones, the nonlinear natural frequency reduces and from a specific waviness it becomes less than the linear one. Also, the frequency-amplitude and response curves of the quadratic model were obtained for primary and harmonic resonances. An interesting finding was that by growth on the waviness, the system behaviour moves from hardening to softening and the vibration amplitude decreases as well. Thus, in a specific value the response resembles the linear system in spite of different nonlinear terms presence. The impact of this parameter on the jump amplitude and position were also investigated for various cases. For the cubic curve, the horizontal position of curve maximum point were taken as the control parameter and it was changed from a point near to the nanotube end to the middle. It was detected that as the point approaches the middle, the nonlinear natural frequency decreases and from a particular position it starts to become less than the linear one. Also in both primary and parametric resonances, this shift on the maximum point position significantly affects the hardening-softening behaviour as well as the jump amplitude and position. Accordingly, the more the position moves toward the middle, the system has more tendency to show softening behaviour.

7.2. RECOMMENDED FUTURE WORKS

Dynamic modeling and nonlinear vibration of piezoelectric-based nano structures are very fascinating research topics due to the comprehensive application and importance of understanding the behaviour of such structures. As a result, a variety of problems can be developed which have not been investigated yet. Thus, the following recommendations can be proposed in order to continue the future studies:

1- Other non-classical theories can be employed in order to investigate the effect of small scale nano system and the results can be compared with the proposed non-local model. For example coupled stress theory, modified strain gradient theory and so on are other non-classical theories for this purpose.

2- The proposed structures can be investigated and evaluated using other mechanical techniques such as molecular dynamics, finite element method and experimental approaches and the obtained findings can be checked by the presented work.

3- Other continuum mechanic theories can be applied for the whole system. For example Timoshenko and/or Rayleigh beam theory can be used. Also, the shell theory can be employed when the piezoelectric layer is not considered to be slender and the structure can be taken as cylindrical model.

4- Other resonance cases which were not considered in this work can be taken into the account and their influence on the frequency responses, jump phenomena and hardening-softening behaviour can be investigated.

5- Buckling analysis and Chaotic vibration of the piezoelectric-layered nanotubes under constant and/or harmonic axial loads and fluid motion are other aspects of the proposed systems dynamics and afterward the stability analysis can be carried

out to find out when the corresponding behaviours are periodic, quasi-periodic and chaotic. Then the control methods can be developed to control the system vibration and to stabilize the problem.

6- Design and analyze of mass sensors, humidity detection tools, AFM devises, nano-fluid injectors, gas storage systems, nano scale energy harvesters and many other mechanical systems can be done considering the methodology that used for the proposed models of this study.

7- Other geometries and curvatures can be taken for the configuration of the proposed structures and different techniques like NURBS method can be utilized to model and investigate the effect of the structures non-uniformity.

References

[1] S. Iijima, "Helical microtubules of graphitic carbon," *nature*, vol. 354, pp. 56-58, 1991.

[2] J. N. Coleman, U. Khan, W. J. Blau, and Y. K. Gun'ko, "Small but strong: a review of the mechanical properties of carbon nanotube–polymer composites," *Carbon*, vol. 44, pp. 1624-1652, 2006.

[3] M. J. O'connell, *Carbon nanotubes: properties and applications*: CRC press, 2006.

[4] K. Hata, D. N. Futaba, K. Mizuno, T. Namai, M. Yumura, and S. Iijima, "Water-assisted highly efficient synthesis of impurity-free single-walled carbon nanotubes," *Science*, vol. 306, pp. 1362-1364, 2004.

[5] E. W. Wong, P. E. Sheehan, and C. M. Lieber, "Nanobeam mechanics: elasticity, strength, and toughness of nanorods and nanotubes," *Science*, vol. 277, pp. 1971-1975, 1997.

[6] X. Wang, Q. Li, J. Xie, Z. Jin, J. Wang, Y. Li, *et al.*, "Fabrication of ultralong and electrically uniform single-walled carbon nanotubes on clean substrates," *Nano letters*, vol. 9, pp. 3137-3141, 2009.

[7] R. H. Baughman, A. A. Zakhidov, and W. A. de Heer, "Carbon nanotubes--the route toward applications," *Science*, vol. 297, pp. 787-792, 2002.

[8] H. Askari, "Nonlinear vibration and chaotic motion of uniform and non-uniform carbon nanotube resonators," University of Ontario Institute of Technology, 2014.

[9] J. Cao, Q. Wang, and H. Dai, "Electromechanical properties of metallic, quasimetallic, and semiconducting carbon nanotubes under stretching," *Physical review letters*, vol. 90, p. 157601, 2003.

[10] L. Yang and J. Han, "Electronic structure of deformed carbon nanotubes," *Physical Review Letters*, vol. 85, p. 154, 2000.

[11] S. Berber, Y.-K. Kwon, and D. Tomanek, "Unusually high thermal conductivity of carbon nanotubes," *Physical review letters*, vol. 84, p. 4613, 2000.

[12] Z. Han and A. Fina, "Thermal conductivity of carbon nanotubes and their polymer nanocomposites: a review," *Progress in polymer science*, vol. 36, pp. 914-944, 2011.

[13] O. Meincke, D. Kaempfer, H. Weickmann, C. Friedrich, M. Vathauer, and H. Warth, "Mechanical properties and electrical conductivity of carbon-nanotube filled polyamide-6 and its blends with acrylonitrile/butadiene/styrene," *Polymer*, vol. 45, pp. 739-748, 2004.

[14] E. T. Thostenson, Z. Ren, and T.-W. Chou, "Advances in the science and technology of carbon nanotubes and their composites: a review," *Composites science and technology*, vol. 61, pp. 1899-1912, 2001.

[15] Y. Lu and S. Chen, "Micro and nano-fabrication of biodegradable polymers for drug delivery," *Advanced drug delivery reviews*, vol. 56, pp. 1621-1633, 2004.

[16] C. Li and T.-W. Chou, "Mass detection using carbon nanotube-based nanomechanical resonators," *Applied Physics Letters*, vol. 84, pp. 5246-5248, 2004.

[17] B. Lassagne, D. Garcia-Sanchez, A. Aguasca, and A. Bachtold, "Ultrasensitive mass sensing with a nanotube electromechanical resonator," *Nano letters*, vol. 8, pp. 3735-3738, 2008.

[18] K. S. Hwang, S.-M. Lee, S. K. Kim, J. H. Lee, and T. S. Kim, "Micro-and nanocantilever devices and systems for biomolecule detection," *Annual Review of Analytical Chemistry*, vol. 2, pp. 77-98, 2009.

[19] T. Kuroyanagi, Y. Terada, K. Takei, S. Akita, and T. Arie, "Cantilevered carbon nanotube hygrometer," *Applied Physics Letters*, vol. 104, p. 193104, 2014.

[20] S. Babu, P. Ndungu, J.-C. Bradley, M. P. Rossi, and Y. Gogotsi, "Guiding water into carbon nanopipes with the aid of bipolar electrochemistry," *Microfluidics and Nanofluidics,* vol. 1, pp. 284-288, 2005.
[21] M. Majumder, N. Chopra, R. Andrews, and B. J. Hinds, "Nanoscale hydrodynamics: enhanced flow in carbon nanotubes," *Nature,* vol. 438, pp. 44-44, 2005.
[22] S. Supple and N. Quirke, "Rapid imbibition of fluids in carbon nanotubes," *Physical review letters,* vol. 90, p. 214501, 2003.
[23] B. Bourlon, D. C. Glattli, C. Miko, L. Forró, and A. Bachtold, "Carbon nanotube based bearing for rotational motions," *Nano Letters,* vol. 4, pp. 709-712, 2004.
[24] L. Dong, A. Subramanian, and B. J. Nelson, "Carbon nanotubes for nanorobotics," *Nano Today,* vol. 2, pp. 12-21, 2007.
[25] S. Fujita, K. Nomura, K. Abe, and T. H. Lee, "3-d nanoarchitectures with carbon nanotube mechanical switches for future on-chip network beyond cmos architecture," *Circuits and Systems I: Regular Papers, IEEE Transactions on,* vol. 54, pp. 2472-2479, 2007.
[26] B. Regan, S. Aloni, R. Ritchie, U. Dahmen, and A. Zettl, "Carbon nanotubes as nanoscale mass conveyors," *Nature,* vol. 428, pp. 924-927, 2004.
[27] A. Fennimore, T. Yuzvinsky, W.-Q. Han, M. Fuhrer, J. Cumings, and A. Zettl, "Rotational actuators based on carbon nanotubes," *Nature,* vol. 424, pp. 408-410, 2003.
[28] R. H. Baughman, C. Cui, A. A. Zakhidov, Z. Iqbal, J. N. Barisci, G. M. Spinks, *et al.*, "Carbon nanotube actuators," *Science,* vol. 284, pp. 1340-1344, 1999.
[29] L. Sudak, "Column buckling of multiwalled carbon nanotubes using nonlocal continuum mechanics," *Journal of Applied Physics,* vol. 94, pp. 7281-7287, 2003.
[30] A. C. Eringen and D. Edelen, "On nonlocal elasticity," *International Journal of Engineering Science,* vol. 10, pp. 233-248, 1972.
[31] A. C. Eringen, "Nonlocal polar elastic continua," *International Journal of Engineering Science,* vol. 10, pp. 1-16, 1972.
[32] A. C. Eringen, "On differential equations of nonlocal elasticity and solutions of screw dislocation and surface waves," *Journal of Applied Physics,* vol. 54, pp. 4703-4710, 1983.
[33] A. Eringen, "Nonlocal polar field models," *Academic, New York,* 1976.
[34] J. Peddieson, G. R. Buchanan, and R. P. McNitt, "Application of nonlocal continuum models to nanotechnology," *International Journal of Engineering Science,* vol. 41, pp. 305-312, 2003.
[35] Q. Wang, "Wave propagation in carbon nanotubes via nonlocal continuum mechanics," *Journal of Applied Physics,* vol. 98, p. 124301, 2005.
[36] J. Reddy and S. Pang, "Nonlocal continuum theories of beams for the analysis of carbon nanotubes," *Journal of Applied Physics,* vol. 103, p. 023511, 2008.
[37] J. Reddy, "Nonlocal nonlinear formulations for bending of classical and shear deformation theories of beams and plates," *International Journal of Engineering Science,* vol. 48, pp. 1507-1518, 2010.
[38] H.-S. Shen and C.-L. Zhang, "Nonlocal beam model for nonlinear analysis of carbon nanotubes on elastomeric substrates," *Computational Materials Science,* vol. 50, pp. 1022-1029, 2011.
[39] T. Murmu and S. Adhikari, "Nonlocal elasticity based vibration of initially pre-stressed coupled nanobeam systems," *European Journal of Mechanics-A/Solids,* vol. 34, pp. 52-62, 2012.
[40] J. R. Claeyssen, T. Tsukazan, and R. D. Coppeti, "Nonlocal effects in modal analysis of forced responses with single carbon nanotubes," *Mechanical Systems and Signal Processing,* vol. 38, pp. 299-311, 2013.
[41] X.-F. Li, G.-J. Tang, Z.-B. Shen, and K. Y. Lee, "Resonance frequency and mass identification of zeptogram-scale nanosensor based on the nonlocal beam theory," *Ultrasonics,* vol. 55, pp. 75-84, 2015.

[42] N. Jalili, *Piezoelectric-based vibration control: from macro to micro/nano scale systems*: Springer Science & Business Media, 2009.
[43] S. N. Mahmoodi, "Nonlinear vibration and frequency response analysis of nanomechanical cantilever beams," CLEMSON UNIVERSITY, 2007.
[44] M. Brissaud, "Three-dimensional modeling of piezoelectric materials," *Ultrasonics, Ferroelectrics, and Frequency Control, IEEE Transactions on,* vol. 57, pp. 2051-2065, 2010.
[45] Y. Gao and Z. L. Wang, "Electrostatic potential in a bent piezoelectric nanowire. The fundamental theory of nanogenerator and nanopiezotronics," *Nano letters,* vol. 7, pp. 2499-2505, 2007.
[46] C.-Y. Wang and S. Adhikari, "ZnO-CNT composite nanotubes as nanoresonators," *Physics Letters A,* vol. 375, pp. 2171-2175, 2011.
[47] J. Zhang, R. Wang, and C. Wang, "Piezoelectric ZnO-CNT nanotubes under axial strain and electrical voltage," *Physica E: Low-Dimensional Systems and Nanostructures,* vol. 46, pp. 105-112, 2012.
[48] K. Momeni and H. Attariani, "Electromechanical properties of 1D ZnO nanostructures: nanopiezotronics building blocks, surface and size-scale effects," *Physical Chemistry Chemical Physics,* vol. 16, pp. 4522-4527, 2014.
[49] A. Khan, J. Edberg, O. Nur, and M. Willander, "A novel investigation on carbon nanotube/ZnO, Ag/ZnO and Ag/carbon nanotube/ZnO nanowires junctions for harvesting piezoelectric potential on textile," *Journal of Applied Physics,* vol. 116, p. 034505, 2014.
[50] P. Poncharal, Z. Wang, D. Ugarte, and W. A. De Heer, "Electrostatic deflections and electromechanical resonances of carbon nanotubes," *Science,* vol. 283, pp. 1513-1516, 1999.
[51] G. Abadal, Z. J. Davis, X. Borrisé, O. Hansen, A. Boisen, N. Barniol, *et al.*, "Atomic force microscope characterization of a resonating nanocantilever," *Ultramicroscopy,* vol. 97, pp. 127-133, 2003.
[52] Z. J. Davis and A. Boisen, "Aluminum nanocantilevers for high sensitivity mass sensors," *Applied Physics Letters,* vol. 87, p. 013102, 2005.
[53] J. Kim, S. Park, J. Park, and J. Lee, "Molecular dynamics simulation of elastic properties of silicon nanocantilevers," *Nanoscale and Microscale Thermophysical Engineering,* vol. 10, pp. 55-65, 2006.
[54] S. Adali, "Variational Principles for Transversely Vibrating Multiwalled Carbon Nanotubes Based on Nonlocal Euler− Bernoulli Beam Model," *Nano letters,* vol. 9, pp. 1737-1741, 2009.
[55] Y. Fu, J. Zhang, and Y. Jiang, "Influences of the surface energies on the nonlinear static and dynamic behaviors of nanobeams," *Physica E: Low-dimensional Systems and Nanostructures,* vol. 42, pp. 2268-2273, 2010.
[56] N. Kacem, S. Baguet, S. Hentz, and R. Dufour, "Computational and quasi-analytical models for non-linear vibrations of resonant MEMS and NEMS sensors," *International Journal of Non-Linear Mechanics,* vol. 46, pp. 532-542, 2011.
[57] A. Farshidianfar, "An efficient GDQ model for vibration analysis of a multiwall carbon nanotube on Pasternak foundationwith general boundary conditions," *Proceedings of the Institution of Mechanical Engineers-Part C,* vol. 225, 2011.
[58] T. Murmu and S. Adhikari, "Nonlocal vibration of carbon nanotubes with attached buckyballs at tip," *Mechanics Research Communications,* vol. 38, pp. 62-67, 2011.
[59] M. D. Dai, C.-W. Kim, and K. Eom, "Nonlinear vibration behavior of graphene resonators and their applications in sensitive mass detection," *Nanoscale research letters,* vol. 7, pp. 1-10, 2012.
[60] T. Murmu and S. Adhikari, "Nonlocal frequency analysis of nanoscale biosensors," *Sensors and Actuators A: Physical,* vol. 173, pp. 41-48, 2012.

[61] M. Rafiee, S. Mareishi, and M. Mohammadi, "An investigation on primary resonance phenomena of elastic medium based single walled carbon nanotubes," *Mechanics Research Communications,* vol. 44, pp. 51-56, 2012.
[62] A. Noghrehabadi, M. Ghalambaz, and A. Ghanbarzadeh, "A new approach to the electrostatic pull-in instability of nanocantilever actuators using the ADM–Padé technique," *Computers & Mathematics with Applications,* vol. 64, pp. 2806-2815, 2012.
[63] J. A. Storch and I. Elishakoff, "Analytical solutions to the free vibration of a double-walled carbon nanotube carrying a bacterium at its tip," *Journal of Applied Physics,* vol. 114, p. 174309, 2013.
[64] A. Nordenfelt, "Selective self-excitation of higher vibrational modes of graphene nano-ribbons and carbon nanotubes through magnetomotive instability," *Journal of Computational and Nonlinear Dynamics,* vol. 8, p. 011011, 2013.
[65] E. M. Miandoab, A. Yousefi-Koma, H. N. Pishkenari, and M. Fathi, "Nano-resonator frequency response based on strain gradient theory," *Journal of Physics D: Applied Physics,* vol. 47, p. 365303, 2014.
[66] N. Khosravian and H. Rafii-Tabar, "Computational modelling of the flow of viscous fluids in carbon nanotubes," *Journal of Physics D: Applied Physics,* vol. 40, p. 7046, 2007.
[67] M. Rasekh and S. Khadem, "Nonlinear vibration and stability analysis of axially loaded embedded carbon nanotubes conveying fluid," *Journal of Physics D: Applied Physics,* vol. 42, p. 135112, 2009.
[68] L. Wang, "Dynamical behaviors of double-walled carbon nanotubes conveying fluid accounting for the role of small length scale," *Computational Materials Science,* vol. 45, pp. 584-588, 2009.
[69] L.-L. Ke and Y.-S. Wang, "Thermoelectric-mechanical vibration of piezoelectric nanobeams based on the nonlocal theory," *Smart Materials and Structures,* vol. 21, p. 025018, 2012.
[70] E. Ghavanloo, F. Daneshmand, and M. Rafiei, "Vibration and instability analysis of carbon nanotubes conveying fluid and resting on a linear viscoelastic Winkler foundation," *Physica E: Low-dimensional Systems and Nanostructures,* vol. 42, pp. 2218-2224, 2010.
[71] P. Soltani, M. Taherian, and A. Farshidianfar, "Vibration and instability of a viscous-fluid-conveying single-walled carbon nanotube embedded in a visco-elastic medium," *Journal of Physics D: Applied Physics,* vol. 43, p. 425401, 2010.
[72] L. Wang, "Vibration analysis of fluid-conveying nanotubes with consideration of surface effects," *Physica E: Low-dimensional Systems and Nanostructures,* vol. 43, pp. 437-439, 2010.
[73] K. Hashemnia, M. Farid, and H. Emdad, "Dynamical analysis of carbon nanotubes conveying water considering carbon–water bond potential energy and nonlocal effects," *Computational Materials Science,* vol. 50, pp. 828-834, 2011.
[74] L. Wang, "A modified nonlocal beam model for vibration and stability of nanotubes conveying fluid," *Physica E: Low-dimensional Systems and Nanostructures,* vol. 44, pp. 25-28, 2011.
[75] L. Wang, "Vibration analysis of nanotubes conveying fluid based on gradient elasticity theory," *Journal of Vibration and Control,* p. 1077546311403957, 2011.
[76] P. Soltani and A. Farshidianfar, "Periodic solution for nonlinear vibration of a fluid-conveying carbon nanotube, based on the nonlocal continuum theory by energy balance method," *Applied Mathematical Modelling,* vol. 36, pp. 3712-3724, 2012.
[77] K. Kiani, "Vibration behavior of simply supported inclined single-walled carbon nanotubes conveying viscous fluids flow using nonlocal Rayleigh beam model," *Applied Mathematical Modelling,* vol. 37, pp. 1836-1850, 2013.

[78] F. Liang and Y. Su, "Stability analysis of a single-walled carbon nanotube conveying pulsating and viscous fluid with nonlocal effect," *Applied Mathematical Modelling*, vol. 37, pp. 6821-6828, 2013.
[79] A. M. Patel and A. Y. Joshi, "Investigating the influence of surface deviations in double walled carbon nanotube based nanomechanical sensors," *Computational Materials Science*, vol. 89, pp. 157-164, 6/15/ 2014.
[80] L. Berhan, Y. Yi, and A. Sastry, "Effect of nanorope waviness on the effective moduli of nanotube sheets," *Journal of applied physics*, vol. 95, pp. 5027-5034, 2004.
[81] F. N. Mayoof and M. A. Hawwa, "Chaotic behavior of a curved carbon nanotube under harmonic excitation," *Chaos, Solitons & Fractals*, vol. 42, pp. 1860-1867, 2009.
[82] W. Xia and L. Wang, "Vibration characteristics of fluid-conveying carbon nanotubes with curved longitudinal shape," *Computational Materials Science*, vol. 49, pp. 99-103, 2010.
[83] H.-L. Lee and W.-J. Chang, "Surface and small-scale effects on vibration analysis of a nonuniform nanocantilever beam," *Physica E: Low-dimensional Systems and Nanostructures*, vol. 43, pp. 466-469, 2010.
[84] K. Yazdchi and M. Salehi, "The effects of CNT waviness on interfacial stress transfer characteristics of CNT/polymer composites," *Composites Part A: Applied Science and Manufacturing*, vol. 42, pp. 1301-1309, 2011.
[85] H. M. Ouakad and M. I. Younis, "Natural frequencies and mode shapes of initially curved carbon nanotube resonators under electric excitation," *Journal of Sound and Vibration*, vol. 330, pp. 3182-3195, 2011.
[86] Z. Saadatnia, A. Barari, and E. Esmailzadeh, "Nonlinear forced vibration analysis of free-form nanotube conveying fluid," in *Nanotechnology (IEEE-NANO), 2014 IEEE 14th International Conference on*, 2014, pp. 689-692.
[87] Z. Yan and L. Jiang, "The vibrational and buckling behaviors of piezoelectric nanobeams with surface effects," *Nanotechnology*, vol. 22, p. 245703, 2011.
[88] C. Wang, L. Li, and Z. Chew, "Vibrating ZnO–CNT nanotubes as pressure/stress sensors," *Physica E: Low-dimensional Systems and Nanostructures*, vol. 43, pp. 1288-1293, 2011.
[89] L.-L. Ke, Y.-S. Wang, and Z.-D. Wang, "Nonlinear vibration of the piezoelectric nanobeams based on the nonlocal theory," *Composite Structures*, vol. 94, pp. 2038-2047, 2012.
[90] A. G. Arani, A. Shajari, S. Amir, and A. Loghman, "Electro-thermo-mechanical nonlinear nonlocal vibration and instability of embedded micro-tube reinforced by BNNT, conveying fluid," *Physica E: Low-dimensional Systems and Nanostructures*, vol. 45, pp. 109-121, 2012.
[91] M. Rafiee, J. Yang, and S. Kitipornchai, "Large amplitude vibration of carbon nanotube reinforced functionally graded composite beams with piezoelectric layers," *Composite Structures*, vol. 96, pp. 716-725, 2013.
[92] A. G. Arani, M. Abdollahian, R. Kolahchi, and A. Rahmati, "Electro-thermo-torsional buckling of an embedded armchair DWBNNT using nonlocal shear deformable shell model," *Composites Part B: Engineering*, vol. 51, pp. 291-299, 2013.
[93] S. Hosseini-Hashemi, I. Nahas, M. Fakher, and R. Nazemnezhad, "Nonlinear free vibration of piezoelectric nanobeams incorporating surface effects," *Smart Materials and Structures*, vol. 23, p. 035012, 2014.
[94] H. Asemi, S. Asemi, A. Farajpour, and M. Mohammadi, "Nanoscale mass detection based on vibrating piezoelectric ultrathin films under thermo-electro-mechanical loads," *Physica E: Low-dimensional Systems and Nanostructures*, vol. 68, pp. 112-122, 2015.
[95] A. C. J. Luo and R. P. S. Han, "Analytical predictions of chaos in a non-linear rod," *Journal of Sound and Vibration*, vol. 227, pp. 523-544, 1999.
[96] S. S. Rao and S. S. Rao, *Mechanical Vibrations*: Pearson Prentice Hall, 2004.
[97] A. H. Nayfeh and D. T. Mook, *Nonlinear oscillations*: John Wiley & Sons, 2008.

[98] H. Cho, M.-F. Yu, A. F. Vakakis, L. A. Bergman, and D. M. McFarland, "Tunable, broadband nonlinear nanomechanical resonator," *Nano letters,* vol. 10, pp. 1793-1798, 2010.

[99] J. Reddy and C. Wang, "Dynamics of fluid-conveying beams," *Centre for Offshore Research and Engineering, National University of Singapore, CORE Report,* pp. 1-21, 2004.

[100] M. H. Sadeghi and M. H. Karimi-Dona, "Dynamic behavior of a fluid conveying pipe subjected to a moving sprung mass–an FEM-state space approach," *International Journal of Pressure Vessels and Piping,* vol. 88, pp. 123-131, 2011.

[101] C. H. Kim, C.-W. Lee, and N. Perkins, "Nonlinear vibration of sheet metal plates under interacting parametric and external excitation during manufacturing," in *ASME 2003 International Design Engineering Technical Conferences and Computers and Information in Engineering Conference*, 2003, pp. 2481-2489.

[102] J. Reddy and I. Singh, "Large deflections and large-amplitude free vibrations of straight and curved beams," *International Journal for numerical methods in engineering,* vol. 17, pp. 829-852, 1981.

Appendices

- **Appendix *A***

The coefficients of equations (3.26) and (3.53) can be computed by the following relations and integrations:

$$\begin{cases} a_{j0} = \int_0^1 \phi_{j0} X_j \, d\hat{x}, \;\; \omega_j^2 = \dfrac{1}{a_{j0}} \int_0^1 \phi_{j1} X_j \, d\hat{x}, \;\; j = 1, 2 \\ a_1 = \dfrac{1}{a_{10}} \int_0^1 \phi_4 X_1 \, d\hat{x}, a_2 = \dfrac{1}{a_{10}} \int_0^1 \phi_3 X_1 \, d\hat{x}, a_3 = \dfrac{1}{a_{20}} \int_0^1 \phi_5 X_2 \, d\hat{x}, a_4 = \dfrac{1}{a_{20}} \int_0^1 \phi_2 X_2 \, d\hat{x}, \\ b_1 = \dfrac{1}{a_{10}} \int_0^1 \phi_2 X_1 \, d\hat{x}, b_2 = \dfrac{1}{a_{10}} \int_0^1 \phi_5 X_1 \, d\hat{x}, b_3 = \dfrac{1}{a_{20}} \int_0^1 \phi_3 X_2 \, d\hat{x}, b_4 = \dfrac{1}{a_{20}} \int_0^1 \phi_4 X_2 \, d\hat{x}, \\ \hat{q}_j(\hat{t}) = \dfrac{1}{a_{j0}} \int_0^1 \{F(\hat{x}, \hat{t}) \Delta(\hat{x} - \hat{x}_0) - \mu_0^{\,2} \dfrac{\partial^2}{\partial \hat{x}^2} [F(\hat{x}, \hat{t}) \Delta(\hat{x} - \hat{x}_0)]\} X_j d\hat{x} \end{cases} \tag{A.1}$$

Where

$$\begin{cases} \phi_{j0} = (1 + M\Delta(\hat{x} - \hat{x}_m)) X_j - \mu_0^{\,2} \dfrac{\partial^2}{\partial \hat{x}^2} \{(1 + m\Delta(\hat{x} - \hat{x}_m)) X_j\}, \; j = 1, \; 2 \\ \phi_{j1} = X_j'''' - \hat{P} X_j'' + \mu_0^{\,2} \hat{P} X_j'''', \; j = 1, \; 2 \\ \phi_2 = -\dfrac{EAL^2}{2EI} (C_1 X_2'' + C_2 X_1'') + \mu_0^{\,2} \dfrac{\partial^2}{\partial \hat{x}^2} \{\dfrac{EAL^2}{2EI} (C_1 X_2'' + C_2 X_1'')\} \\ \phi_3 = -\dfrac{EAL^2}{2EI} (C_2 X_2'' + C_3 X_1'') + \mu_0^{\,2} \dfrac{\partial^2}{\partial \hat{x}^2} \{\dfrac{EAL^2}{2EI} (C_2 X_2'' + C_3 X_1'')\} \\ \phi_4 = -\dfrac{EAL^2}{2EI} C_1 X_1'' + \mu_0^{\,2} \dfrac{\partial^2}{\partial \hat{x}^2} \{\dfrac{EAL^2}{2EI} (C_1 X_1'')\} \\ \phi_5 = -\dfrac{EA}{2L} C_3 X_2'' + \mu_0^{\,2} \dfrac{\partial^2}{\partial \hat{x}^2} \{\dfrac{EAL^2}{2EI} (C_3 X_2'')\} \end{cases} \tag{A.2}$$

Also,

$$C_1 = \int_0^1 X_1'^2 d\hat{x}, \;\; C_2 = \int_0^1 2 X_1' X_2' d\hat{x}, \;\; C_3 = \int_0^1 X_2'^2 d\hat{x}, \tag{A.3}$$

- **Appendix *B***

The constant coefficients in equations (4.21) and (4.35) are computed as follows

$$\begin{cases} b_0 = \int_0^1 \psi_0 X_1 \, d\hat{x}, \\ \omega_1^2 = \dfrac{1}{b_0} \int_0^1 \psi_1 X_1 \, d\hat{x}, \\ b_1 = \dfrac{1}{b_0} \int_0^1 \psi_2 X_1 \, d\hat{x}, \\ \widehat{F}(\hat{t}) = \dfrac{1}{b_0} \int_0^1 [F(\hat{x},\hat{t}) + \mu_0{}^2 \dfrac{\partial^2}{\partial \hat{x}^2} F(\hat{x},\hat{t})] X_1 d\hat{x}, \end{cases} \tag{B.1}$$

Where

$$\begin{cases} \psi_0 = X_1 + MX\Delta(\hat{x} - \hat{x}_m) - \mu_0{}^2 \dfrac{\partial^2}{\partial \hat{x}^2} \{X_1 + MX_1\Delta(\hat{x} - \hat{x}_m)\}, \\ \psi_1 = X_1'''' + (\hat{P} - \hat{V}_0) X_1'' - \mu_0{}^2 (\hat{P} - \hat{V}_0) X_1'''', \\ \psi_2 = -\dfrac{\overline{EA}L^2}{2\overline{EI}} (C_1 X_1'') + \mu_0{}^2 \dfrac{\partial^2}{\partial \hat{x}^2} \{\dfrac{\overline{EA}L^2}{2\overline{EI}} (C_1 X_1'')\}, \\ C_1 = \int_0^1 X_1'^2 d\hat{x} \end{cases} \tag{B.2}$$

The dimensionless parameters are

$$x = L\hat{x},\ t = \tau\hat{t},\ w = L\hat{w},\ \tau = \sqrt{\frac{\overline{\rho A}L^4}{\overline{EI}}},\ M = \frac{m}{\overline{\rho A}L}, \mu_0 = \frac{e_0 a}{L}, \hat{P} = \frac{2pL^2}{\overline{EI}}, \hat{V}_0 = \frac{A_1 e_1 E_0 L^2}{\overline{EI}} \tag{B.3}$$

Where $E_0 = \dfrac{V_0}{L}$ is the constant electric field directly related to the applied voltage [47].

- **Appendix *C***

The constant coefficients Eq. (5.13) are

$$\begin{cases} c_0 = \int_0^L \Gamma_0 X \, dx, \\ \omega_0^2 = \dfrac{1}{c_0}\int_0^1 \Gamma_1 X_1 \, d\hat{x}, \\ c_1 = \dfrac{1}{c_0}\int_0^1 \Gamma_2 X_1 \, d\hat{x}, \\ c_2 = \dfrac{1}{c_0}\int_0^1 \Gamma_3 X_1 \, d\hat{x}, \\ F_0 = \dfrac{\hat{F}_0}{c_0}\int_0^1 [\Delta(\hat{x}-\hat{x}_o) + \mu_0{}^2 \dfrac{\partial^2}{\partial \hat{x}^2}\Delta(\hat{x}-\hat{x}_o)] X_1 d\hat{x}, \end{cases} \tag{C.1}$$

In which $\hat{F}_0$ is the amplitude of applied point load. Also

$$\begin{cases} \Gamma_0 = X_1 + MX\Delta(\hat{x}-\hat{x}_m) - \mu_0{}^2 \dfrac{\partial^2}{\partial \hat{x}^2}\{X_1 + MX_1\Delta(\hat{x}-\hat{x}_m)\}, \\ \Gamma_1 = X_1'''' + (\hat{U} - \hat{V}_0 + \hat{P})X_1'' - \mu_0{}^2(\hat{U} + \hat{P} - \hat{V}_0)X_1'''', \\ \Gamma_2 = -\hat{V}_1 X_1'' + \mu_0{}^2 \hat{V}_1 X_1'''', \\ \Gamma_3 = -\dfrac{\overline{EA}L^2}{2\overline{EI}}(C_1 X_1') + \mu_0{}^2 \dfrac{\partial^2}{\partial \hat{x}^2}\{\dfrac{\overline{EA}L^2}{2\overline{EI}}(C_1 X_1')\}, \\ C_1 = \int_0^1 X_1'^2 d\hat{x} \end{cases} \tag{C.2}$$

The dimensionless parameters are

$$\begin{aligned} &x = L\hat{x},\ t = \tau\hat{t},\ w = L\hat{w},\ \tau = \sqrt{\frac{(\overline{\rho A} + \rho_f A_f)L^4}{\overline{EI}}},\ M = \frac{m}{\overline{\rho A}L},\ \mu_0 = \frac{e_0 a}{L}, \\ &\hat{P} = \frac{2pL^2}{\overline{EI}}, \hat{V}_0 = \frac{A_1 e_1 V_0 L}{\overline{EI}}, \hat{V}_1 = \frac{A_1 e_1 V_1 L}{\overline{EI}}, \hat{U} = \frac{\rho_f A_f (vL)^2}{\overline{EI}} \end{aligned} \tag{C.3}$$

where V_0 and V_1 are the amplitudes of constant and harmonic voltages, and $\hat{U}$ shows the dimensionless fluid velocity.

- **Appendix *D***

The constant coefficients of Eq. (6.9) with the amplitude of applied point load, $\hat{F}_1$ are

$$\begin{cases} d_0 = \int_0^L \eta_0 X \, dx, \\ \omega_0^2 = \dfrac{1}{d_0}\int_0^1 \eta_1 X_1 \, d\hat{x}, \\ d_1 = \dfrac{1}{d_0}\int_0^1 \eta_2 X_1 \, d\hat{x}, \\ d_2 = \dfrac{1}{d_0}\int_0^1 \eta_3 X_1 \, d\hat{x}, \\ d_3 = \dfrac{1}{d_0}\int_0^1 \eta_4 X_1 \, d\hat{x}, \\ F_0 = \dfrac{1}{d_0}\int_0^1 \eta_5 X_1 \, d\hat{x}, \\ F_1 = \dfrac{\hat{F}_1}{d_0}\int_0^1 [\Delta(\hat{x}-\hat{x}_o) + \mu_0{}^2 \dfrac{\partial^2}{\partial \hat{x}^2}\Delta(\hat{x}-\hat{x}_o)] X_1 d\hat{x}, \end{cases} \tag{D.1}$$

$$\begin{cases} \eta_0 = X_1 - \mu_0{}^2 X_1'', \\ \eta_1 = X_1'''' - \dfrac{\overline{EA}L^2}{\overline{EI}} C_2 \hat{\bar{Z}}'' + \mu_0{}^2 \dfrac{\overline{EA}L^2}{\overline{EI}} C_2 \hat{\bar{Z}}'''', \\ \eta_2 = -\hat{V}_1 X_1'' + \mu_0{}^2 \hat{V}_1 X_1'''', \\ \eta_3 = -\dfrac{\overline{EA}L^2}{\overline{EI}}(\dfrac{C_1}{2}\hat{\bar{Z}}'' + C_2 X'') + \mu_0{}^2 \dfrac{\overline{EA}L^2}{\overline{EI}} \dfrac{\partial^2}{\partial \hat{x}^2}(\dfrac{C_1}{2}\hat{\bar{Z}}'' + C_2 X''), \\ \eta_4 = -\dfrac{\overline{EA}L^2}{2\overline{EI}}(C_1 X_1'') + \mu_0{}^2 \dfrac{\partial^2}{\partial \hat{x}^2}\{\dfrac{\overline{EA}L^2}{2\overline{EI}}(C_1 X_1'')\}, \\ \eta_5 = -\hat{V}_1 \hat{\bar{Z}}'' + \mu_0{}^2 \hat{V}_1 \hat{\bar{Z}}'''' \\ C_1 = \int_0^1 X_1'^2 d\hat{x}, C_2 = \int_0^1 X_1' \hat{\bar{Z}}' d\hat{x}, \end{cases} \tag{D.2}$$

The dimensionless parameters are

$$x = L\hat{x},\ t = \tau \hat{t},\ w = L\hat{w},\ \bar{Z} = L\hat{\bar{Z}},\ \tau = \sqrt{\frac{\overline{\rho A}L^4}{\overline{EI}}},\ M = \frac{m}{\overline{\rho A}L},\ \mu_0 = \frac{e_0 a}{L}, \hat{V}_1 = \frac{A_1 e_1 V_1 L}{\overline{EI}} \tag{D.3}$$

V_1 is the harmonic voltage amplitude and $\hat{\bar{Z}}$ is the dimensionless structure curvature[86].